DOE-Arizona-0031854

Final Report

U.S. Department of Energy National Energy Technology Laboratory

Grant: DE-FE0031854

Non-Fouling, Low Cost Electrolytic Coagulation & Disinfection for Treating Flowback and Produced Water for Reuse

PI: James Farrell, Professor, farrellj@email.arizona.edu, (520) 940-0487

Submitted By: James Farrell, 

Submission Date: September 1, 2023

DUNS Number: 806345617

Recipient: University of Arizona, 888 N Euclid Ave, Tucson, AZ 85719

Initial Grant Period: 1/1/2020 through 12/31/2021

Revised Grant Period: 1/1/2020 through 6/30/2023

Reporting Period End Date: 6/30/2023

Report Term: Final

DISCLAIMER

Executive Summary

This *Final Report* is composed of two major sections. The first section presents experimental results obtained in the laboratory during Budget Period 1. The second section presents results from the field test conducted during Budget Period 2.

Laboratory Results

This research investigated a novel electrochemical process for producing a ferric iron coagulant for use in treating flowback and produced water from hydraulic fracturing and oil production operations. The treatment system improves the effectiveness and lowers the cost of coagulation processes using Fe^{3+} as the coagulant. The electrolytic coagulant generation (ECG) system uses an electrochemical cell to produce acid and base from oilfield brine solutions. The acid is used to dissolve scrap iron to provide a Fe^{3+} coagulating agent. The base is used to neutralize the treated water. Compared to conventional electrocoagulation (EC), the main advantage of the ECG system is an order of magnitude lower cost for the source of iron. The second advantage over conventional EC is that it can deliver Fe^{3+} doses greater than 1 mM, since it is not limited by the amount of dissolved oxygen in the water required to oxidize ferrous to ferric iron. The capital costs for conventional EC and the ECG system are similar, but the operational costs for the ECG system are an order of magnitude lower than conventional EC. The combined costs for iron and electrical energy for treating 1 m^3 of FPW with 1 mM Fe^{3+} is estimated to be $0.87 for conventional EC, and $0.087 for the ECG system. The estimated all-in cost for treating FPW with a 2 mM Fe^{3+} dose is $0.73/$m^3$ ($0.12/bbl).

Field Test Results

The field test was conducted at the Paul Foster Central Tank Battery (CTB) in Lea County, New Mexico from November 10, 2022 through December 15, 2022. The feed water to the system was produced water from the Tatanka 1H formation. After approximately two weeks of testing, the initial batch of produced water had been treated and no untreated produced water was available. Thus, after this time, the feed water to

the system consisted of previously treated water (*i.e.*, recycled water). The recycled water had nearly all colloidal particles removed, and had a much lower alkalinity due to precipitation of carbonate minerals during the first pass through the system. Although the recycled water was not an ideal test solution due to its low particulate concentrations, its lower alkalinity did allow us to identify the main problem with the treatment system.

The main problem with the treatment system was caused by the high alkalinity of the initial feed water (5.4 meq/L) that consumed a significant fraction of the electrochemically generated acid. This resulted in pH values exiting the iron contact tank that were too high to dissolve enough iron to effectively treat the produced water. Tests performed with recycled water with lower alkalinity did not have this issue, and dissolved iron concentrations greater than 20 mM could be achieved.

One consistent observation was that effluent water from the iron contact tank was always free of particulates, even when fed with circumneutral solutions. This suggests that there is no need to dissolve high concentrations of iron if all the water to be treated is passed through the scrap iron canister. In this case, dissolved O_2 and hypochlorous acid can promote sufficient iron corrosion to provide an effective coagulating agent – even in neutral pH water. This solves the problem resulting from highly alkaline produced water.

Modifications to the design of the treatment system were made based on the field test results. These modifications will add minimal additional cost, and were tested in bench-scale laboratory experiments. In short-term testing, the modified treatment process was able to remove colloidal FeS particulates to levels below detection. Long-term, steady state testing will be required to determine whether the modified process is suitable for commercial treatment systems.

Introduction – Laboratory Experiments

The use of hydraulic fracturing for recovering oil and gas from low permeability formations requires large quantities of water. In the Permian basin of the southwestern United States, 5 to 12 acre-ft of water are needed to complete each hydraulic fracture (1). In many cases, areas with high levels of unconventional oil and gas production are in water-stressed regions (2). This results in high costs for obtaining and transporting the water needed for hydraulic fracturing operations. Also problematic is that a large fraction of the injected water is recovered as flowback over the early stages of oil and gas production. Flowback and produced water (FPW) recovered along with oil or gas are contaminated with dissolved hydrocarbons, emulsified oil, and suspended and dissolved solids, and must be treated before disposal or reuse.

Treatment options for most FPW are limited by its high salt content, which is generally greater than that of seawater (35,000 mg/L) and is often greater than 200,000 mg/L (3). The most practical and commonly used options for disposal of FPW are deep well injection or reuse in hydraulic fracturing or secondary oil recovery (4,5,6). Treatment of FPW for these uses requires removal of: 1) solids; 2) H_2S; 3) dispersed oil; 4) Fe^{2+}, and sometimes partial removal of other scale forming cations (*e.g.*, Ba^{2+}, Sr^{2+}, Ca^{2+}). Disinfection prior to storage is also desirable to reduce the need for organic disinfectants (*e.g.*, glutaraldehyde) during reuse.

A recent publication reviewed 16 commercialized FPW treatment technologies and 15 of these used electrocoagulation (EC) (7,8,9,10,11). EC targets particulate and emulsified oil removal so that the water can be reused in hydraulic fracturing and secondary oil recovery. Other FPW treatment technologies include biological processes

focused on dissolved hydrocarbon removal (12), and membrane methods that remove particulate, salts, and hydrocarbons (13).

Electrolytic Coagulant Production

Electrocoagulation adds Fe^{2+} or Al^{3+} coagulants into solution via anodic dissolution of metal sheets or plates. The ECG process adds Fe^{3+} to the solution and solves several problems with EC and is illustrated in Figure 1. An electrochemical cell is used to produce acid (H^+) and base (OH^-) via electrolysis of water:

$$anode\ reaction \quad 2\,H_2O \rightarrow O_2 + 4\,H^+ + 4\,e^- \tag{1}$$

$$cathode\ reaction \quad 4\,H_2O + 4\,e^- \rightarrow 2\,H_2 + 4\,OH^- \tag{2}$$

The acid is used to dissolve steel scrap in the form of machine shop turnings or filings to produce the Fe^{2+} necessary to form the coagulant:

$$iron\ dissolution\ reaction \quad 2\,H^+ + Fe \rightarrow Fe^{2+} + H_2 \tag{3}$$

Dissolved O_2 generated by reaction 1 oxidizes Fe^{2+} to Fe^{3+}. The cathode reaction raises the pH of the catholyte solution, which is later used to neutralize the treated water back to its original pH value. In addition to water oxidation, oxidation of Cl^- may also occur and produce $Cl_{2(aq)}$:

$$2\,Cl^-_{(aq)} \rightarrow Cl_{2(aq)} + 2\,e^- \tag{4}$$

The dissolved chlorine rapidly reacts with water to produce hypochlorous (HOCl) and hydrochloric (HCl) acids:

$$Cl_{2(aq)} + H_2O_{(l)} \rightarrow HOCl_{(aq)} + H^+{}_{(aq)} + Cl^-_{(aq)} \tag{5}$$

A small fraction of the anolyte solution that bypasses the scrap iron canister can be used to provide a disinfectant during water storage.

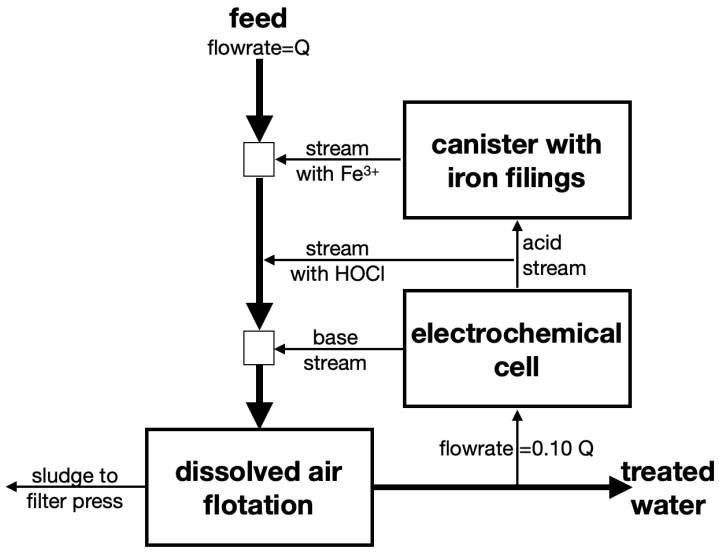

Figure 1. Diagram of the electrolytic coagulant generation system. A fraction of the acid stream bypasses the scrap iron to provide a HOCl disinfectant in the treated water.

The ECG process has advantages over both chemical coagulation and EC. Advantages over chemical coagulation are: 1) no net acid is produced since the H^+ formed during ferric hydroxide precipitation is neutralized by OH^- produced at the cathode; 2) coagulant is added more uniformly to the water thereby requiring lower coagulant doses; 3) smaller sludge volume resulting from lower coagulant doses; and 4) lower total cost for the ferric iron coagulant. Advantages of ECG over conventional EC are: 1) significantly lower cost for the iron coagulant; 2) elimination of cathode fouling by mineral scale; 3) elimination of anode fouling at high current densities due to precipitation of coagulant species on anode surface (14); 4) elimination of incomplete iron coagulant usage at high doses (15). In conventional EC, coagulant doses greater than 1 mM lead to magnetite precipitation due to insufficient dissolved oxygen to completely oxidize the Fe^{2+} to Fe^{3+}. The dense particles of magnetite formed under these conditions are not effective for coagulation. This is especially problematic at the high dosages needed for treating FPW,

which have been reported to range from 2.09 (16) to 6.5 mM (17) for iron EC, and 1.83 to 11 mM (18,19) for aluminum EC. A final advantage of the ECG process is its smaller footprint, since the electrochemical cell can operate at current densities more than an order of magnitude greater than those for conventional EC, where the maximum current density is limited to ~10 mA/cm^2 (15). Higher current densities result in oxygen evolution and precipitation of ferric hydroxide and magnetite on the iron anode surface (15).

The goal of this research was to investigate the technical and economic feasibility for replacing conventional EC with electrolytically generated ferric iron. Towards that end, experiments were performed to determine the costs for acid and base production as a function of current density and brine salt concentration. The stoichiometry and kinetics for dissolution of scrap iron were determined and potential electrode fouling issues were investigated. The operating costs for the ECG process were then compared to those for conventional EC, and the levelized cost for treatment of FPW were determined for a 190 liters per minute (lpm) mobile treatment system.

Materials and Methods

Electrolysis experiments

Electrolysis experiments were performed to determine the energy costs for producing acid and base, and to investigate the formation of hypochlorous acid resulting from oxidation of chloride ions. These experiments employed an ElectroSyn Cell® from Electrocell North America using 2 to 24-unit cells. Both the anode and cathode were platinized titanium with a 2.5 µm-Pt coating and an electroactive area of 400 cm^2 per side. The electrodes were arranged in a monopolar configuration with a 5 mm interelectrode gap. Both sides of each electrode were active, yielding a total anode area of 0.96 m^2 and

a total cathode area of 1.0 m^2, as illustrated in Figure 2. Nafion® N-424 cation exchange membranes were used as dividers between the anolyte and catholyte solutions. A Hydroflow® model S38 electronic water conditioner attached to the catholyte feed pipe was used to reduce mineral scale formation on the cathodes and ion exchange membranes.

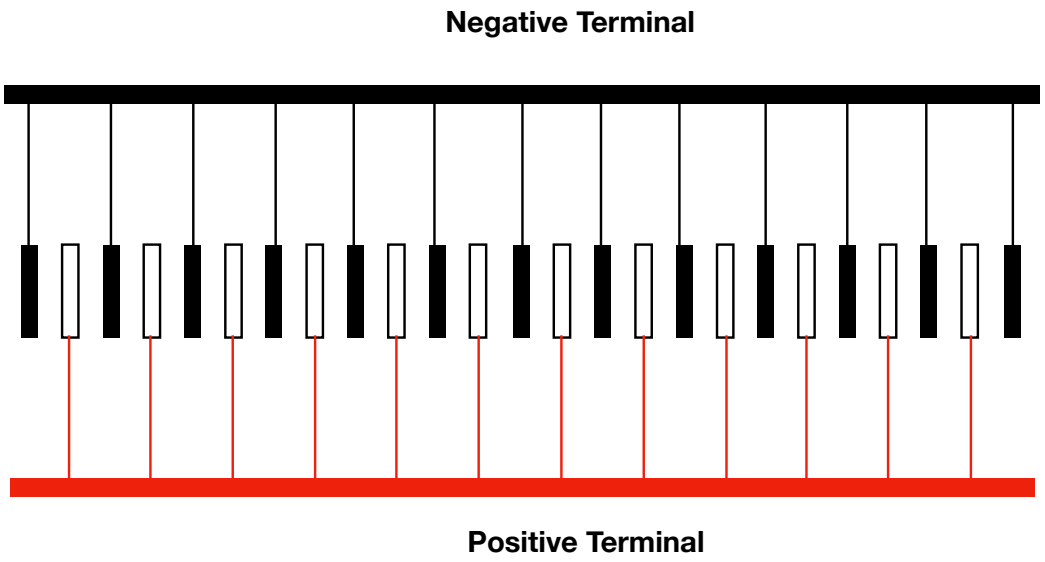

Figure 2. Electrode wiring diagram for 24-unit cells containing 12 anodes (positive) and 13 cathodes (negative) with both electrode faces active (excepting the end cathodes).

Experiments were conducted in a single pass using Na_2SO_4, NaCl and simulated oilfield brine solutions. The experiments were run galvanostatically using current densities ranging from 6.25 to 100 mA/cm^2. Flow rates ranged from 0.125 to 1 L/min per unit cell, yielding mean hydraulic detention times ranging from 0.2 to 1.6 min. Influent and effluent pH values were measured using an Accumet AE10 pH-meter. The concentrations of H^+ and OH^- in the effluent solutions were determined via titration using standardized NaOH and HCl solutions. The applied voltage was recorded over the

course of the experiments. Chlorine concentrations in the solutions were measured using the total chlorine DPD method (20). The Faradaic efficiency (ξ) was determined by:

$$\xi = \frac{C\,Q}{I/_F} \times 100\% \quad (6)$$

where C (M) is the concentration of acid or base, Q (L/s) is the volumetric flow rate, I (A) is the applied current and F is the Faraday constant. The energy to generate 1 kmol of acid or base was calculated from:

$$E = \frac{I\,\bar{U}}{2\,C\,Q} \quad (7)$$

where $E\left(\frac{kWh}{kmol}\right)$ is the energy and $\bar{U}(V)$ is the average voltage over the course of each experiment. Because acid and base are produced at the same time and in equal quantities, the total energy required to operate the cell in each experiment was divided by a factor of two to determine separate energy requirements for generation of 1 kmol of acid or 1 kmol of base.

Iron Dissolution Experiments

Experiments were performed to investigate the stoichiometry and kinetics of iron dissolution by the electrochemically produced acid and oxygen. These experiments used Connelly-GPM (Chicago, IL) CC-1004, -8 to +50 mesh metallic iron filings contained in a 30 L PVC tank. Empty bed contact times (EBCT) between the acid solutions and the filings ranged from 1.8 to 14 minutes. Iron concentrations in the effluent stream were determined using a spectrophotometer via the 1,10 phenanthroline method (21).

Suspended Solids Removal

The effect of the electrochemically generated coagulant for lowering turbidity via coagulation/flocculation of suspended solids was investigated using bentonite clay in a simulated oilfield brine solution whose composition is listed in Table 1. Suspensions containing 500 to 1500 mg/L of bentonite were treated with electrochemically generated ferric iron doses ranging from 1.25 to 2.5 mM. Final turbidity and pH values were measured after 2 hours of settling in 1 L Erlenmeyer flasks.

Table 1. Composition of simulated brine solution compared to an oilfield brine from Jal, New Mexico, USA (22).

Parameter	**Jal Well**	**Experiment**
pH	7.3	7.6
Ca^{2+}	4247 mg/L	4240 mg/L
Mg^{2+}	727 mg/L	730 mg/L
HCO_3^-	2867 mg/L	3050 mg/L
Na^+	42,720 mg/L	36,800 mg/L
Cl^-	65,800 mg/L	56,800 mg/L

Results and Discussion

Electrolysis Experiments

Electrochemical production of reagents is often performed in recirculation mode using short hydraulic detention times to minimize mass transfer limitations on reactant conversion. However, for operational simplicity it is desirable to produce high acid and base concentrations in a single pass through the electrochemical cell. This requires high Faradaic efficiencies at low flow rates. Experiments were performed to determine the effect of flow rate on the Faradaic efficiency and concentrations of acid and base that could be produced in a single pass. These experiments were run at a fixed current density

of 25 mA/cm^2 using 0.5 M NaCl as the feed solution. At this current density, there were negligible O_2 and H_2 gas bubbles that could decrease the electrical conductivity of the solution and thereby affect the operating voltage.

Figure 3a shows the total acid concentrations, which are the sum of the hydronium ion (H_3O) and the hypochlorous acid (HOCl) concentrations. Increasing the flow rate had a less than proportional decrease in the total acid concentration, yielding increased Faradic efficiencies with increasing flow rate. This can be attributed to greater H^+ diffusion across the Nafion® membrane at lower flow rates due to greater acid concentrations and increased hydraulic detention times in the anode chamber of the electrochemical cell. Figure 3b shows that the Faradaic efficiency reached 96% at a flow rate of 0.5 L/min, which indicates that flow rates in excess of 0.5 L/min per unit cell are not needed to achieve high efficiencies. As shown in Figure 3c, the ratio of HOCl to the total amount of acid produced ranged from 35 to 40% and was only marginally affected by the flow rate. Considering that more than half the H^+ ions passed through the Nafion® membrane at the lowest flow rate, the near constant ratio of HOCl to total acid indicates that chloride oxidation accounted for a smaller fraction of the total current at lower flow rates. This is consistent with slower rates of Cl^- mass transfer to the electrode surface at lower flow rates, as predicted by boundary layer theory (23). Figure 3d shows the energy requirements per kmol of acid and base produced as a function of flow rate. The decreasing energy costs with increasing flow rate are the result of higher Faradaic efficiencies with increasing flow rate.

Electrolysis experiments were also performed to determine the effect of current density and feed solution composition on the energy costs for producing acid and base.

Figure 4 shows the energy costs for producing 1 kmol of acid and 1 kmol of base from Na_2SO_4 and NaCl electrolyte solutions. Persulfate concentrations in the effluent solutions were below the detection limit which indicated no appreciable sulfate oxidation in these experiments. For all feed solutions, the energy requirements increased in a near linear manner with current density. This is expected since the rate of acid production is proportional to the current density but ohmic power dissipation is proportional to the second power of the current density (15). For feed solutions containing only Na_2SO_4, the energy costs decreased with increasing salt concentrations. This can be attributed to increasing solution electrical conductivity with increasing salt concentration. The lowest salt concentration investigated was 35 mM Na_2SO_4, which is equivalent to 5000 mg/L total dissolved solids (TDS). This is at the low end of TDS concentrations in real flowback and produced water (3). The highest salt concentration of 704 mM Na_2SO_4 is equivalent to a TDS concentration of 100,000 mg/L, which is in the mid-range of TDS values found in FPW, which often exceed 250,000 mg/L TDS (3). The two NaCl containing solutions, which had ionic strength values of 299 and 334 mM, had similar energy costs as the 176 mM Na_2SO_4 solution, which had an ionic strength of 528 mM. This indicates that oxidation

of Cl^- was more energetically favorable than water oxidation under these operating conditions.

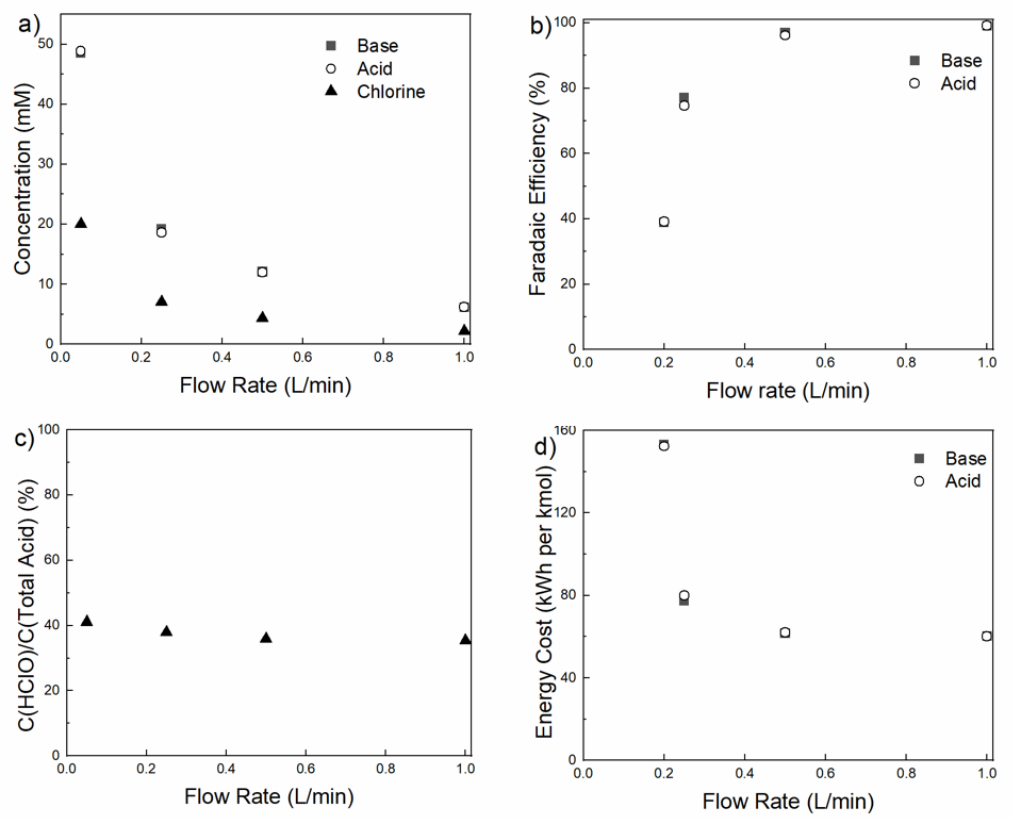

Figure 3. a) Acid, base and HOCl concentrations as a function of flow rate per unit cell; b) Faradaic efficiency for acid and base production; c) fraction of acid present as HOCl; d) Energy requirements per kmol of acid or base as calculated by equation 7.

The energy costs for electrolytic acid and base production are considerably less than costs for purchasing technical grade (*i.e.*, lowest grade) acid and base in multiple ton quantities. Based on the highest energy cost in Figure 4 of 150 kWh per kmol and a US average industrial electricity cost of $0.083 (24), the cost for producing 1 kmol of acid plus

1 kmol of base is $24.90. Approximate costs for technical grade acid and base are $135/kmol for H_2SO_4 (25) and $140 /kmol for NaOH (26). Thus, the electrical energy cost was less than 10% of the cost for purchasing technical grade chemicals.

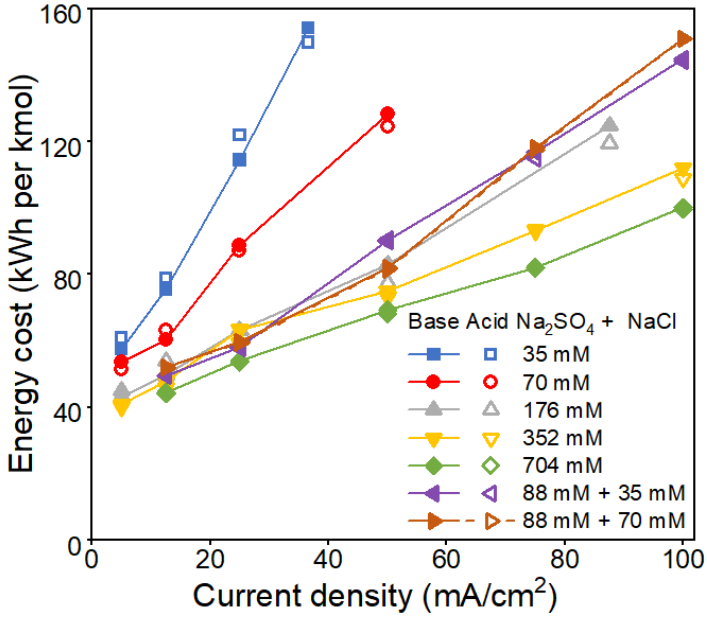

Figure 4. Energy costs per kmol of acid or base produced for different electrolyte solutions.

Iron Dissolution Experiments

Experiments were conducted to determine the stoichiometry between acid consumption and ferric iron generation. Figure 5 shows the moles of acid consumed per mole of iron dissolved. For dissolution of metallic iron by acid, two moles of H^+ are required per mol of Fe^{2+}, as illustrated by equation 3. In addition, one mol of acid is required to oxidize one mole of Fe^{2+}:

$$2Fe^{2+} + 2H^+ + 0.5\ O_{2(aq)} \rightarrow 2Fe^{3+} + H_2O \qquad (8)$$

Thus, three moles of acid should be consumed per mole of Fe^{3+}. However, the data in Figure 5 shows that each mole of Fe^{3+} produced required only 1.6 moles of acid. This can be explained by the fact that O_2 dissolved in the acid can also oxidize metallic iron according to:

$$4Fe_{(s)} + 3O_{2(aq)} + 2H_2O \leftrightarrow 2\,Fe_2O_3 \cdot H_2O_{(s)} \quad (9)$$

Dissolved oxygen may also oxidize Fe^{2+} with concomitant generation of acid, according to: (27,28):

$$4\,Fe^{2+} + O_{2(aq)} + 6H_2O \leftrightarrow 4\,FeOOH_{(s)} + 8\,H^+ \quad (10)$$

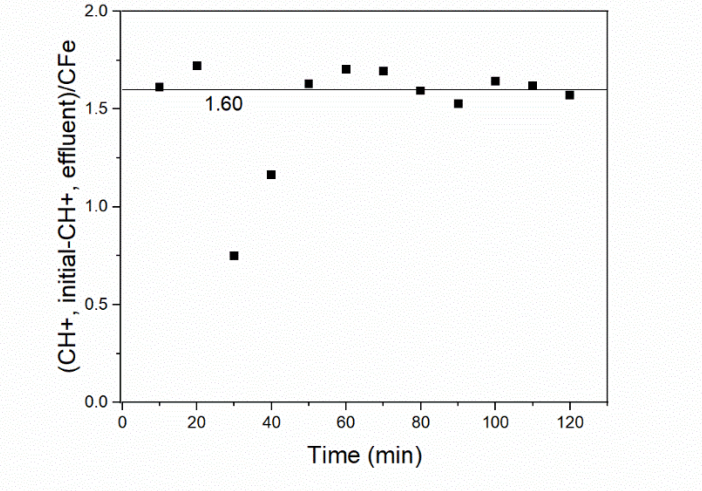

Figure 5. Equivalents of acid consumed per aqueous phase Fe versus elapsed time of operation by electrochemically generated acid.

The technical feasibility for electrochemical coagulant generation requires that the reaction between the acid and the iron filings be sufficiently fast so that only a short contact time is needed. Figure 6 shows the fraction of the acid consumed as a function of the EBCT. In 88 mM sodium sulfate solutions, the fraction of the acid consumed

increased from 36% to 96% by increasing the EBCT from 1.8 to 14 minutes. However, in solutions containing 88 mM Na_2SO_4 plus 35 mM NaCl, >99% of the acid reacted with an EBCT of 2 minutes or less. The faster dissolution results from Cl^- ions preventing formation of a ferric hydroxide passivating layer on the iron (29). Thus, since most FPW contains more than 35 mM of Cl^- ions, a short EBCT can be used to dissolve the iron filings.

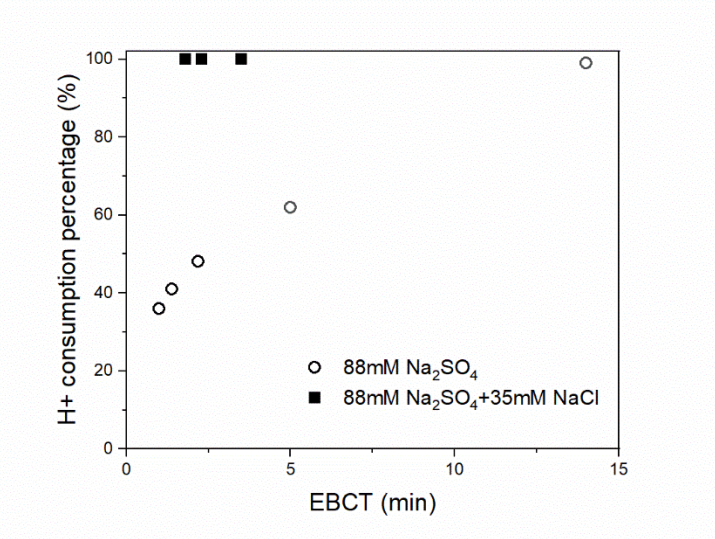

Figure 6. Fractional acid consumption as a function of empty bed contact time (EBCT) in iron filings tank.

Electrode and Membrane Fouling

FPW often contains high concentrations of Ca^{2+} and Mg^{2+} ions that can form $CaCO_3$ or $Mg(OH)_2$ mineral scale at the high pH values in the cathode compartment of the electrochemical cell. Precipitation of $CaCO_3$ or $Mg(OH)_2$ in solution is not problematic since those precipitates will exit the cell in the catholyte stream. However, precipitation of mineral solids on the electrode surface will block electroactive sites and make areas of the electrode surface inactive. In addition, precipitation of mineral solids on the

membrane dividing the electrochemical cell will impede ion transport through the membrane in areas covered with precipitate. If precipitated mineral solids build up on the electrode or membrane, increasing voltages will be needed to maintain the same current. Precipitates on the electrode and membrane can be removed by reversing the polarity of the electrochemical cell. By reversing polarity, the electrode previously serving as the cathode is converted to an anode that produces O_2 and H^+ via water oxidation. The H^+ ions can dissolve precipitated mineral scale on both the membrane and electrode surface.

To investigate electrode and membrane fouling, experiments were performed with feed solutions containing high concentrations of Ca^{2+}, Mg^{2+} and HCO_3^-. The concentrations chosen were selected to approximate produced water from an oil production well in the Permian Basin, as shown in Table 1 (22). Figure 7 shows the applied voltage as a function of time when the cell was operated at a current density of 100 mA/cm^2 in both forward and reverse polarity. Forward polarity corresponds to the operating condition of the treatment system and reverse polarity corresponds to the cleaning cycle. Figure 7 shows the system operating in forward polarity for seven hours. During that time, the cell voltage increased from 6.9 V to 7.1 V. This small change in voltage indicates that fouling by mineral scale does not appear to be a problem. When the polarity was reversed after 7 hours of operation, the voltage increased to 7.6 V but remained relatively stable thereafter. The small increase in voltage in reverse polarity can be attributed to a coating on one side of the Nafion® N-24 membrane that reduces proton diffusion through the membrane. This coating should be facing the anode, and results in greater ohmic voltage loss across the membrane when operated facing the cathode.

At other current densities and for up to 15.5 hours of continuous operation, no significant increases in voltage or cell pressure were observed, as shown in Figure 8. These data show that there was only a small effect of operating time on cell voltage and suggests that there was minimal electrode and membrane fouling. To confirm this, the electrochemical cell was taken apart after operating for two hours in forward polarity at 100 mA/cm^2. Figure 9 shows pictures of the cathode and cathode facing membrane from one of the unit cells. There were no visible precipitates on either the membrane or the electrode. This confirms that electrode and membrane fouling was not a problem under the conditions of these experiments.

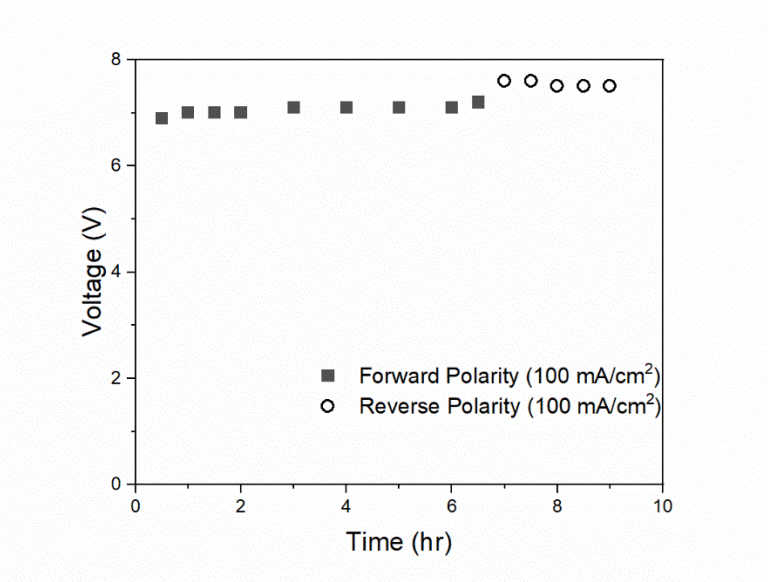

Figure 7. Voltage versus time of operation for forward and reverse polarity at 100 mA/cm^2 using feed water with ion concentrations given in Table 1.

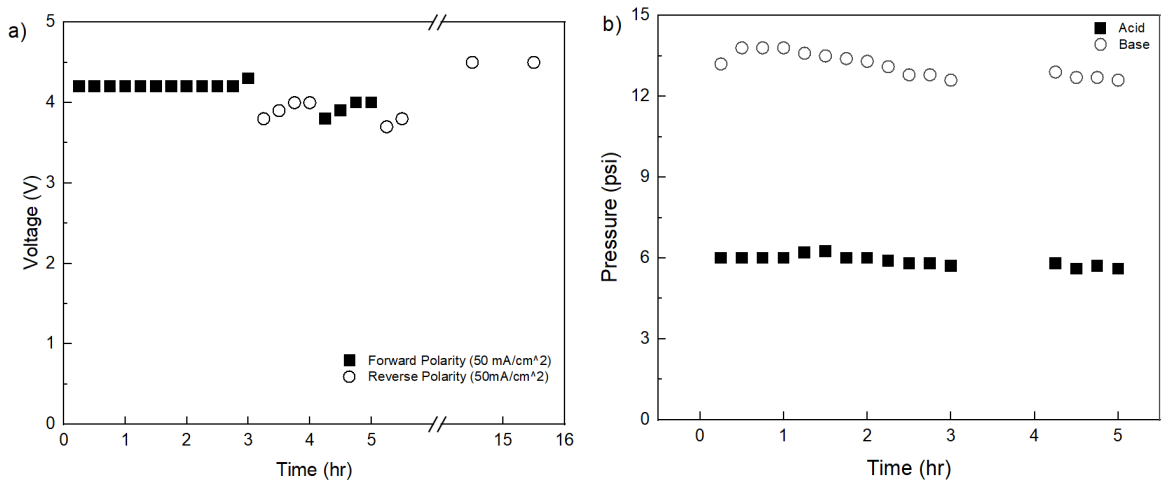

Figure 8. a) Voltage versus time of operation in forward and reverse polarity at 50 mA/cm^2. b) Influent pressure to the acid and base chambers of the electrochemical cell at a constant flow rate of 1 liter per minute per unit cell.

Figure 9. Cathode and cathode facing membrane after 2 hours of operation at a current density of 100 mA/cm^2 using feed water with the composition given in Table 1. No cleaning cycle was used in this experiment.

Suspended Solids Removal

Experiments were performed to investigate the effectiveness of the coagulant produced by the ECG process for removing suspended solids. Figure 10 shows initial and final turbidity and pH values, and final dissolved iron concentrations for a suspension with 1500 mg/L of bentonite clay at an initial pH value of 6.5. Treatment with 1.25 to 2.5 mM ferric iron reduced the turbidity values from 93 NTU to a range of 1.3 to 2.1. These values are lower than the recommended values of <10 NTU for use in hydraulic fracturing (4). Final pH values ranged from 6 to 4.5 and decreased with increasing Fe^{3+} dosage. A possible explanation for the decreases in pH may be a greater contribution of reaction 10 to Fe^{2+} oxidation as compared to reaction 8. Final dissolved iron concentrations ranged from 10 to 13 μM (0.5 – 0.73 mg/L). These values are well below the <10 mg/L guideline for reuse of produced water in hydraulic fracturing (5).

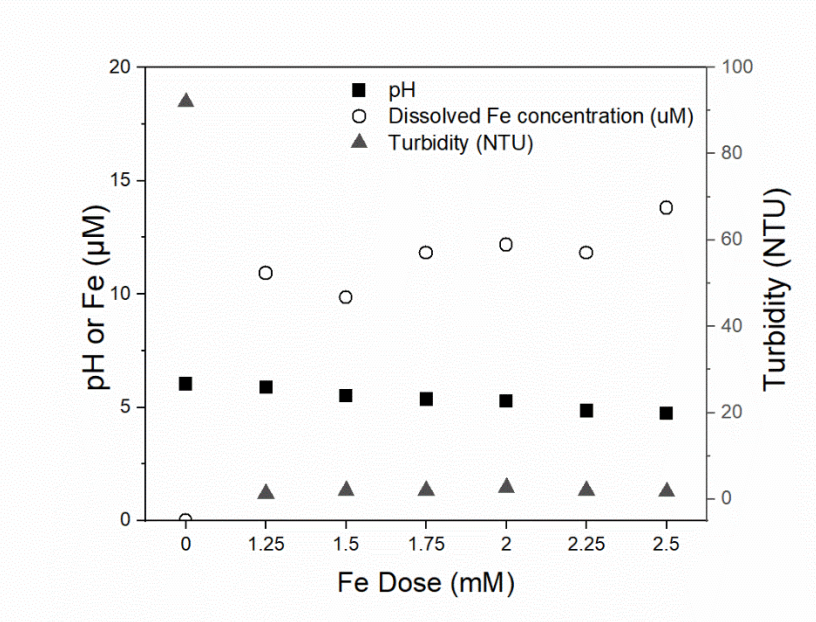

Figure 10. Initial and final pH, turbidity, and dissolved iron concentrations (μM) as a function of iron coagulant dose. Composition of the feed water is given in Table 1. Initial suspended solids concentration was 1500 m/L of bentonite clay with a turbidity of 93 NTU.

Economic Analysis

The feasibility of the ECG process for replacing traditional electrocoagulation depends on a cost comparison between the two processes. The ECG process shares many similar components with electrocoagulation, such as: power supply, pumps, and solids separation equipment. Thus, the total capital costs for the two processes are expected to be similar. The main cost differences between conventional EC and the ECG process are the electrical energy and iron metal costs. Another difference is that the ECG process requires up to 10% of the treated water to be recycled for acid and base production. In a recent field test of the ECG process, a 50 meq/L acid solution was produced for the cell operating at a current density of 48 mA/cm^2 and a flow rate of 15 L/min. This is sufficient acid to produce a 31 mM ferric iron solution. Dilution of this by a factor of 11 would result in a 2.8 mM dose of ferric iron, which is typical of those used in treatment of produced water (16).

Electrical Energy Costs

Figure 11 shows the energy (kWh) required to treat 1 m^3 of water with 1 mM Fe^{3+} coagulant for different feed solutions for the ECG process. The electrical energy costs for traditional electrocoagulation as a function of the current density, solution conductivity, and electrode spacing were determined in a previous publication (15). For an electrocoagulation system operating at 10 mA/cm^2 and 1 cm electrode spacing with a solution conductivity equivalent to 0.5 M NaCl (conductivity = 0.032 S/cm), the energy required for dosing 1 m^3 of water with 1 mM Fe^{3+} is 0.060 $\frac{kWh}{mM-m^3}$. This is half of that required by the ECG system at 10 mA/cm^2 for the 353 and 704 mM Na_2SO_4 solutions, as

shown in Figure 11. However, with increasing current density, the energy costs for the ECG system reached as high as 0.48 $\frac{kWh}{mM-m^3}$ at a current density of 100 mA/cm^2.

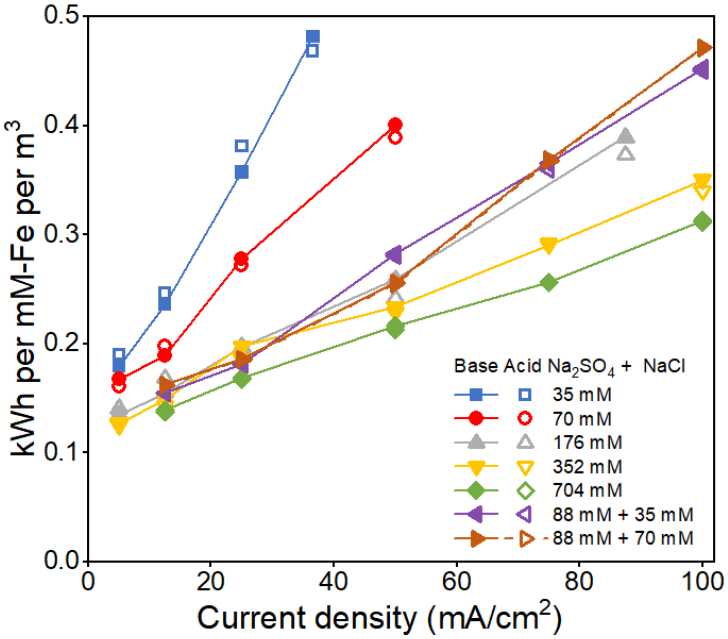

Figure 11. Electrical energy in kWh required for delivering a 1 mM Fe^{3+} dose per cubic meter of water as a function of current density.

Iron Costs

Current costs for scrap iron shavings are $0.35 per lb. For sheets of iron that are typical of the size used in electrocoagulation (0.75 m^2, 5 mm thick), the cost for a 7-gauge sheet that weighs 61.3 lbs is $284, which amounts to $4.63/lb (30). The electrical and iron costs can be added to obtain the total operating costs for delivering 1 mM Fe^{3+} coagulant per cubic meter of water, as shown in Table 2. The costs in Table 2 were based on the highest energy requirement in Figure 11 of $0.48\ \frac{kWh}{mM-m^3}$ and the U.S. average industrial electricity cost of $0.083 per kWh (31). A utilization of 66% was used

for the iron sheet metal for conventional EC. Incomplete utilization of the iron sheets in conventional EC results from hole formation in the center of each sheet before the entire sheet can be electrochemically dissolved. The costs in Table 2 show that the dominant cost for both processes is the cost for the iron. The total cost for delivering 1 mM Fe^{3+} per cubic meter of water treated is $0.87 for conventional EC and $0.087 for the ECG process. Including the expense for loss of Pt from the electrodes has a negligible impact on the costs in Table 2. The cell used in this investigation operating at 100 mA/cm^2 passes 1000 A-yr of charge for delivering 2 mM Fe^{3+} into 100,000 m^3 of water. Previous studies have reported a Pt loss of 8 mg/A-yr when operating at 0.1 A/cm^2 in 0.1 M NaCl (32). This corresponds to 8 g of Pt loss per year, which is equivalent to 8 x 10^{-5} g/m^3 of water treated.

Table 2. Costs for energy, iron and combined operational cost for conventional EC and the ECG process for treating 1 m^3 of FPW with 1 mM Fe^{3+}. Costs for the ECG process were increased by 10% to account for treated water recycling.

Operating Costs	Conventional EC	ECG Process
electrical	$0.0050	$0.044
iron	$0.86	$0.043
total	$0.87	$0.087

Capital Cost Comparison of ECG with Conventional EC

We estimate that the capital costs for electrolytic coagulant generation (ECG) and conventional electrocoagulation will be similar. For the system used in this investigation, the cost for electrochemical cell was 17% of the total cost for the treatment system. Thus, even if the cell costs for conventional EC were significantly lower than those for ECG, this

would not appreciably reduce the total capital cost of the treatment system. Although conventional EC does not require non-consumable platinized titanium electrodes, it does require more than 10 times greater electrode area as the ECG process. Data from this study showed that the ECG process could be economically operated at a current density of 100 mA/cm^2. With conventional EC, the maximum current density is limited to ~10 mA/cm^2 (15). Higher current densities result in oxygen evolution on the anode, and precipitation of ferric hydroxide and magnetite on the anode surface (15). Thus, extra cost for the ECG electrodes is compensated by greater costs for electrode housing in conventional EC.

Total Treatment Costs

Estimated total costs for treating FPW by the ECG system are shown in Table 3. Operating at a current density of 100 mA/cm^2, the system used in this study can treat 190 Lpm with a coagulant dose of 2 mM-Fe^{3+}. The costs in Table 3 are based on a useful life for the system of 10 years, and a five-year useful life of the membranes. The electrical requirements are from Figure 11 of 0.48 $\frac{kWh}{mM-m^3}$. The capital costs are based on the actual cost of purchasing the treatment system. A significant fraction of this costs is for the design of the system and its control software. Thus, the capital costs here are likely greater than those for mass production. The system can be completely automated, since the only labor required is to add one 25 kg bag of iron to the contact tank per day.

Table 3. Treatment costs for operating the system at 190 Lpm over a 10-year period with a coagulant dose of 2 mM-Fe^{3+}.

Item	Amount
Capital Cost (actual cost from this project)	$368,750
Interest Expense @ 5%/yr	$184,375
Capital plus Interest	$553,125
Operational Expense @$0.087/mM-Fe/$m^3$	$172,967
Total Cost for 10 years	$726,092
Volume of FPW Treated @ 190 Lpm gpm	994,064 m^3
Cost per m^3 FPW Treated	$0.73/$m^3$
Cost per bbl FPW Treated	**$0.12/bbl**

Conclusions

The ECG process is functionally similar to conventional electrocoagulation in that metallic iron is used to provide a ferric iron coagulant. However, in addition to lower iron costs, the ECG process overcomes several limitations of EC, especially when treating flowback and produced water. Brines generated during oil production contain suspended particles and emulsified oil that can foul EC electrodes and are usually anoxic. The ECG process eliminates electrode fouling by passing only treated water through the electrochemical cell. Anoxic waters require aeration prior to EC using iron electrodes, whereas the ECG process aerates the water at oxygen partial pressures greater than 1 atmosphere. The ECG process is also beneficial in other applications requiring high coagulant doses where a high salinity brine stream is available, such as in treatment of concentrate solutions generated during reverse osmosis production of potable water.

Acknowledgements

This research was funded by the US Department of Energy and administered by the National Energy Technology Laboratory through agreement DE-FE0031854. Additional funding was provided by the Stevens Family Trust through a gift to the University of Arizona.

Data Tables for Laboratory Section

Data for Figure 3a.

Flow Rate (L/min)	Base (mM)	Acid (mM)	Chlorine (mM)
0.05	48.5	48.8	20.0
0.25	19.2	18.6	7.0
0.5	12.1	12.0	4.3
1	6.17	6.18	2.18

Data for Figure 3b.

Flow rate (L/min)	Faradaic Efficiency Base (%)	Faradaic Efficiency Acid (%)
0.2	38.9	39.2
0.25	77.2	74.7
0.5	96.9	96.1
1	99.1	99.1

Data for Figure 3c.

Flow Rate (L/min)	HClO/Total Acid (%)
0.05	41.0
0.25	37.8
0.5	35.9
1	35.3

Data for Figure 3d.

Flow Rate (L/min)	Energy Cost Base (kWh per kmol)	Energy Cost Acid (kWh per kmol)
0.2	153.1	152.2
0.25	77.3	79.9
0.5	61.5	62.0
1	60.2	60.1

Data for Figure 4.

Current Density $\frac{mA}{cm^2}$	Base Energy Cost ($\frac{kWh}{kmol}$)						
	35 mM Na_2SO_4	70 mM Na_2SO_4	176 mM Na_2SO_4	352 mM Na_2SO_4	704 mM Na_2SO_4	88 mM Na_2SO_4 + 35 mM NaCl	88 mM Na_2SO_4 + 70 mM NaCl
5	57.5	53.6	43.2	40.7			
12.5	75.6	60.4	49.7	47.9	44.5	49.6	52.0
25	114.4	88.8	63.1	63.3	54.0	58.0	59.6
36.6	154.1			75.0	69.2	90.4	81.9
50		128.1	83.0				
75				93.1	82.0	116.8	118.0
87.5			124.7				
100				112.1	100.1	144.8	151.0

Current Density $\frac{mA}{cm^2}$	Acid Energy Cost ($\frac{kWh}{kmol}$)						
	35 mM Na_2SO_4	70 mM Na_2SO_4	176 mM Na_2SO_4	352 mM Na_2SO_4	704 mM Na_2SO_4	88 mM Na_2SO_4 + 35 mM NaCl	88 mM Na_2SO_4 + 70 mM NaCl
5.0	60.8	51.5	45.0	40.1			
12.5	78.8	63.3	53.9	45.8	44.2	49.5	51.8
25.0	121.9	87.1	63.2	59.4	53.5	57.9	59.4
36.6	149.8			73.3	68.1	89.9	81.6
50.0		124.6	77.3				
75.0				93.6	82.1	115.0	117.5
87.5			119.5				
100.0				108.8	99.7	144.2	150.8

Data for Figure 5.

Time (min)	$\frac{CH^{+}_{initial} - CH^{+}_{effluent}}{CFe}$
10	1.61
20	1.72
30	0.75
40	1.16
50	1.63
60	1.70
70	1.69
80	1.59
90	1.53
100	1.64
110	1.62
120	1.57

Data for Figure 6.

EBCT (min)	H+ consumption percentage (%)	
	88 mM Na_2SO_4	88 mM Na_2SO_4 + 35 mM NaCl
14	99	
5	62	
2.2	48	
1.4	41	
1	36	
3.5		99.98
2.3		99.97
1.8		99.97

Data for Figure 7.

Time (hr)	Forward Polarity (V)	Reverse Polarity (V)
0.5	6.9	
1	7	
1.5	7	
2	7	
3	7.1	
4	7.1	
5	7.1	
6	7.1	
6.5	7.2	
7		7.6
7.5		7.6
8		7.5
8.5		7.5
9		7.5

Data for Figure 8a.

Time (hr)	Forward Polarity (V)	Reverse Polarity (V)
0.25	4.2	
0.5	4.2	
0.75	4.2	
1	4.2	
1.25	4.2	
1.5	4.2	
1.75	4.2	
2	4.2	
2.25	4.2	
2.5	4.2	
2.75	4.2	
3	4.3	
3.25		3.8
3.5		3.9
3.75		4
4		4
4.25	3.8	
4.5	3.9	
4.75	4	
5	4	
5.25		3.7
5.5		3.8
14.5		4.5
15.5		4.5

Data for Figure 8b.

Time (hr)	Acid Pressure (psi)	Base Pressure (psi)
0.25	6	13.2
0.5	6	13.8
0.75	6	13.8
1	6	13.8
1.25	6.2	13.6
1.5	6.25	13.5
1.75	6	13.4
2	6	13.3
2.25	5.9	13.1
2.5	5.8	12.8
2.75	5.8	12.8
3	5.7	12.6
4.25	5.8	12.9
4.5	5.6	12.7
4.75	5.7	12.7
5	5.6	12.6

Data for Figure 10.

Fe Dose (mM)	pH	Turbidity (NTU)	Dissolved Fe concentration (μM)
0	6.04	92	0
1.25	5.9	1.33	10.92
1.5	5.52	2.05	9.85
1.75	5.36	1.97	11.82
2	5.28	2.7	12.18
2.25	4.85	2.03	11.82
2.5	4.74	1.77	13.79

Data for Figure 11.

Current Density $\frac{mA}{cm^2}$	Base Energy Cost $\left(\frac{kWh}{mM-Fe\ m^3}\right)$						
	35 mM Na_2SO_4	70 mM Na_2SO_4	176 mM Na_2SO_4	352 mM Na_2SO_4	704 mM Na_2SO_4	88 mM Na_2SO_4 + 35 mM NaCl	88 mM Na_2SO_4 + 70 mM NaCl
5	0.18	0.17	0.13	0.13			
12.5	0.24	0.19	0.16	0.15	0.14	0.15	0.16
25	0.36	0.28	0.20	0.20	0.17	0.18	0.19
36.6	0.48						
50		0.40	0.25946	0.23	0.22	0.28	0.26
75				0.29	0.26	0.37	0.37
87.5			0.39				
100				0.35	0.31	0.45	0.47

Current Density $\frac{mA}{cm^2}$	Acid Energy Cost $\left(\frac{kWh}{mM-Fe\ m^3}\right)$						
	35 mM Na_2SO_4	70 mM Na_2SO_4	176 mM Na_2SO_4	352 mM Na_2SO_4	704 mM Na_2SO_4	88 mM Na_2SO_4 + 35 mM NaCl	88 mM Na_2SO_4 + 70 mM NaCl
5	0.19	0.16	0.14	0.13			
12.5	0.25	0.20	0.17	0.14	0.14	0.15	0.16
25	0.38	0.27	0.20	0.19	0.17	0.18	0.19
36.6	0.47						
50		0.39	0.24	0.23	0.21	0.28	0.25
75				0.29	0.26	0.36	0.37
87.5			0.37				
100				0.34	0.31	0.45	0.47

References

(1) Lowry, T.S.; Schuhen, M.D.; Lofton, O.W.; Walker, L.T.N.; Johnson, P.B.; Powers, D.W.; Bowman, D.O. Water Resource Assessment in the New Mexico Permian Basin, Sandia Report SAND2018-12018 Unlimited Release, Printed October 2018.

(2) Roland, J; Sungchung, S., The Water Stressed American West, Center for American Progress, June 26, 2019, https://www.americanprogress.org/article/oil-gas-development-creating-problem-arid-west/. accessed 2/3/2023

(3) Otton, J.K.; Mercier, T. Produced Water Brine and Stream Salinity, US Geological Survey, https://water.usgs.gov/orh/nrwww/Otten.pdf. accessed 2/3/2023

(4) Hoagland, F.M., Recycling Produced Water, presented at: Fundamentals of Produced Water Treatment in the Oil and Gas Industry, Upstream O&G Subcommittee of Industrial Wastewater Committee (IWWC), Water Environment Federation with Produced Water Society, April 25, 2019.

(5) Wilson, B.C.; Lucero, A.A., Romero, J.T.; Romero, P.J.; Water Use by Categories in New Mexico Counties and River Basins, and Irrigated Acreage in 2000, New Mexico Office of the State Engineer, Technical Report 51, February 2003.

(6) Hoagland, F.M. Introduction to Produced Water Management, presented at: Fundamentals of Produced Water Treatment in the Oil and Gas Industry Conference, Upstream O&G Subcommittee of Industrial Wastewater Committee (IWWC), Water Environment Federation with Produced Water Society, April 25, 2019.

(7) Mohammad-Pajooh, E.; Weichgrebe, D.; Cuff, G.; Tosarkani, B.M.; Rosenwinkel, K.H. On-site treatment of flowback and produced water from shale gas hydraulic fracturing: A review and economic evaluation. *Chemosphere* **2018**, 2012, 898-914.

(8) http://www.bosquesystems.com/water-treatment.html. accessed 2/3/23

(9) https://www.originclear.com/hubfs/pdf/CLEAN-FRAC-Model-60K-Data-Sheet.pdf. accessed 2/3/2023

(10) https://www.bakercorp.com/en-us/products/filtration/kaselco-systems/electrocoagulation-solutions/. accessed 2/3/2023

(11) http://www.veoliawatertech.com/news-resources/datasheets/ross-flowback-produced-water.htm. accessed 2/3/2023

(12) Freedman, D.E., Riley, S.M., Jones, Z.L., Rosenblum, J.S., Sharp, J.O., Spear, J.R. and Cath, T.Y. Biologically active filtration for fracturing flowback and produced water treatment. *Journal of Water Process Engineering* **2017,** *18*, 29-40.

(13) Chang, H., Li, T., Liu, B., Vidic, R.D., Elimelech, M. and Crittenden, J.C. Potential and implemented membrane-based technologies for the treatment and reuse of flowback and produced water from shale gas and oil plays: A review. *Desalination* **2019**, *455*, 34-57.

(14) Schulz, M.C.; Baygents, J.C.; Farrell, J. Laboratory and Pilot Testing of Electrocoagulation for removing scale-forming species from industrial process waters. *Int. J. Env. Sci. Technol.* **2009**, 6, 521-526.

(15) Gu, Z; Liao, Z.; Schulz, M.; Davis, J. R.; Baygents, J. C.; Farrell, J. Estimating dosing rates and energy consumption for electrocoagulation using iron and aluminum electrodes. *Ind. Eng. Chem. Res.* **2009**, 48, 3112-3117.

(16) Esmaeilirad, N.; Carlson, K.; Ozbek, O. Influence of softening sequence on electrocoagulation treatment of produced water. *J. Hazard. Mater.* **2015**, 283, 721-729.
(17) Aly, D.T.A. A Novel Electrocoagulation System of Produced Water Treatment, M.S. Thesis, Qatar Univeristy, January 2018.
(18) Ammar, S.H.; Akbar, A.S. Oilfield produced water treatment in internal-loop airlift reactor using electrocoagulation/flotation technique. *Chinese J. Chem. Eng*. **2018**, 26, 879-885.
(19) Lobo, F.L.; Wang, H.; Huggins, T.; Rosenblum, J.; Linden, K G., Low-energy hydraulic fracturing wastewater treatment via AC powered electrocoagulation with biochar. *J. Hazard. Mater.* **2016**, 309, 180-184.
(20) Cooper,W.J.; Roscher,N.M.; Slifker, R.A. Determining free available chlorine by DPD-colorimetric, DPD-Steadifac (colorimetric), and FACTS procedures. *Journal-American Water Works Association* **1982***,* 74.7, 362-368.
(21) Tamura, H.; Goto, K., Yotsuyanagi, T.; Nagayama, M., Spectrophotometric determination of iron (II) with 1,10-phenanthroline in the presence of large amounts of iron (III). *Talanta* **1974**, 21(4), 314-318.
(22) Zendejas Rodriguez, A.; Wang, H.; Hu, L.; Zhang, Y.; Xu, P. Treatment of produced water in the Permian Basin for hydraulic fracturing: comparison of different coagulation processes and innovative filter media. *Water* **2020**, *12*, 770; doi:10.3390/w12030770
(23) Sáez, A.E.; Baygents, J.C. *Environmental transport phenomena*. CRC Press, 2014.
(24) https://www.eia.gov/totalenergy/data/monthly/pdf/sec9_11.pdf. accessed on 5/4/2023
(25) https://alliancechemical.com/product/sulfuric-acid-93/?attribute_pa_size=275-gallon&attribute_pa_packaging-type=tote&gclid=EAIaIQobChMI9JX469Xm_gIVNh-tBh2NzglVEAQYASABEgLf6PD_BwE. accessed 5/9/2023
(26) https://alliancechemical.com/product/sodium-hydroxide-50/. accessed on 5/9/2023
(27) Burke, S.P., Banwart, S.A. A geochemical model for removal of iron(II)(aq) from mine water discharges. *Appl. Geochem*. **2002**, 17, 431-443.
(28) Wehrli, B. Redox Reactions of Metal Ions at Mineral Surfaces, In: Aquatic Chemical Kinetics, W. Stumm, Ed., Wiley-Interscience, New York, 1990.
(29) Revie, R. Winston, ed. *Uhlig's corrosion handbook*. Vol. 51, John Wiley & Sons, 2011.
(30) https://www.metalsdepot.com/steel-products/steel-sheet. accessed on 5/9/2023
(31) https://www.eia.gov/totalenergy/data/monthly/pdf/sec9_11.pdf. accessed on 5/4/2023
(32) Juchniewicz, R.; Walaszkowski, J.; Bohdanowicz, W.; Sokolski, W.; Widuchowski, A. Influence of pulsed current on platinized titanium and tantalum durability. *Corrosion Science* **1986**, 26, 55-61.

Introduction – Field Test

The field test was conducted at the Paul Foster Central Tank Battery (CTB) in Lea County, New Mexico from November 10, 2022 through December 15, 2022. An aerial photograph of the site is shown in Figure 1, and the treatment equipment layout is shown in Figure 2. The Paul Foster CTB receives oil and produced water from multiple wells from multiple pay zones in Lea County. At the time of testing, the produced water was from the Tatanka 1H formation. However, during the testing period there was a pause in oil production, and thus there was a limited amount of produced water available. This water was contained in two 25,000 gallon tanks, labelled as tank #3 and #4 in Figure 3. The treated water and solids removed by the treatment system were pumped into tank #4, shown in Figure 3. The initial supply of produced water in tank #3 was exhausted after approximately two weeks of testing. After that time, water in tank #4 was pumped back to tank #3 to serve as the feed water to the treatment system. Because tank #4 contained both treated and untreated water, the suspended solids concentrations in the recycled feed water were greatly reduced compared to earlier dates.

Figure 1. Field test location off State Road 128 in Lea County, New Mexico.

Figure 2. Equipment set-up at field test site. Four clear wells are shown in foreground. Product water from the treatment system was collected in a 500 gallon polyethylene tank.

Figure 3. Tanks #3 & #4 contained the produced water that was treated. Treated water was pumped back into tank #4.

Because of the limited amount of produced water, the testing period was condensed to approximately 30 days. Secondary containment was installed prior to setting up the equipment, as shown in Figure 2. In order to take as much data as possible, the plan for one operator was amended to having two or three operators during the testing period. Samples were taken from 11 different collection points within the treatment system. Each experiment sampled only a subset of collection points. The water parameters tested on-site included: pH values, turbidity, iron, and chlorine concentrations. Pressures and flow rates were also recorded at six different points in the treatment system. Other data included current and voltage measurements, and photographs of water samples. Selected water samples were shipped back to the University of Arizona for additional analyses. On December 16, 2022, the treatment system was returned to the University of Arizona.

The purpose of the field test was to identify weak or failure points in the treatment system and to evaluate modifications to overcome the recognized problems. Therefore, issues of concern prior to the field test will be discussed first. A complicating factor in analyzing the field test data results from changing properties of the feed water to the system. Thus, data taken during different days may not be comparable. Issues associated with changing water properties will be mentioned where appropriate.

At the commencement of testing, the produced water contained high concentrations of suspended and colloidal solids, as shown in Figure 4. Comparison of Figures 4a and 4b shows that a significant fraction of the solids settled from the suspension after one hour. Figure 4c shows that colloidal particles remained suspended and contributed to a

significant amount of turbidity. Major ion concentrations and potential precipitates contained in the feed water at the start of the experiments are listed in Table 1.

Table 1. Major ion concentrations and dissolved minerals in feed water. An analysis of the Tatanka 1H water is included in Appendix 1.

Cations (mg/L)		Anions (mg/L)		Supersaturated Minerals	Carbonate Precipitation Potential lbs/1000 bbl
Na^{+}	37417	Cl^{-}	63102	Calcite ($CaCO_3$)	104.91
Ca^{2+}	2771	SO_4^{-}	1448	Aragonite ($CaCO_3$)	102.77
Mg^{2+}	367	CO_2	110.9	Strontianite ($SrCO_3$)	26.95
K^{+}	673	HCO_3^{-}	329.4	Magnesite ($MgCO_3$)	39.99
Sr^{2+}	191	H_2S	6.8	Siderite ($FeCO_3$)	3.18
Fe	4.6	B	45		

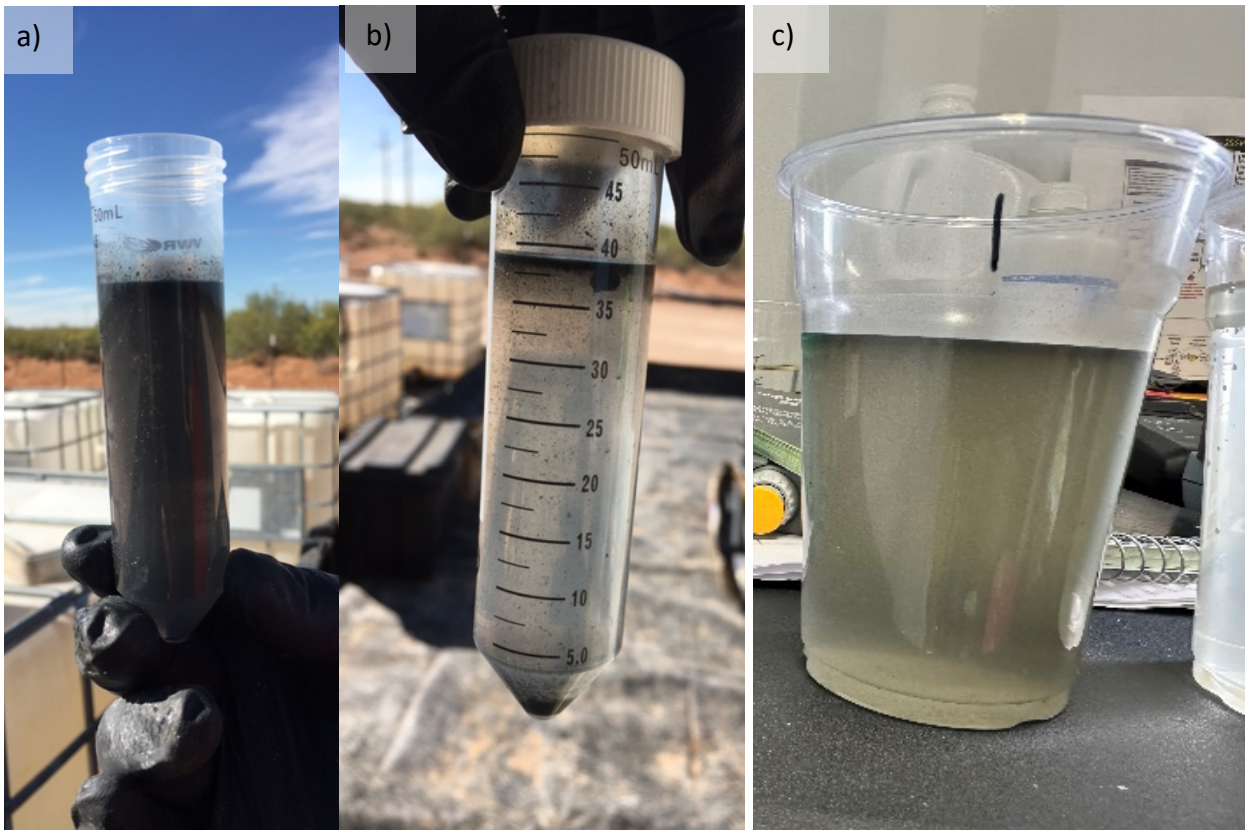

Figure 4. a) Water from tank #3 on November 10, 2022. b) Water from tank #3 on November 10, 2022 after approximately 1 hour settling period. c) Influent water to treatment system at sampling point 1 on November 15, 2022.

The data analysis will reference the simplified process flow diagram of the system in Figure 5. The process uses an electrochemical cell to make acid and base via water electrolysis. The acid is used to dissolve scrap iron to provide a coagulation agent for treating flowback and produced water (FPW). The acid stream containing dissolved Fe^{3+} is added to the feed water, which is then neutralized via addition of base. Neutralization of the stream results in precipitation of a ferric hydroxide coagulating agent that serves to coalesce small colloidal particles into larger particles that can be removed via dissolved air flotation (DAF). A media filter is used to remove any particulates not removed via the DAF process. Treated water with all particulates removed is used as the feed water for the electrochemical cell.

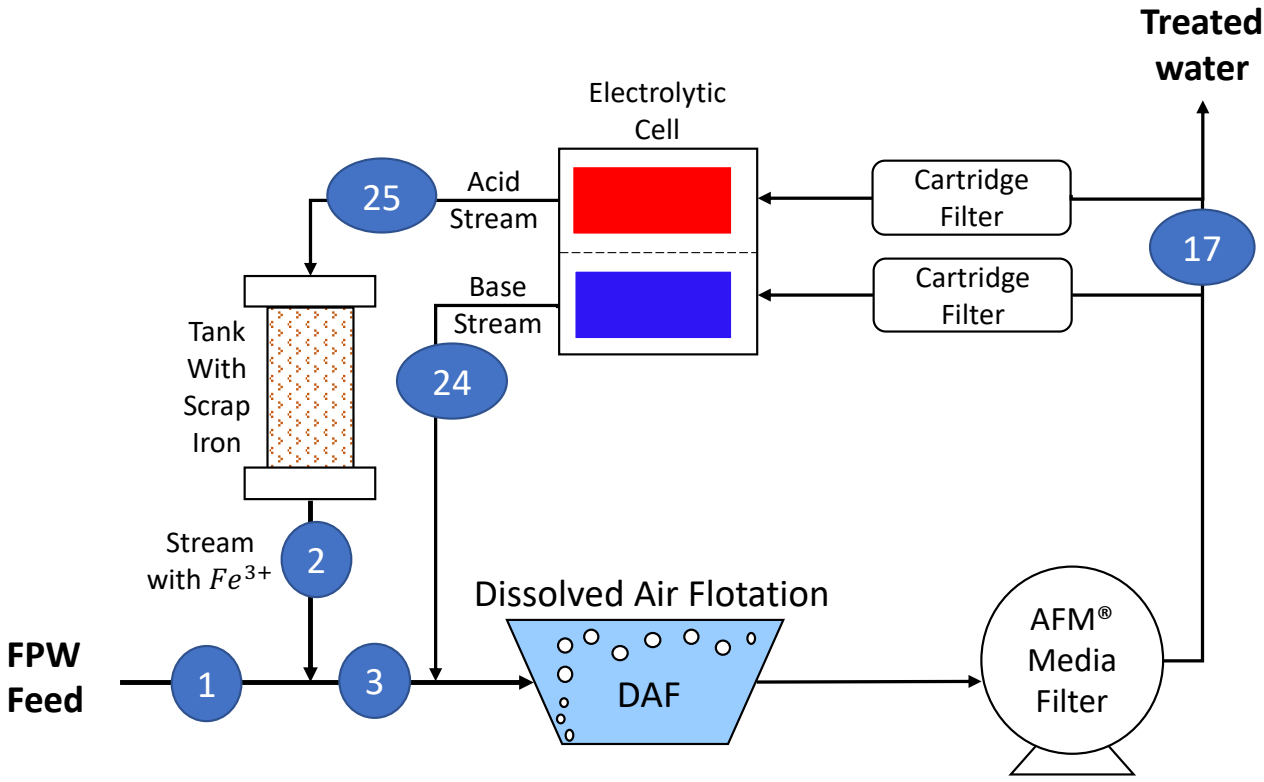

Figure 5. Simplified process flow diagram illustrating points where samples were taken. The line numbers correspond to those in the complete system process flow diagram. AFM® media is produced by the Dryden Aqua Corp.

Anticipated Problems

The two primary issues of concern prior to the field test were:

1. Mineral precipitation promoted by the high pH in the cathode chamber could foul the electrode and impede catholyte flow.

2. Acid consumption via reaction with bicarbonate may limit the amount of acid available for oxidizing the iron filings.

These issues will be addressed with supporting data below.

Electrode Fouling Issues

1. **Mineral precipitation promoted by the high pH in the cathode chamber could foul the electrode and impede catholyte flow.** This turned out not to be a problem since the plan of reversing the cell polarity every 0.5 hours was sufficient to obviate this concern.

The high precipitation potential for the carbonate minerals listed in Table 1 indicate that significant quantities of these minerals could form if bicarbonate (HCO_3^-) in the feed water was converted to carbonate (CO_3^{2-}). The cathode reaction produces hydroxide ions which raise the pH of the catholyte solution, as indicated by reaction 1. The hydroxide ions promote conversion of bicarbonate to carbonate, as indicated by reaction 2.

$$cathode\ reaction \quad 4\,H_2O + 4\,e^- \rightarrow 2\,H_2 + 4\,OH^- \tag{1}$$

$$carbonate\ production \quad OH^- + HCO_3^- \rightarrow CO_3^{2-} + H_2O \tag{2}$$

The carbonate ions may react with the divalent metal ions listed in Table 1 to form carbonate minerals. Mineral precipitation may occur on the cathode surface, on the ion exchange membrane, or in bulk solution.

The electrochemical cell was operated at anolyte feed rates of 4 and 10 gallons per minute (gpm). The catholyte flow rate was initially set so that there would be equivalent pressure drops across the anolyte and catholyte chambers of the electrochemical cell. The stoichiometry of the anode and cathode reactions results in twice as much hydrogen gas generation at the cathode than oxygen gas at the anode. Gas in the flow stream increases the pressure drop for water flow through the cell. Thus, in most experiments the catholyte flow rates were less than anolyte flow rates, and were allowed to vary without adjustment.

Figure 6 shows flow rates of the anolyte and catholyte solutions as a function of time for anolyte flow rates of 4 and 10 gpm. The decline in catholyte flow rates can be attributed to mineral precipitation in the cathode chamber. Catholyte compartment clogging was greater at higher currents and lower flow rates. However, this problem was solved by reversing polarity of the electrodes every half hour. Polarity reversal does not affect operation of the treatment system, since effluent from the electrochemical cell is connected to a stream switching valve that directs flows to their desired points in the system. Figure 7 shows the anolyte and catholyte flow rates as a function of time with polarity reversal. The initial catholyte flow rate of 2 gpm could be maintained indefinitely via polarity reversal every 0.5 hours. Cell voltages ranged from 5.8 to 6.9 V over the 4.5-hour period of operation.

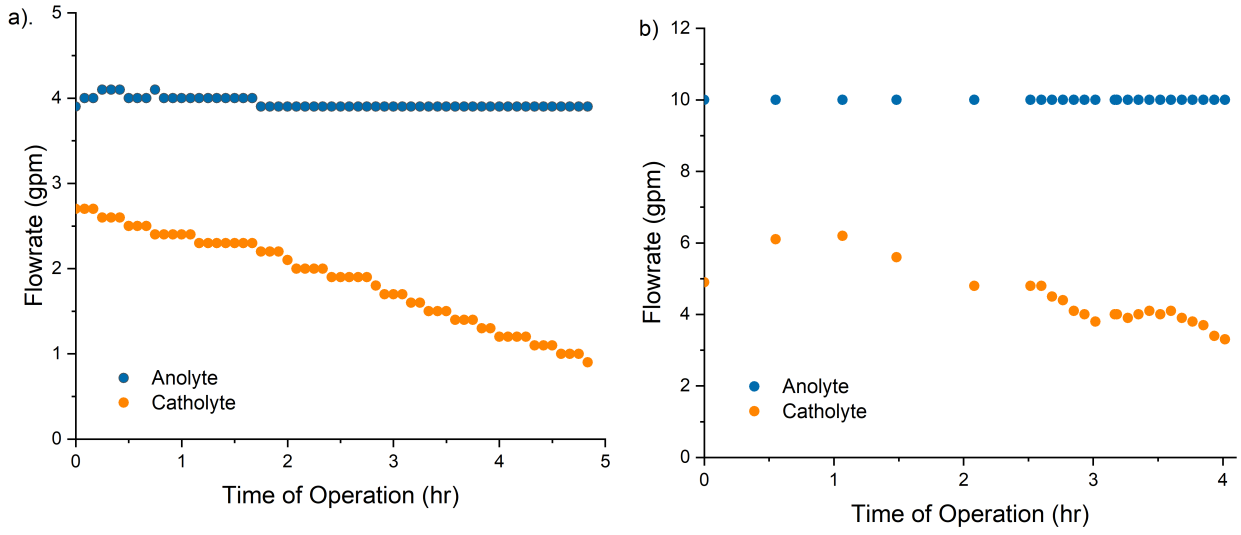

Figure 6. a) Decline in catholyte flow rate at a current 236 A (23.6 mA/cm^2) and anolyte flow rate of 4 gpm. b) Catholyte flow rates at a current of 500 A (50 mA/cm^2) and anolyte flow rate of 10 gpm.

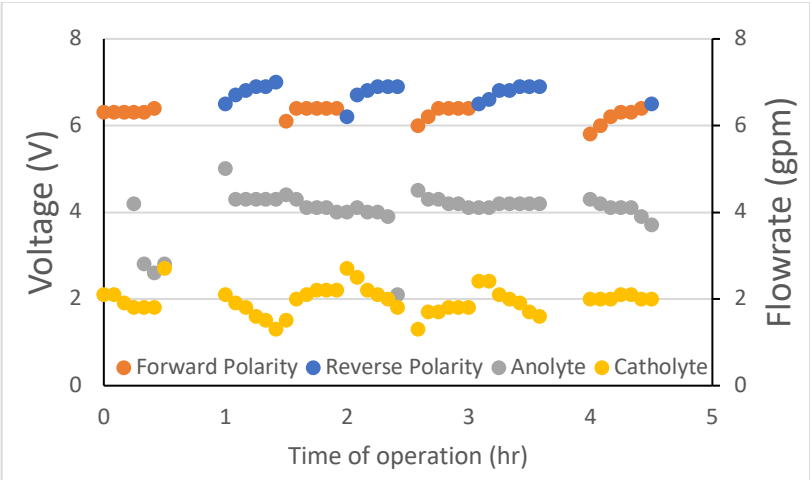

Figure 7. Catholyte and anolyte flow rates versus time under forward and reverse polarity at a current of 965 A (96.5 mA/cm^2). Also shown are the cell voltages as a function of time.

Alkalinity Issues

2. **Acid consumption via reaction with bicarbonate may limit the amount of acid available for oxidizing the scrap iron.** This turned out to be a problem, but we believe that this problem can be solved by a change in system design.

The hydrogen ions (H^+) ions produced by the anode reactions can react with bicarbonate (HCO_3^-) to produce carbonic acid (H_2CO_3), as shown in reactions 3 and 4.

$$anode\ reaction \qquad 2\ H_2O \rightarrow O_2 + 4\ H^+ + 4\ e^- \tag{3}$$

$$carbonic\ acid\ generation \qquad H^+ + HCO_3^- \rightarrow\ H_2CO_3 \tag{4}$$

The reaction of H^+ with bicarbonate serves to buffer the anolyte pH value and produces a weak acid that is less reactive for oxidizing the scrap iron. Thus, dissolved carbonate in the feed water decreased the amount of acid available for iron corrosion. Using Faraday's law, the measured cell current and flow rate were used to calculate the hypothetical anolyte pH value in the absence of buffering. Figure 8 compares the measured anolyte pH values in line 25 with theoretical pH values in the absence of buffering and unit activity coefficients. This comparison shows that more than 99% of the acid was consumed via reaction with bicarbonate.

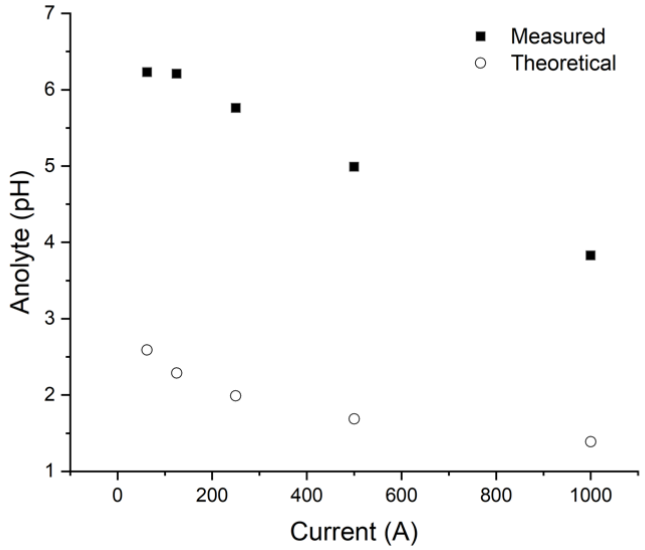

Figure 8. Measured anolyte pH values in line 25 versus theoretical values with no buffering and unit activity coefficients calculated using Faraday's law. Data measured on 11/20/22.

Figure 9 shows anolyte pH values in line 25 going into the scrap iron tank. Also shown are the dissolved iron concentrations in the effluent from the iron tank in line 2. The pH values in the iron tank effluent were close to neutral (pH=7±0.5). Data in Figure 9 shows that dissolved iron concentrations were approximately 1 ± 0.5 mM. Thus, consumption of hydrogen ions in the iron tank was less than that required to produce the observed amounts of dissolved iron. If all iron oxidation were due to reaction with H^+, the stoichiometry in reaction 5 indicates that a change in acid concentration of at least 2 mM is needed to produce a dissolved iron concentration of 1 mM. The 4 gpm data in Figure 9 indicates that hydrogen ion consumption ranged from approximately 0.001 mM to 0.1 mM. This indicates that other oxidants were involved in iron oxidation. In addition to hydrogen ions, the anode also produces oxygen gas (reaction 3) and hypochlorous acid (HOCl), as shown by reactions 6 and 7. Both oxygen and HOCl can oxidize the iron filings.

$$iron\ dissolution\ reaction \quad 2\,H^+ + Fe \rightarrow Fe^{2+} + H_2 \tag{5}$$

$$minor\ anode\ reaction \quad 2Cl^- \rightarrow Cl_{2(aq)} + 2e^- \tag{6}$$

$$chlorine\ hydrolysis \quad Cl_{2(aq)} + H_2O_{(l)} \rightarrow HOCl_{(aq)} + H^+{}_{(aq)} + Cl^-_{(aq)} \tag{7}$$

The dissolved chlorine concentrations in the anolyte solution (line 25) as a function of current density are shown in Figure 10. Effluent chlorine concentrations in line 2 exiting the iron tank were not measured for these experiments. However, in other experiments, 87% to 93% of the chlorine reacted with the iron filings, as shown in Figure 11. Thus, except for the data at 1000 A, the consumption of chlorine and H^+ in the iron tank was too low to explain the dissolved iron concentrations in Figure 9. This indicates oxygen was the primary oxidant for corrosion of the scrap iron at low currents. Using Faraday's law

and the measured currents and flow rates, the concentration of oxygen available to dissolve in the solution was calculated. The available oxygen ranged from 10 to 155 millimoles per liter of anolyte solution for currents ranging from 62.5 to 1000 A. Although not all of this oxygen will dissolve in the solution, it is much more than enough for producing the observed iron concentrations in Figure 9. The dissolved iron concentrations in Figure 9 were nearly independent of the feed solution pH value, chlorine concentration, and oxygen content. Thus, the iron concentrations exiting the contact tank were not significantly dependent on the oxidant concentrations going into the tank. This suggests that there was precipitation of ferric hydroxide in the tank, and the measured dissolved iron concentrations of 1 ± 0.5 mM were likely representative of the solubility of iron in the water.

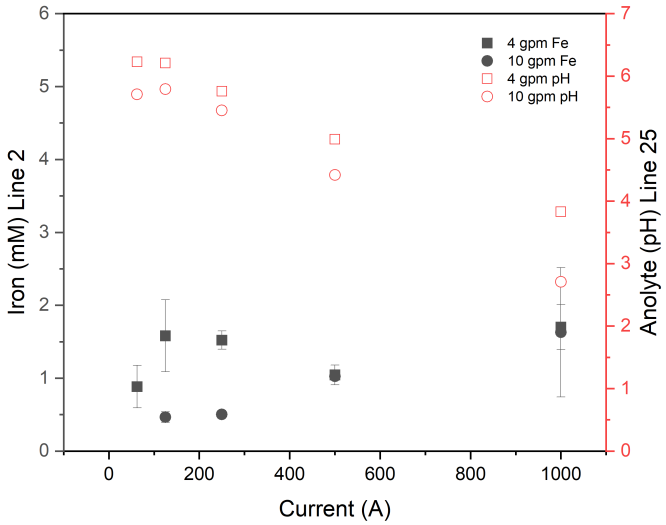

Figure 9. Dissolved iron in line 2 exiting the scrap iron tank. Also shown are the influent pH values to the scrap iron tank (line 25). Effluent pH values from the iron tank were near neutral . Data at 4 gpm measured on 11/20/22. Data at 10 gpm measured on 11/25/22.

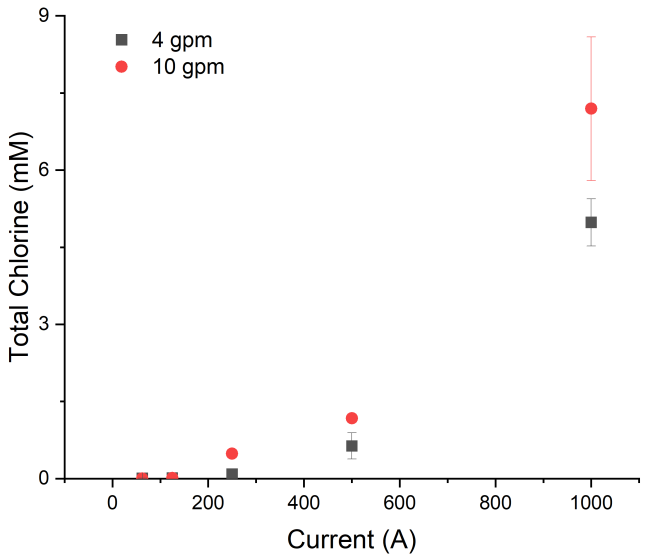

Figure 10. Chlorine concentrations in the anolyte solution fed into the scrap iron tank via line 25. The total chlorine consists primarily of HOCl, but for pH values less than 3, Cl_2 is the predominant species.

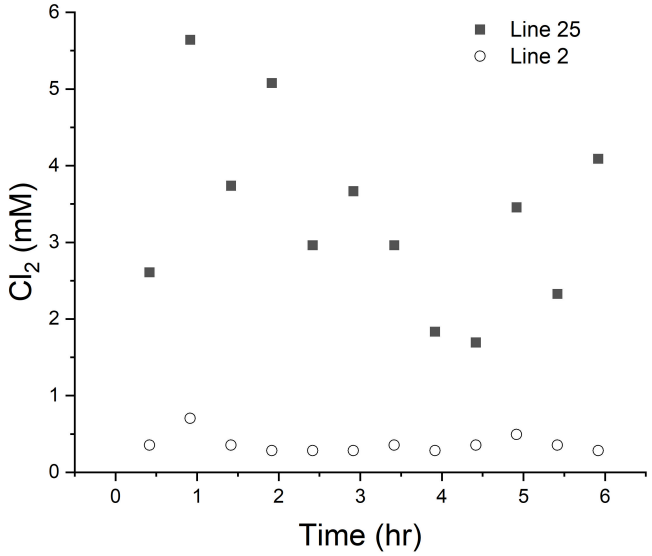

Figure 11. Chlorine concentrations entering the scrap iron tank via line 25 and exiting the iron tank in line 2. Electrochemical cell was operated at 1000 A and 4 gpm.

Turbidity Removal

Precipitation of ferric hydroxide in the scrap iron tank resulted in significant removal of turbidity. Figure 12 shows that the turbidity in line 2 could be reduced to values below 1 NTU. As shown by the photograph in Figure 13, line 2 was essentially free of particulate

matter. However, the low amount of dissolved iron in line 2 was insufficient for removing turbidity after line 2 was combined with the influent water (line 1) to form line 3. When the iron containing line 2 (4 gpm) was combined with the influent water from line 1 (15 gpm) and the catholyte stream in line 24 (4 gpm), the Fe^{3+} concentrations were diluted by a factor of approximately 6. Thus, there was less than 0.25 mM of Fe^{3+} available for coagulating the suspended solids in the feed water. This resulted in only a small amount of turbidity removal in other parts of the system. Figures 12, 13 and 14 show that the final turbidity of the treated water in line 17 was significantly higher than that in line 2.

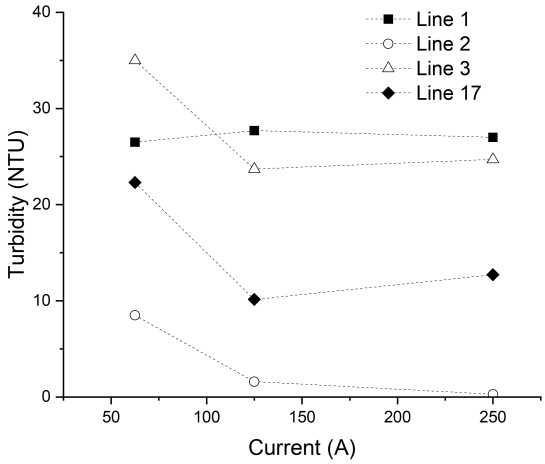

Figure 12. Turbidity values measured at different points in the treatment system on 11/23/22.

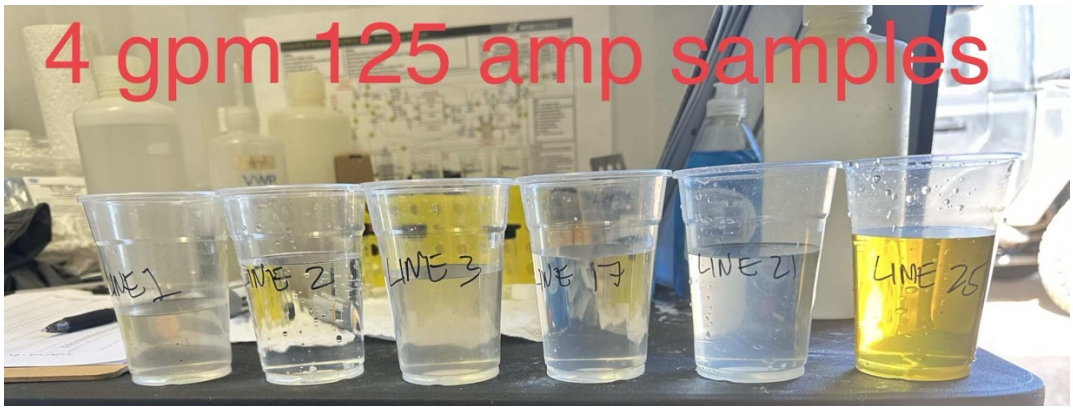

Figure 13. Photographs of water samples taken 11/23/22 corresponding to the data in Figure 12.

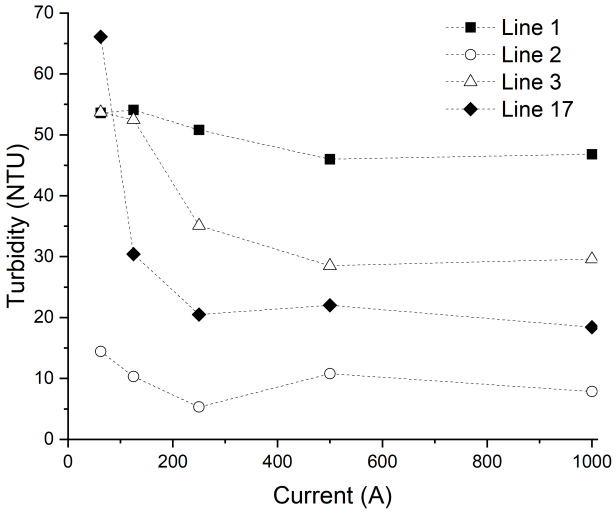

Figure 14. Turbidity values measured at different points in the treatment system on 11/24/22 and 11/25/22.

We speculate that the turbidity removal in line 2 was due to coagulation/flocculation with ferric hydroxide, and not due to filtration by the scrap iron media. The iron media used in the field test consisted of ferrous metal machine shop turnings, as shown in Figure 15. The irregular shape of the media resulted in a void fraction in the scrap iron tank of 93%. The large particle size and high void fraction of the media would not be an effective filter for uncoagulated colloidal particles. Figures 12-14 can be used to compare turbidity removal in the scrap iron tank to turbidity removal by the combination of dissolved air flotation and AFM media filtration. The AFM media consisted of fine crushed glass particles with a void fraction of less than 40%, and is shown in Figure 16. Thus, for a filtration removal mechanism, the AFM media should provide more turbidity removal than the iron tank. However, the turbidity of the water coming out of the iron tank in line 2 was always significantly lower than the treated water turbidity in line 17, as shown in Figures 12-14. In addition, the color removal from line 25 in the iron tank indicates a coagulation/flocculation mechanism, as opposed a simple filtration removal mechanism.

Figure 15. Ferrous machine shop turnings used in the scrap iron tank.

Figure 16. AFM® filtration media used after the dissolved air flotation process.

Effect of Water Recycling

The use of recycled water solved the problem of the alkalinity neutralizing most of the electrochemically generated acid. Figure 17 shows pH values in different parts of the system using recycled water on December 8, 2022. Although the alkalinity was not measured, its effect can be assessed by the pH values in the anolyte solution exiting the electrochemical cell. Anolyte pH values as low as 1.5 could be reached at a current of 500 A using recycled water. In contrast, the lowest anolyte pH value using untreated water at 500 A was 4.3 (Figure 9).

Table 2 shows anolyte pH values for the system operating at 500 and 1000 A at a flow rate of approximately 4 gpm. In the high alkalinity water at the commencement of the field test, anolyte pH values ranged from 4.8 to 3.8 over the current range 500 to 1000 A. This resulted in iron tank effluent pH values in the range of 6.5-7.5, and dissolved iron concentrations of 1 ± 0.5 mM, as shown in Table 2. Treatment of the water reduced the alkalinity via precipitation of carbonate minerals. Thus, in recycled water, anolyte pH values of 1.5 to 2.3 and dissolved iron concentrations of 8-9 mM could be achieved on December 8, 2022 at a current of 500 A. At a current of 1000 A on December 10, 2022, anolyte pH values ranging from 1.3 to 1.6 could be achieved, as shown in Table 2. This resulted in pH values near 2 in the iron tank effluent and dissolved iron concentrations of 20-24 mM, as shown in Figure 18.

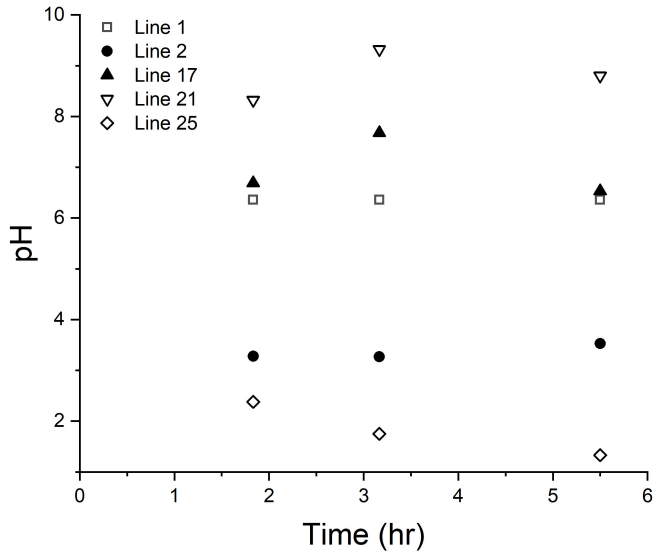

Figure 17. Solution pH values at different points in the system at a current of 580 A on December 8. Line 25 shows pH values entering the iron contact tank, and line 2 shows effluent pH values.

Table 2. Effect of feed solution alkalinity on anolyte pH values at currents of 500 to 1000 A. Also shown are pH values and dissolved iron concentrations in the effluent solutions from the iron contact tank.

alkalinity	anolyte pH	iron tank effluent pH	dissolved Fe (mM)
high (5.4 meq/L)	3.8-4.8	6.5-7.5	1±0.5
medium (recycled)	1.5-2.3	3.3-3.5	8-9
low (recycled)	1.3-1.6	2.04-2.08	20-24

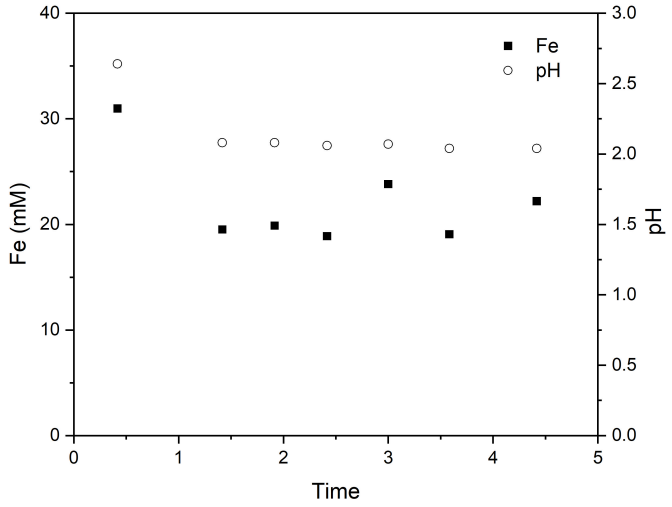

Figure 18. Dissolved iron concentrations and pH in the effluent stream from the scrap iron tank. The influent to the iron tank had pH values ranging from 1.43 to 1.59. Data taken after system start-up at 30 minutes elapsed are not representative of steady state values.

Unanticipated Problems

Cartridge Filter Clogging

The system was designed to pass treated water containing little to no particulate matter through the electrochemical cell. However, incomplete particulate removal by the treatment system resulted in particulate concentrations in the treated water that were sufficient to clog the cartridge filters feeding the electrochemical after a few hours of

operation. Figure 19 shows cartridge filters clogged with black and brown solids. This problem subsided when recycled water was used to run the experiments, since most of the particulates were removed during the first pass through the treatment system.

Figure 19. Clogged cartridge filters on November 19, 2022. Cartridge filters prevent particulates from entering the electrochemical cell.

Hydrogenation of Unsaturated Hydrocarbons

Platinized titanium cathodes may promote hydrogenation of unsaturated hydrocarbons. Reduction of hydrogen ions on platinum produces adsorbed atomic hydrogen (H^*) on the cathode surface, according to:

$$cathode\ reaction\ \ Pt + H^+ + e^- \rightarrow Pt - H^* \quad (6)$$

The adsorbed atomic hydrogen can react with double bonds in dissolved hydrocarbons and convert them to single bonds, according to:

$$2\,Pt - H^* + R - CH = CH - R \;\rightarrow\; R - CH_2 - CH_2 - R + 2\,Pt \qquad (7)$$

Alkanes produced by these reactions are less water soluble than the corresponding alkenes. This resulted in precipitation of paraffinic hydrocarbons, that congealed and floated to the surface of the water. Figure 20 shows wax-like substances floating on top of the water in the clear-wells prior to media filtration. Although the hydrogenation reactions occur in the electrochemical cell, it takes several minutes for the precipitated hydrocarbons to congeal into the solids shown in Figure 20.

Figure 20. Congealed hydrocarbons floating in clear wells on November 15, 2022.

Proposed System Modifications

The main problem with the system is that high concentrations of bicarbonate in the feed water resulted in effluent pH values from the iron tank that were too high to dissolve sufficient Fe^{3+} into the feed water stream. Treatment system performance could be improved by reducing the system alkalinity and passing all the water through the scrap iron tank. A process flow diagram of an improved treatment system is shown in Figure 21 and contains the elements described below.

1. **Aeration** - Produced water is anaerobic and usually contains toxic gases, such as H_2S. Aeration of the water can strip out the H_2S and provide an oxidant for corroding the scrap iron. Thus, the first element in the modified system is aeration using a venturi tube.

2. **Fluidized bed crystallization** - The liquid/air mixture is then added to a fluidized bed crystallization reactor (FBCR) to precipitate carbonate mineral solids and thereby reduce the alkalinity. The pH of the water is raised to ~10.5 via addition of a cathodically generated base stream. The carbonate minerals then precipitate on seed crystals in the reactor. A significant fraction of the paraffinic hydrocarbons will likely be removed via adsorption to the mineral solids. The precipitated mineral solids will grow over time and be periodically purged from the bottom of the reactor when they reach diameters greater than 1 mm. Solids of this size are easily dewatered via gravity drainage. Fluidized bed crystallization is a commercialized process used extensively in mineral processing and municipal water treatment.

3. **Reactive filtration/coagulation** – The water exiting the FBCR will then be passed through a canister containing scrap iron, such as the machine shop turnings used in the field test. The pH of the water entering the scrap iron tank will be lowered by addition of anodically generated acid. The anodically generated acid will also contain HOCl and oxygen that will act as oxidants for iron corrosion. If necessary, effluent from the iron canister can be neutralized using cathodically generated base. If the solution pH exiting the scrap iron tank is above 3-4, some of the corroded iron may precipitate from solution and be filtered by the iron media — as was the case in the field test. Under all operating conditions, effluent from the iron canister was free of particulates. This indicates that passing water through the iron contact tank was sufficient to remove particulates. The removal mechanism is likely coagulation/flocculation combined with filtration of the flocculated solids. The iron contact tank had a high void fraction (93%), and thus clogging of the media should not be a problem until a considerable amount of the iron has formed coagulated solids. Periodically, the iron contact tank could be backwashed with a concentrated, anodically generated, acid solution to dissolve the precipitates and produce a low volume, highly concentrated stream of solids. Neutralization of the concentrated stream would precipitate the ferric hydroxide and thereby coagulate the removed solids.

4. **Dissolved air flotation** – Dissolved Fe^{3+} and particulates exiting the scrap iron tank can be flocculated and separated from the treated water using dissolved air flotation. This is the same process used by the original treatment system.

5. **Electrochemical acid and base generation** – An electrochemical cell similar to the one used in this investigation will be used to generate acid and base. The feed to the cell is treated water where the particulates and most of the bicarbonate have been removed.

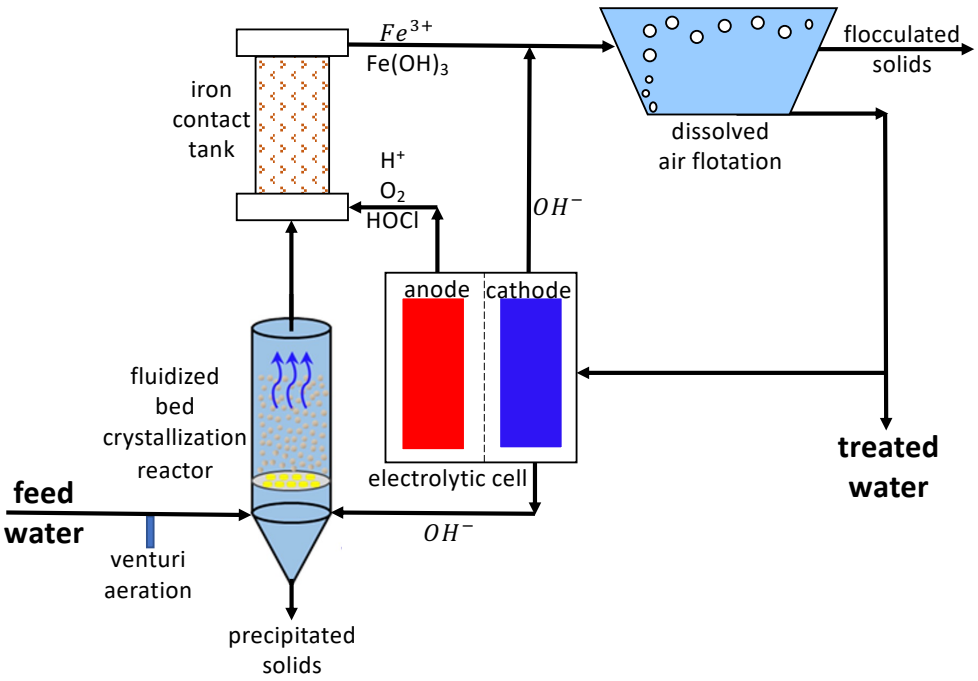

Figure 21. Process flow diagram for revised treatment system.

With the proposed system modifications, the pH values of solutions entering the iron contact tank are likely to be near neutral. Thus, the major oxidants for iron corrosion will be oxygen and HOCl. The effectiveness of these two oxidants for providing sufficient iron corrosion for coagulation/flocculation purposes was investigated in laboratory experiments, as described below.

Laboratory Experiments Investigating System Design Changes

Materials and Methods

Column Experiments

Experiments measuring removal of colloidal FeS particles were performed in a 60 cm long by 2.5 cm internal diameter PVC column packed with the ferrous machine shop turnings used in the field test. A schematic diagram of the experimental set-up is illustrated in Figure 22. FeS particles were used since the majority of particulates in the field test consisted of FeS. The bulk density of the column packing was 0.81 g/mL, which corresponds to a void fraction of 90%. The feed solution was at a pH value of 7.6, and was purged with air in order to achieve a dissolved oxygen concentration of 8 mg/L. The NaCl and bicarbonate concentrations in the feed solution were similar to those from the field test. The packed column contained no water at the start of the experiment and the suspension of colloidal FeS was fed into the bottom of the column at a flow rate of 21.5 mL/min, resulting in an empty bed contact time (EBCT) of 15 minutes. The turbidity of influent and effluent samples were measured over an eight hour period using a turbidity meter.

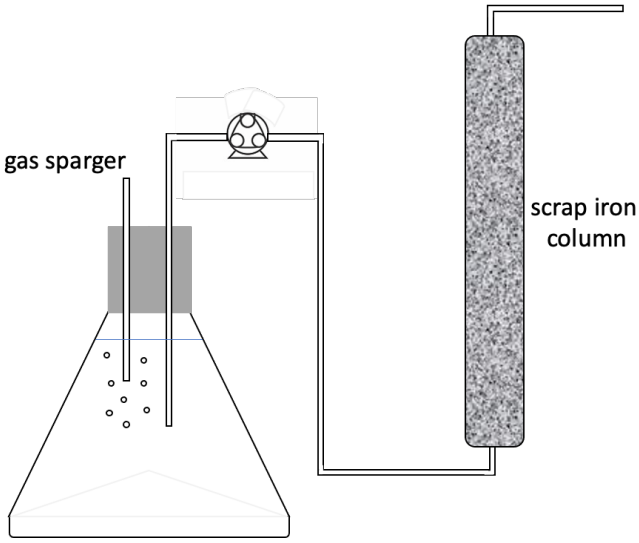

Figure 22. Schematic diagram of column experiment measuring removal of colloidal FeS .

Iron Corrosion Experiments

The effects of dissolved oxygen concentrations and solution pH values on iron corrosion rates were investigated using Tafel analysis. These experiments employed 4 cm long by 2 mm diameter iron wires (Aesar), a Ag/AgCl reference electrode, and a platinum mesh counter electrode. The measurements were performed in a stirred glass corrosion cell purged with N_2, air or O_2 gases, as illustrated in Figure 23. Linear sweep voltammetry scans were performed ±200 mV with respect to the open circuit potential. Duplicate or triplicate measurements were made for each set of experimental conditions.

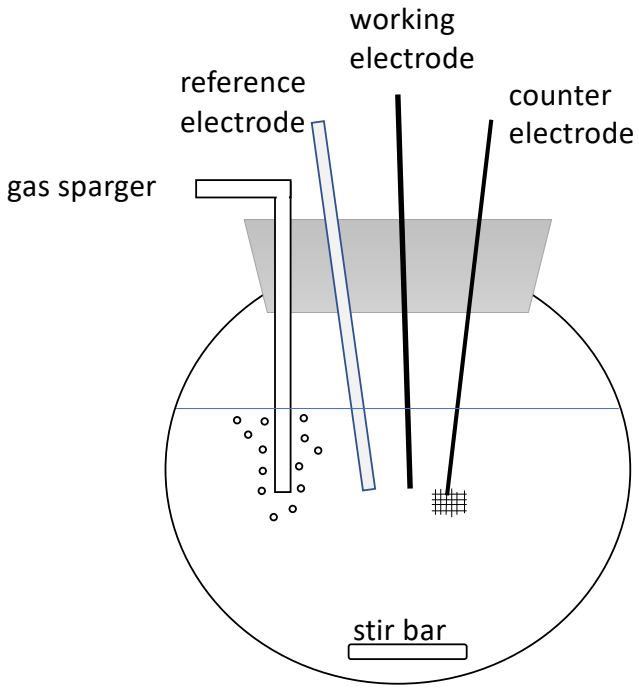

Figure 23. Schematic diagram of cell used for iron wire corrosion rate experiments.

Results and Discussion

Column Experiments

The column experiments were performed to determine if a circumneutral solution containing 8 mg/L of dissolved oxygen could promote iron corrosion rates sufficiently high to remove FeS colloids from the feed water. The feed water to the column is shown in

Figure 24a and Figure 24b shows the turbidity values of the effluent water over an eight hour period. The first effluent sample at 0.5 hours was taken after passage of two empty bed volumes of feed solution were passed through the column. The turbidity of this sample of 159 NTU indicates that only a small amount of the initial turbidity of 173 NTU had been removed. The small amount of turbidity removal can be attributed to a time lag for initiation of iron corrosion. The low turbidity removal after two empty bed volumes indicates that filtration contributes, at most, only a small amount to turbidity removal. Increasing iron corrosion with elapsed time resulted in increasing turbidity removal. By three hours elapsed, the effluent turbidity had been reduced to less than 4 NTU, which is below the recommendation of < 10 NTU for the use of produced water in hydraulic fracturing. By eight hours elapsed, the effluent turbidity had been reduced to ≤ 0.22 NTU, which is equivalent to > 99.8% turbidity removal. Continuous, long-term experiments are needed to validate this concept.

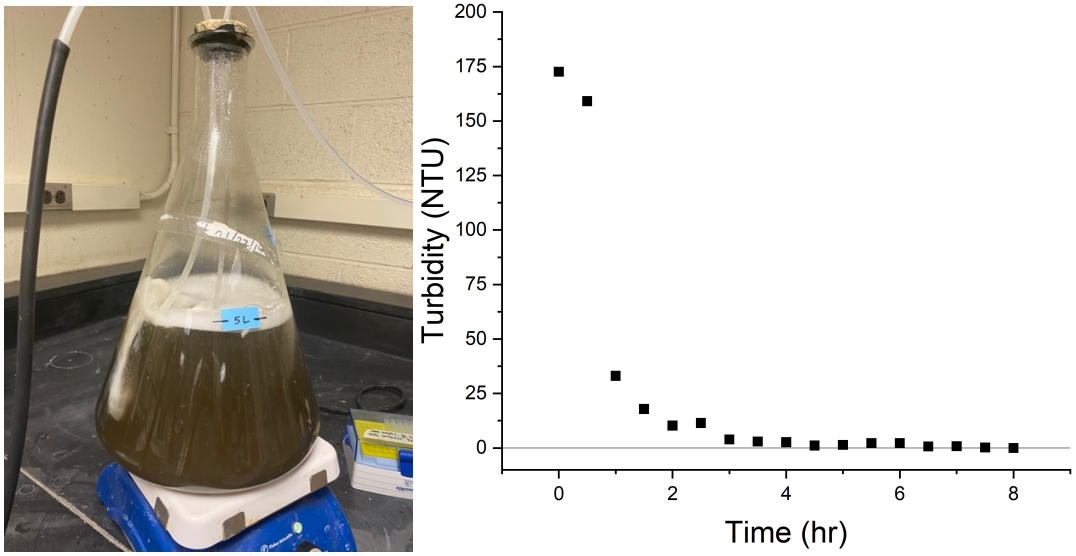

Figure 24. a) Feed water containing colloidal FeS with a turbidity of 173 NTU. b) Effluent turbidity from column of scrap iron operated at an EBCT of 15 minutes.

The high void fraction of the column (90%) would allow large volumes of water to be treated before any clogging problems would likely occur —even if all the corrosion products remained in the column. The 33 mL of iron (density= 7.88 g/mL) in the column would occupy a volume of 230 mL if it were all converted to hydrous ferric hydroxide (density=1.8 g/mL). The column would then still have a void fraction of 29%, which is typical of packed-bed media used in water treatment operations. Although the removed particulates would also fill the void space in the column, it would take 9787 bed volumes of 500 mg/L FeS particles to fill the 323 mL of column volume.

Iron Corrosion Experiments

The effect of dissolved oxygen concentration on iron corrosion rates was investigated in 0.5 M NaCl solutions at a pH value of 7. Figure 25a shows the current density (i) versus potential with respect to the standard hydrogen electrode (E/SHE) for an iron wire in water with dissolved oxygen concentrations of 0, 8 and 38 mg/L, corresponding to solutions purged with nitrogen, air and oxygen gases. The similar anodic current densities at potentials greater than -0.1 V indicates that the dissolved oxygen concentration had only a small effect on the anodic reaction for iron corrosion, which is:

$$Fe \rightarrow Fe^{2+} + 2\,e^{-} \quad (8)$$

The dissolved oxygen concentration had a marked effect on the cathodic reactions. The different slope for the cathodic branch of the nitrogen purged solution compared to those purged with air and O_2 indicate different cathodic reactions. For the nitrogen purged solution, the predominant cathodic reaction was reduction of hydrogen ions:

$$2H^{+} + 2e^{-} \rightarrow H_2 \quad (9)$$

For the solutions purged with air and O_2, the predominant cathodic reaction was:

$$O_2 + 4\,H^+ + 4e^- \rightarrow 2\,H_2O \qquad (10)$$

Figure 25b shows the free corrosion current densities and free corrosion potentials calculated from the polarization plots in Figure 25a. Water in equilibrium with air had a factor of 54 times greater corrosion current density as the anaerobic solution purged with N_2. Purging the solution with oxygen gas at a pressure of 1 atmosphere increased the corrosion rate by a factor of 113 over the anaerobic solution.

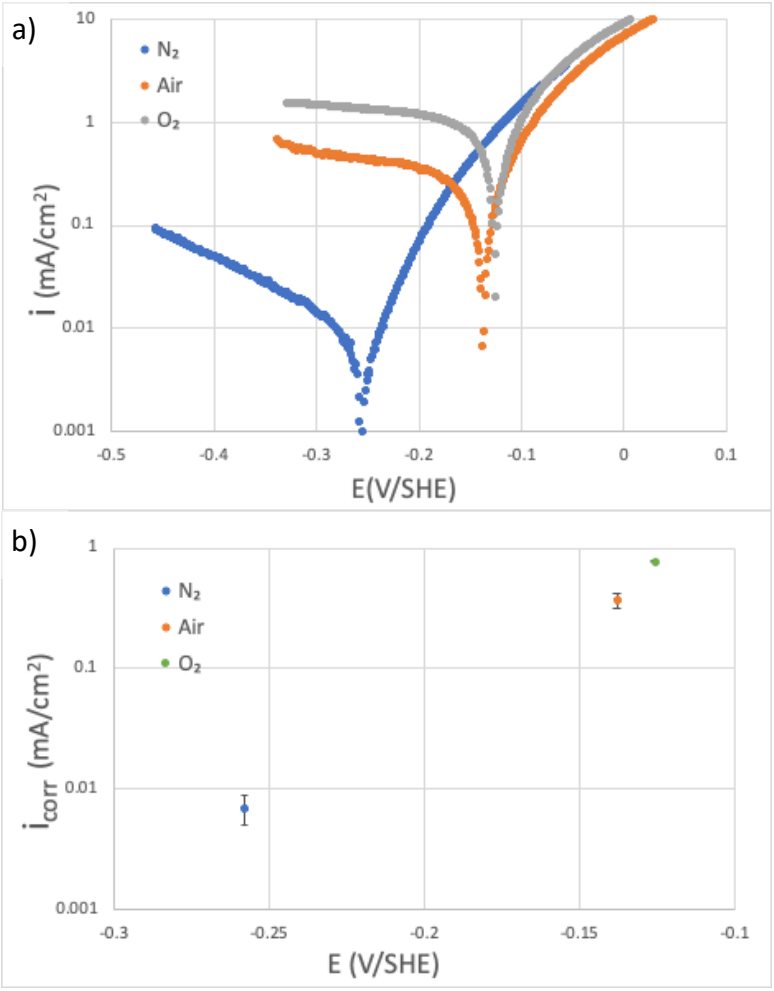

Figure 25. a) Current density (i) versus potential (E) for iron wires in solutions purged with N_2, air and O_2 gases. b) Corrosion current density (i_{corr}) versus free corrosion potential (E) calculated from Tafel analyses of the polarization plots.

The effect of solution pH value on iron corrosion rates was investigated in air and nitrogen purged solutions. Figure 26a shows polarization plots in air purged solutions over the pH range 1 to 7. Decreasing the solution pH from 7 to 3 resulted in gradual increases corrosion currents, as shown in Figure 26b. However, a large increase in the currents occurred when the pH was reduced to 2. This indicates there is only a small advantage in lowering the pH to 3 when trying to maximize iron corrosion rates. Comparison of corrosion rates in nitrogen and air purged solutions in Figure 26b shows that the increase in corrosion rates by lowering the pH from 7 to 3 was smaller than the increase resulting from aeration of the solution.

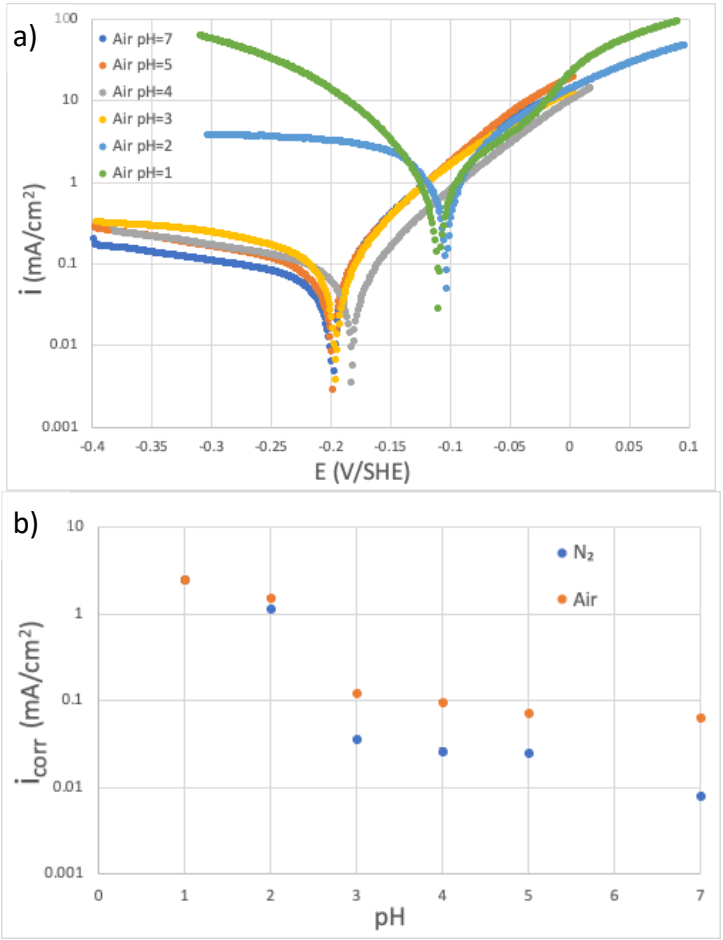

Figure 26. a) Polarization plots for iron wire in 0.5 M NaCl air purged solutions over the pH range 1 to 7. b) Comparison of corrosion current densities in air and N_2 purged solutions.

The column test results and the corrosion rate measurements indicate that it may be possible to treat flowback and produced water via passage through a packed bed of machine shop turnings without the use of an electrochemical cell to lower the pH of the feed water.

Data Tables for Field Test Section

Data for Figure 6a.

Time of Operation hr	Anolyte Flowrate gpm	Catholyte Flowrate gpm
0.00	3.9	2.7
0.08	4	2.7
0.17	4	2.7
0.25	4.1	2.6
0.33	4.1	2.6
0.42	4.1	2.6
0.50	4	2.5
0.58	4	2.5
0.67	4	2.5
0.75	4.1	2.4
0.83	4	2.4
0.92	4	2.4
1.00	4	2.4
1.08	4	2.4
1.17	4	2.3
1.25	4	2.3
1.33	4	2.3
1.42	4	2.3
1.50	4	2.3
1.58	4	2.3
1.67	4	2.3
1.75	3.9	2.2
1.83	3.9	2.2
1.92	3.9	2.2
2.00	3.9	2.1
2.08	3.9	2.0
2.17	3.9	2.0
2.25	3.9	2.0
2.33	3.9	2.0
2.42	3.9	1.9
2.50	3.9	1.9
2.58	3.9	1.9
2.67	3.9	1.9
2.75	3.9	1.9
2.83	3.9	1.8
2.92	3.9	1.7
3.00	3.9	1.7
3.08	3.9	1.7
3.17	3.9	1.6
3.25	3.9	1.6

3.33	3.9	1.5
3.42	3.9	1.5
3.50	3.9	1.5
3.58	3.9	1.4
3.67	3.9	1.4
3.75	3.9	1.4
3.83	3.9	1.3
3.92	3.9	1.3
4.00	3.9	1.2
4.08	3.9	1.2
4.17	3.9	1.2
4.25	3.9	1.2
4.33	3.9	1.1
4.42	3.9	1.1
4.50	3.9	1.1
4.58	3.9	1.0
4.67	3.9	1.0
4.75	3.9	1.0
4.83	3.9	0.9

Data for Figure 6b.

Time of Operation hr	Anolyte Flowrate gpm	Catholyte Flowrate gpm
0.00	10	4.9
0.55	10	6.1
1.07	10	6.2
1.48	10	5.6
2.08	10	4.8
2.52	10	4.8
2.60	10	4.8
2.68	10	4.5
2.77	10	4.4
2.85	10	4.1
2.93	10	4.0
3.02	10	3.8
3.17	10	4.0
3.18	10	4.0
3.27	10	3.9
3.35	10	4.0
3.43	10	4.1
3.52	10	4.0
3.60	10	4.1
3.68	10	3.9
3.77	10	3.8
3.85	10	3.7

3.93	10	3.4
4.02	10	3.3

Data for Figure 7.

Time	Forward Polarity	Anolyte	Reverse Polarity	Catholyte
hr	V	gpm	V	gpm
0	6.3	6.3		2.1
0.08	6.3	6.3		2.1
0.17	6.3	5.9		1.9
0.25	6.3	4.2		1.8
0.33	6.3	2.8		1.8
0.42	6.4	2.6		1.8
0.50		2.8		2.7
1.00		5.0	6.5	2.1
1.08		4.3	6.7	1.9
1.17		4.3	6.8	1.8
1.25		4.3	6.9	1.6
1.33		4.3	6.9	1.5
1.42		4.3	7.0	1.3
1.50	6.1	4.4		1.5
1.58	6.4	4.3		2.0
1.67	6.4	4.1		2.1
1.75	6.4	4.1		2.2
1.83	6.4	4.1		2.2
1.92	6.4	4.0		2.2
2.00		4.0	6.2	2.7
2.08		4.1	6.7	2.5
2.17		4.0	6.8	2.2
2.25		4.0	6.9	2.1
2.33		3.9	6.9	2.0
2.42		2.1	6.9	1.8
2.58	6.0	4.5		1.3
2.67	6.2	4.3		1.7
2.75	6.4	4.3		1.7
2.83	6.4	4.2		1.8
2.92	6.4	4.2		1.8
3.00	6.4	4.1		1.8
3.08		4.1	6.5	2.4
3.17		4.1	6.6	2.4
3.25		4.2	6.8	2.1
3.33		4.2	6.8	2.0
3.42		4.2	6.9	1.9
3.50		4.2	6.9	1.7
3.58		4.2	6.9	1.6

4.00	5.8	4.3		2.0
4.08	6.0	4.2		2.0
4.17	6.2	4.1		2.0
4.25	6.3	4.1		2.1
4.33	6.3	4.1		2.1
4.42	6.4	3.9		2.0
4.50		3.7	6.5	2.0

Data for Figure 8

Current A	Measured pH	Theoretical pH
62.5	6.23	2.59
125	6.21	2.29
250	5.76	1.99
500	4.99	1.69
1000	3.83	1.39

Data for Figure 9.

Current A	4 gpm Fe mM	Error ±	4 gpm pH	10 gpm Fe mM	Error ±	10 gpm pH
62.5	0.88	0.29	6.23			5.71
125	1.58	0.49	6.21	0.48	0.072	5.79
250	1.52	0.13	5.76	0.50	0.036	5.45
500	1.04	0.14	4.99	1.02	0.055	4.42
1000	1.70	0.31	3.83	1.63	0.89	2.71

Data for Figure 10.

Current A	4 gpm mM	Error ±	10 gpm	Error ±
62.5	0.0083	0.00102	0	0
125	0.013	0.0009	0.014	0.0029
250	0.087	0.030	0.49	0.010
500	0.63	0.25	1.2	0.060
1000	5.0	0.46	7.2	1.4

Data for Figure 11.

Time hr	Line 25 mM Cl_2	Line 2 mM Cl_2
0.42	2.6	0.35
0.92	5.6	0.71
1.42	3.7	0.35
1.92	5.1	0.28
2.42	3.0	0.28
2.92	3.7	0.28
3.42	3.0	0.35
3.92	1.8	0.28
4.42	1.7	0.36
4.92	3.5	0.50
5.42	2.3	0.35
5.92	4.1	0.28

Data for Figure 12.

Current A	Line 1 NTU	Line 2	Line 3	Line 17
62.5	26.5	8.49	35.0	22.3
125	27.7	1.60	23.7	10.1
250	27.0	0.28	24.7	12.7

Data for Figure 14.

Current A	Line 1 NTU	Line 2 NTU	Line 3 NTU	Line 17 NTU
62.5	53.6	14.4	53.7	66.1
125	54.1	10.3	52.5	30.4
250	50.8	5.31	35.1	20.5
500	46.0	10.8	28.5	22.0
1000	46.8	7.84	29.6	18.4

Data for Figure 17.

Time hr	Line 1 pH	Line 2 pH	Line 17 pH	Line 21 pH	Line 25 pH
1.83	6.36	3.28	6.69	8.32	2.38
3.17	6.36	3.27	7.68	9.32	1.75
5.5	6.36	3.53	6.53	8.8	1.33

Data for Figure 18.

Time hr	pH	Fe mM
0.42	2.64	30.98

1.42	2.08	19.52
1.92	2.08	19.88
2.42	2.06	18.89
3.00	2.07	23.82
3.58	2.04	19.07
4.42	2.04	22.20

Data for Figure 24b.

T (hr)	Turbidity (NTU)
0	173
0.5	159
1.0	33.1
1.5	17.9
2.0	10.3
2.5	11.5
3.0	3.90
3.5	2.97
4.0	2.69
4.5	1.12
5.0	1.40
5.5	2.21
6.0	2.17
6.5	0.72
7.0	0.84
7.5	0.24
8.0	0

Data for Figure 25a.

N_2		Air		O_2	
E (V/SHE)	i (mA/cm^2)	E (V/SHE)	i (mA/cm^2)	E (V/SHE)	i (mA/cm^2)
-0.281	2.12E-05	-0.162	4.39E-06	-0.153	2.75E-05
-0.283	1.25E-03	-0.163	6.78E-03	-0.154	1.05E-01
-0.284	2.15E-03	-0.164	2.47E-02	-0.155	1.74E-01
-0.285	3.59E-03	-0.165	3.06E-02	-0.156	2.25E-01
-0.287	4.51E-03	-0.166	4.47E-02	-0.157	2.76E-01
-0.288	4.03E-03	-0.167	5.73E-02	-0.158	3.08E-01
-0.289	4.76E-03	-0.168	6.56E-02	-0.159	3.54E-01
-0.290	4.90E-03	-0.169	7.86E-02	-0.160	3.83E-01
-0.291	5.62E-03	-0.170	8.69E-02	-0.161	4.08E-01
-0.292	7.37E-03	-0.171	9.37E-02	-0.162	4.30E-01
-0.293	6.46E-03	-0.172	1.07E-01	-0.163	4.69E-01

-0.295	6.56E-03	-0.173	1.16E-01	-0.163	5.06E-01
-0.296	8.18E-03	-0.174	1.24E-01	-0.165	5.23E-01
-0.297	7.28E-03	-0.176	1.28E-01	-0.165	5.56E-01
-0.298	7.33E-03	-0.176	1.34E-01	-0.166	5.80E-01
-0.299	7.48E-03	-0.177	1.45E-01	-0.168	6.04E-01
-0.300	7.93E-03	-0.179	1.53E-01	-0.169	6.19E-01
-0.301	8.87E-03	-0.179	1.63E-01	-0.169	6.40E-01
-0.302	9.21E-03	-0.180	1.67E-01	-0.171	6.75E-01
-0.303	9.36E-03	-0.181	1.78E-01	-0.172	6.87E-01
-0.304	9.53E-03	-0.182	1.85E-01	-0.173	7.26E-01
-0.305	1.01E-02	-0.183	1.87E-01	-0.174	7.25E-01
-0.306	1.01E-02	-0.185	1.92E-01	-0.174	7.53E-01
-0.307	1.06E-02	-0.185	1.95E-01	-0.176	7.67E-01
-0.308	1.07E-02	-0.186	2.09E-01	-0.177	7.77E-01
-0.309	1.08E-02	-0.187	2.11E-01	-0.178	7.95E-01
-0.310	1.17E-02	-0.188	2.21E-01	-0.178	8.11E-01
-0.311	1.15E-02	-0.189	2.28E-01	-0.180	8.26E-01
-0.312	1.19E-02	-0.190	2.30E-01	-0.181	8.36E-01
-0.313	1.20E-02	-0.191	2.39E-01	-0.182	8.42E-01
-0.314	1.20E-02	-0.192	2.41E-01	-0.183	8.63E-01
-0.315	1.28E-02	-0.193	2.51E-01	-0.184	8.77E-01
-0.316	1.30E-02	-0.194	2.57E-01	-0.185	8.83E-01
-0.317	1.34E-02	-0.195	2.61E-01	-0.185	9.03E-01
-0.318	1.32E-02	-0.196	2.69E-01	-0.187	9.15E-01
-0.319	1.33E-02	-0.197	2.74E-01	-0.188	9.24E-01
-0.320	1.32E-02	-0.198	2.79E-01	-0.189	9.31E-01
-0.321	1.38E-02	-0.199	2.86E-01	-0.190	9.50E-01
-0.322	1.37E-02	-0.200	2.81E-01	-0.191	9.66E-01
-0.323	1.39E-02	-0.201	2.77E-01	-0.192	9.60E-01
-0.324	1.42E-02	-0.202	2.88E-01	-0.192	9.78E-01
-0.325	1.43E-02	-0.203	2.95E-01	-0.193	9.92E-01
-0.326	1.50E-02	-0.204	2.96E-01	-0.195	9.99E-01
-0.327	1.51E-02	-0.205	2.93E-01	-0.195	1.01E+00
-0.328	1.52E-02	-0.206	3.04E-01	-0.197	1.01E+00
-0.329	1.55E-02	-0.207	3.22E-01	-0.197	1.03E+00
-0.330	1.65E-02	-0.208	3.22E-01	-0.199	1.04E+00
-0.331	1.62E-02	-0.209	3.21E-01	-0.200	1.04E+00
-0.332	1.70E-02	-0.211	3.29E-01	-0.201	1.04E+00
-0.333	1.74E-02	-0.212	3.30E-01	-0.202	1.05E+00
-0.334	1.75E-02	-0.212	3.29E-01	-0.203	1.07E+00
-0.335	1.81E-02	-0.213	3.30E-01	-0.203	1.07E+00
-0.336	1.82E-02	-0.214	3.41E-01	-0.205	1.08E+00
-0.337	1.87E-02	-0.215	3.45E-01	-0.206	1.08E+00
-0.338	1.80E-02	-0.216	3.41E-01	-0.207	1.09E+00
-0.339	1.84E-02	-0.217	3.44E-01	-0.208	1.11E+00
-0.340	1.84E-02	-0.218	3.55E-01	-0.209	1.10E+00
-0.341	1.94E-02	-0.219	3.45E-01	-0.209	1.11E+00

-0.342	1.85E-02	-0.221	3.50E-01	-0.211	1.13E+00
-0.343	1.91E-02	-0.221	3.54E-01	-0.212	1.12E+00
-0.344	1.94E-02	-0.223	3.45E-01	-0.213	1.13E+00
-0.345	1.99E-02	-0.224	3.45E-01	-0.214	1.14E+00
-0.346	1.96E-02	-0.225	3.59E-01	-0.215	1.15E+00
-0.347	2.01E-02	-0.226	3.64E-01	-0.216	1.16E+00
-0.348	1.99E-02	-0.226	3.64E-01	-0.217	1.16E+00
-0.349	2.03E-02	-0.227	3.71E-01	-0.218	1.16E+00
-0.350	2.14E-02	-0.228	3.83E-01	-0.219	1.16E+00
-0.351	2.14E-02	-0.229	3.73E-01	-0.220	1.18E+00
-0.352	2.11E-02	-0.231	3.76E-01	-0.221	1.20E+00
-0.353	2.08E-02	-0.231	3.75E-01	-0.222	1.19E+00
-0.354	2.24E-02	-0.233	3.80E-01	-0.223	1.20E+00
-0.355	2.18E-02	-0.233	3.84E-01	-0.223	1.19E+00
-0.356	2.19E-02	-0.234	3.79E-01	-0.225	1.20E+00
-0.357	2.30E-02	-0.235	3.91E-01	-0.226	1.21E+00
-0.358	2.28E-02	-0.237	3.86E-01	-0.227	1.19E+00
-0.359	2.34E-02	-0.237	3.96E-01	-0.228	1.22E+00
-0.360	2.29E-02	-0.238	3.89E-01	-0.229	1.22E+00
-0.361	2.37E-02	-0.239	3.85E-01	-0.230	1.22E+00
-0.362	2.35E-02	-0.240	3.93E-01	-0.231	1.22E+00
-0.363	2.44E-02	-0.241	3.95E-01	-0.232	1.22E+00
-0.364	2.47E-02	-0.243	4.05E-01	-0.233	1.23E+00
-0.365	2.52E-02	-0.244	3.96E-01	-0.234	1.24E+00
-0.366	2.46E-02	-0.244	4.02E-01	-0.235	1.25E+00
-0.367	2.61E-02	-0.245	4.09E-01	-0.236	1.24E+00
-0.368	2.55E-02	-0.246	4.08E-01	-0.237	1.24E+00
-0.369	2.60E-02	-0.247	4.04E-01	-0.238	1.25E+00
-0.370	2.63E-02	-0.248	4.03E-01	-0.239	1.26E+00
-0.371	2.81E-02	-0.250	4.05E-01	-0.240	1.25E+00
-0.372	2.93E-02	-0.251	4.10E-01	-0.241	1.24E+00
-0.373	2.92E-02	-0.252	4.11E-01	-0.242	1.27E+00
-0.374	2.72E-02	-0.252	4.14E-01	-0.243	1.26E+00
-0.375	2.71E-02	-0.253	4.06E-01	-0.244	1.26E+00
-0.376	2.91E-02	-0.254	4.17E-01	-0.245	1.27E+00
-0.377	2.87E-02	-0.255	4.08E-01	-0.246	1.27E+00
-0.378	2.88E-02	-0.256	4.06E-01	-0.247	1.28E+00
-0.379	2.92E-02	-0.257	4.11E-01	-0.248	1.27E+00
-0.380	2.95E-02	-0.258	4.12E-01	-0.249	1.28E+00
-0.381	3.11E-02	-0.260	4.22E-01	-0.250	1.28E+00
-0.382	3.14E-02	-0.260	4.29E-01	-0.251	1.28E+00
-0.383	3.13E-02	-0.261	4.24E-01	-0.252	1.29E+00
-0.384	3.17E-02	-0.262	4.25E-01	-0.253	1.29E+00
-0.385	3.23E-02	-0.263	4.27E-01	-0.254	1.29E+00
-0.386	3.28E-02	-0.265	4.18E-01	-0.255	1.29E+00
-0.387	3.25E-02	-0.265	4.16E-01	-0.256	1.30E+00
-0.388	3.31E-02	-0.266	4.20E-01	-0.257	1.31E+00

-0.389	3.33E-02	-0.267	4.16E-01	-0.258	1.31E+00
-0.390	3.43E-02	-0.269	4.34E-01	-0.259	1.30E+00
-0.392	3.42E-02	-0.270	4.30E-01	-0.260	1.31E+00
-0.392	3.45E-02	-0.270	4.26E-01	-0.261	1.30E+00
-0.393	3.53E-02	-0.271	4.29E-01	-0.262	1.31E+00
-0.394	3.46E-02	-0.272	4.45E-01	-0.263	1.32E+00
-0.395	3.73E-02	-0.273	4.32E-01	-0.264	1.31E+00
-0.396	3.62E-02	-0.274	4.31E-01	-0.265	1.32E+00
-0.398	3.77E-02	-0.275	4.26E-01	-0.266	1.33E+00
-0.398	3.70E-02	-0.276	4.34E-01	-0.267	1.33E+00
-0.399	3.76E-02	-0.277	4.38E-01	-0.268	1.33E+00
-0.400	3.81E-02	-0.278	4.47E-01	-0.269	1.34E+00
-0.401	3.82E-02	-0.279	4.49E-01	-0.270	1.34E+00
-0.402	3.90E-02	-0.280	4.47E-01	-0.271	1.34E+00
-0.403	4.02E-02	-0.281	4.39E-01	-0.272	1.34E+00
-0.405	3.92E-02	-0.283	4.43E-01	-0.273	1.34E+00
-0.405	4.00E-02	-0.283	4.42E-01	-0.274	1.35E+00
-0.406	4.21E-02	-0.284	4.50E-01	-0.275	1.34E+00
-0.407	4.09E-02	-0.285	4.55E-01	-0.276	1.35E+00
-0.408	4.12E-02	-0.286	4.57E-01	-0.277	1.36E+00
-0.409	4.25E-02	-0.287	4.60E-01	-0.278	1.36E+00
-0.410	4.29E-02	-0.288	4.52E-01	-0.279	1.38E+00
-0.411	4.25E-02	-0.289	4.57E-01	-0.280	1.35E+00
-0.412	4.32E-02	-0.290	4.59E-01	-0.281	1.37E+00
-0.413	4.51E-02	-0.291	4.45E-01	-0.282	1.37E+00
-0.414	4.53E-02	-0.292	4.62E-01	-0.283	1.37E+00
-0.415	4.54E-02	-0.293	4.56E-01	-0.284	1.38E+00
-0.416	4.62E-02	-0.294	4.64E-01	-0.285	1.37E+00
-0.417	4.71E-02	-0.295	4.58E-01	-0.286	1.37E+00
-0.419	4.61E-02	-0.296	4.55E-01	-0.287	1.37E+00
-0.419	4.78E-02	-0.298	4.56E-01	-0.288	1.37E+00
-0.420	4.86E-02	-0.298	4.68E-01	-0.289	1.38E+00
-0.421	4.93E-02	-0.299	4.78E-01	-0.290	1.39E+00
-0.422	4.92E-02	-0.300	4.60E-01	-0.291	1.40E+00
-0.423	4.90E-02	-0.301	4.78E-01	-0.292	1.40E+00
-0.424	4.99E-02	-0.303	4.83E-01	-0.293	1.40E+00
-0.425	5.07E-02	-0.303	4.91E-01	-0.294	1.41E+00
-0.426	4.99E-02	-0.304	4.63E-01	-0.295	1.40E+00
-0.427	5.00E-02	-0.305	4.76E-01	-0.296	1.41E+00
-0.428	5.07E-02	-0.307	4.83E-01	-0.297	1.41E+00
-0.429	5.26E-02	-0.307	4.90E-01	-0.298	1.39E+00
-0.430	5.22E-02	-0.308	4.81E-01	-0.299	1.41E+00
-0.432	5.37E-02	-0.310	4.79E-01	-0.300	1.41E+00
-0.432	5.41E-02	-0.310	4.80E-01	-0.301	1.42E+00
-0.434	5.38E-02	-0.311	4.91E-01	-0.302	1.41E+00
-0.435	5.46E-02	-0.313	4.82E-01	-0.303	1.42E+00
-0.435	5.55E-02	-0.313	4.88E-01	-0.304	1.43E+00

-0.436	5.56E-02	-0.314	5.06E-01	-0.305	1.43E+00
-0.437	5.62E-02	-0.315	5.00E-01	-0.306	1.43E+00
-0.438	5.66E-02	-0.316	4.95E-01	-0.307	1.43E+00
-0.439	5.79E-02	-0.317	5.04E-01	-0.308	1.42E+00
-0.440	5.87E-02	-0.318	5.01E-01	-0.309	1.44E+00
-0.441	5.88E-02	-0.319	4.83E-01	-0.310	1.44E+00
-0.442	5.89E-02	-0.320	4.96E-01	-0.311	1.44E+00
-0.443	5.89E-02	-0.321	4.87E-01	-0.312	1.44E+00
-0.444	6.07E-02	-0.322	4.99E-01	-0.313	1.43E+00
-0.445	6.11E-02	-0.323	4.94E-01	-0.314	1.45E+00
-0.447	6.17E-02	-0.325	5.01E-01	-0.315	1.46E+00
-0.447	6.27E-02	-0.325	4.93E-01	-0.316	1.47E+00
-0.448	6.41E-02	-0.326	5.05E-01	-0.317	1.46E+00
-0.449	6.42E-02	-0.327	5.16E-01	-0.318	1.45E+00
-0.450	6.68E-02	-0.328	5.28E-01	-0.319	1.46E+00
-0.451	6.60E-02	-0.329	5.28E-01	-0.320	1.47E+00
-0.452	6.73E-02	-0.330	5.24E-01	-0.321	1.48E+00
-0.453	6.67E-02	-0.331	5.43E-01	-0.322	1.48E+00
-0.454	6.94E-02	-0.332	5.27E-01	-0.323	1.47E+00
-0.455	7.04E-02	-0.333	5.46E-01	-0.324	1.49E+00
-0.456	6.88E-02	-0.334	5.27E-01	-0.325	1.47E+00
-0.457	7.06E-02	-0.335	5.33E-01	-0.326	1.48E+00
-0.458	7.01E-02	-0.336	5.30E-01	-0.327	1.47E+00
-0.459	7.14E-02	-0.337	5.39E-01	-0.328	1.48E+00
-0.460	7.48E-02	-0.338	5.40E-01	-0.329	1.48E+00
-0.461	7.39E-02	-0.339	5.51E-01	-0.330	1.50E+00
-0.462	7.33E-02	-0.340	5.65E-01	-0.331	1.50E+00
-0.463	7.47E-02	-0.341	5.47E-01	-0.332	1.50E+00
-0.464	7.66E-02	-0.342	5.49E-01	-0.333	1.50E+00
-0.465	7.68E-02	-0.343	5.41E-01	-0.334	1.51E+00
-0.466	7.78E-02	-0.344	5.33E-01	-0.335	1.51E+00
-0.467	8.06E-02	-0.345	5.43E-01	-0.336	1.52E+00
-0.468	7.96E-02	-0.346	5.67E-01	-0.337	1.51E+00
-0.469	8.00E-02	-0.348	5.62E-01	-0.338	1.52E+00
-0.470	8.21E-02	-0.348	5.59E-01	-0.339	1.53E+00
-0.471	8.31E-02	-0.350	5.84E-01	-0.340	1.52E+00
-0.472	8.27E-02	-0.351	5.94E-01	-0.341	1.52E+00
-0.473	8.26E-02	-0.351	5.90E-01	-0.342	1.52E+00
-0.474	8.41E-02	-0.353	6.12E-01	-0.343	1.53E+00
-0.475	8.57E-02	-0.353	6.10E-01	-0.344	1.53E+00
-0.476	8.56E-02	-0.354	6.08E-01	-0.345	1.52E+00
-0.477	8.77E-02	-0.355	6.23E-01	-0.346	1.52E+00
-0.478	8.76E-02	-0.356	6.22E-01	-0.347	1.54E+00
-0.479	8.79E-02	-0.357	6.15E-01	-0.348	1.55E+00
-0.480	8.99E-02	-0.358	6.22E-01	-0.349	1.54E+00
-0.481	9.19E-02	-0.359	6.38E-01	-0.350	1.54E+00
-0.482	9.55E-02	-0.361	6.44E-01	-0.351	1.54E+00

-0.282	2.76E-05	-0.361	6.53E-01	-0.352	1.55E+00
-0.281	2.75E-04	-0.362	6.68E-01	-0.353	1.55E+00
-0.280	1.01E-03	-0.363	6.73E-01	-0.353	1.52E+00
-0.278	1.96E-03	-0.162	1.04E-05	-0.152	3.01E-05
-0.277	2.53E-03	-0.161	9.42E-03	-0.151	2.04E-02
-0.276	3.11E-03	-0.161	2.08E-02	-0.150	5.31E-02
-0.275	3.69E-03	-0.160	3.41E-02	-0.149	9.99E-02
-0.274	3.97E-03	-0.158	4.66E-02	-0.148	1.39E-01
-0.273	3.65E-03	-0.157	5.67E-02	-0.147	1.68E-01
-0.272	5.12E-03	-0.156	6.95E-02	-0.146	2.02E-01
-0.271	5.51E-03	-0.155	8.63E-02	-0.145	2.35E-01
-0.269	6.18E-03	-0.154	1.00E-01	-0.144	2.71E-01
-0.268	6.23E-03	-0.153	1.21E-01	-0.143	3.02E-01
-0.267	7.24E-03	-0.152	1.28E-01	-0.142	3.50E-01
-0.266	7.51E-03	-0.151	1.41E-01	-0.141	3.85E-01
-0.265	8.28E-03	-0.150	1.55E-01	-0.140	4.31E-01
-0.264	9.07E-03	-0.149	1.73E-01	-0.139	4.54E-01
-0.263	9.50E-03	-0.148	1.85E-01	-0.138	5.05E-01
-0.262	9.93E-03	-0.147	2.07E-01	-0.137	5.29E-01
-0.261	1.09E-02	-0.146	2.21E-01	-0.136	5.77E-01
-0.260	1.07E-02	-0.145	2.38E-01	-0.135	6.08E-01
-0.259	1.20E-02	-0.144	2.49E-01	-0.134	6.65E-01
-0.258	1.31E-02	-0.143	2.70E-01	-0.133	7.04E-01
-0.257	1.38E-02	-0.142	2.86E-01	-0.132	7.46E-01
-0.256	1.46E-02	-0.141	3.09E-01	-0.131	7.82E-01
-0.255	1.51E-02	-0.140	3.22E-01	-0.130	8.33E-01
-0.254	1.56E-02	-0.140	3.38E-01	-0.129	8.70E-01
-0.253	1.73E-02	-0.138	3.54E-01	-0.128	9.19E-01
-0.252	1.81E-02	-0.137	3.75E-01	-0.127	9.59E-01
-0.251	1.92E-02	-0.136	3.95E-01	-0.126	1.01E+00
-0.250	2.01E-02	-0.135	4.20E-01	-0.125	1.05E+00
-0.249	2.11E-02	-0.134	4.34E-01	-0.124	1.10E+00
-0.248	2.28E-02	-0.133	4.58E-01	-0.123	1.15E+00
-0.247	2.44E-02	-0.132	4.80E-01	-0.122	1.19E+00
-0.246	2.58E-02	-0.131	5.04E-01	-0.121	1.25E+00
-0.245	2.71E-02	-0.130	5.26E-01	-0.120	1.30E+00
-0.244	2.83E-02	-0.129	5.48E-01	-0.119	1.36E+00
-0.243	2.93E-02	-0.129	5.74E-01	-0.118	1.41E+00
-0.242	3.13E-02	-0.128	5.97E-01	-0.117	1.47E+00
-0.241	3.29E-02	-0.127	6.20E-01	-0.116	1.52E+00
-0.240	3.47E-02	-0.126	6.44E-01	-0.115	1.57E+00
-0.239	3.67E-02	-0.124	6.72E-01	-0.114	1.62E+00
-0.238	3.80E-02	-0.124	7.01E-01	-0.113	1.68E+00
-0.237	4.00E-02	-0.123	7.26E-01	-0.112	1.74E+00
-0.236	4.23E-02	-0.122	7.52E-01	-0.111	1.80E+00
-0.235	4.43E-02	-0.121	7.80E-01	-0.110	1.86E+00
-0.234	4.66E-02	-0.120	8.12E-01	-0.109	1.91E+00

-0.233	4.86E-02	-0.119	8.42E-01	-0.108	1.97E+00
-0.232	5.13E-02	-0.117	8.71E-01	-0.107	2.03E+00
-0.231	5.38E-02	-0.117	9.01E-01	-0.106	2.10E+00
-0.230	5.63E-02	-0.116	9.32E-01	-0.105	2.15E+00
-0.229	5.90E-02	-0.114	9.64E-01	-0.104	2.22E+00
-0.228	6.12E-02	-0.114	1.00E+00	-0.103	2.28E+00
-0.227	6.40E-02	-0.113	1.03E+00	-0.102	2.35E+00
-0.226	6.70E-02	-0.112	1.07E+00	-0.101	2.41E+00
-0.225	7.07E-02	-0.111	1.10E+00	-0.100	2.47E+00
-0.224	7.39E-02	-0.110	1.14E+00	-0.099	2.54E+00
-0.223	7.74E-02	-0.109	1.18E+00	-0.098	2.61E+00
-0.222	8.05E-02	-0.108	1.22E+00	-0.097	2.68E+00
-0.221	8.42E-02	-0.107	1.26E+00	-0.096	2.74E+00
-0.220	8.81E-02	-0.105	1.30E+00	-0.095	2.82E+00
-0.219	9.14E-02	-0.105	1.34E+00	-0.094	2.88E+00
-0.218	9.53E-02	-0.104	1.37E+00	-0.093	2.95E+00
-0.217	9.94E-02	-0.103	1.42E+00	-0.092	3.02E+00
-0.216	1.03E-01	-0.101	1.46E+00	-0.091	3.09E+00
-0.215	1.08E-01	-0.100	1.50E+00	-0.090	3.17E+00
-0.214	1.12E-01	-0.100	1.54E+00	-0.089	3.24E+00
-0.213	1.17E-01	-0.099	1.59E+00	-0.088	3.31E+00
-0.212	1.22E-01	-0.097	1.64E+00	-0.087	3.39E+00
-0.211	1.27E-01	-0.096	1.68E+00	-0.086	3.46E+00
-0.210	1.31E-01	-0.096	1.72E+00	-0.085	3.54E+00
-0.209	1.37E-01	-0.095	1.77E+00	-0.084	3.63E+00
-0.208	1.43E-01	-0.093	1.82E+00	-0.083	3.69E+00
-0.207	1.48E-01	-0.092	1.88E+00	-0.082	3.77E+00
-0.206	1.54E-01	-0.091	1.92E+00	-0.081	3.85E+00
-0.205	1.58E-01	-0.091	1.97E+00	-0.080	3.93E+00
-0.204	1.64E-01	-0.090	2.02E+00	-0.079	4.01E+00
-0.203	1.70E-01	-0.088	2.07E+00	-0.078	4.09E+00
-0.202	1.76E-01	-0.088	2.13E+00	-0.077	4.17E+00
-0.201	1.83E-01	-0.086	2.18E+00	-0.076	4.26E+00
-0.200	1.90E-01	-0.085	2.23E+00	-0.075	4.34E+00
-0.199	1.97E-01	-0.085	2.29E+00	-0.074	4.42E+00
-0.198	2.03E-01	-0.084	2.35E+00	-0.073	4.50E+00
-0.197	2.12E-01	-0.083	2.40E+00	-0.072	4.59E+00
-0.196	2.19E-01	-0.081	2.47E+00	-0.071	4.67E+00
-0.195	2.26E-01	-0.081	2.52E+00	-0.070	4.75E+00
-0.194	2.35E-01	-0.080	2.58E+00	-0.069	4.84E+00
-0.193	2.41E-01	-0.078	2.64E+00	-0.068	4.93E+00
-0.192	2.50E-01	-0.077	2.70E+00	-0.067	5.01E+00
-0.191	2.57E-01	-0.077	2.76E+00	-0.066	5.11E+00
-0.190	2.66E-01	-0.076	2.82E+00	-0.065	5.19E+00
-0.189	2.76E-01	-0.075	2.88E+00	-0.064	5.28E+00
-0.188	2.85E-01	-0.073	2.95E+00	-0.063	5.37E+00
-0.187	2.93E-01	-0.072	3.02E+00	-0.062	5.47E+00

-0.186	3.03E-01	-0.071	3.08E+00	-0.061	5.56E+00
-0.185	3.12E-01	-0.070	3.15E+00	-0.060	5.64E+00
-0.184	3.22E-01	-0.070	3.23E+00	-0.059	5.74E+00
-0.183	3.32E-01	-0.069	3.30E+00	-0.058	5.83E+00
-0.182	3.45E-01	-0.068	3.36E+00	-0.057	5.93E+00
-0.181	3.55E-01	-0.067	3.43E+00	-0.056	6.01E+00
-0.180	3.65E-01	-0.066	3.50E+00	-0.055	6.12E+00
-0.179	3.75E-01	-0.064	3.57E+00	-0.054	6.21E+00
-0.178	3.87E-01	-0.064	3.65E+00	-0.053	6.30E+00
-0.177	3.99E-01	-0.062	3.71E+00	-0.052	6.40E+00
-0.176	4.10E-01	-0.061	3.79E+00	-0.051	6.50E+00
-0.175	4.23E-01	-0.060	3.87E+00	-0.050	6.60E+00
-0.174	4.37E-01	-0.059	3.94E+00	-0.049	6.69E+00
-0.173	4.49E-01	-0.058	4.03E+00	-0.048	6.79E+00
-0.172	4.62E-01	-0.057	4.12E+00	-0.047	6.89E+00
-0.171	4.76E-01	-0.056	4.17E+00	-0.046	6.99E+00
-0.170	4.93E-01	-0.055	4.23E+00	-0.045	7.09E+00
-0.169	5.05E-01	-0.055	4.32E+00	-0.044	7.19E+00
-0.168	5.18E-01	-0.053	4.41E+00	-0.043	7.30E+00
-0.167	5.37E-01	-0.053	4.49E+00	-0.042	7.41E+00
-0.166	5.50E-01	-0.052	4.55E+00	-0.041	7.50E+00
-0.165	5.65E-01	-0.050	4.67E+00	-0.040	7.61E+00
-0.164	5.82E-01	-0.050	4.77E+00	-0.039	7.71E+00
-0.163	5.97E-01	-0.048	4.83E+00	-0.038	7.81E+00
-0.162	6.14E-01	-0.048	4.92E+00	-0.037	7.91E+00
-0.161	6.30E-01	-0.047	5.00E+00	-0.036	8.02E+00
-0.160	6.44E-01	-0.045	5.06E+00	-0.035	8.12E+00
-0.159	6.64E-01	-0.044	5.17E+00	-0.034	8.23E+00
-0.158	6.81E-01	-0.044	5.29E+00	-0.033	8.33E+00
-0.157	6.96E-01	-0.042	5.34E+00	-0.032	8.44E+00
-0.156	7.16E-01	-0.041	5.42E+00	-0.031	8.55E+00
-0.155	7.35E-01	-0.040	5.51E+00	-0.030	8.66E+00
-0.154	7.55E-01	-0.039	5.64E+00	-0.029	8.77E+00
-0.153	7.76E-01	-0.039	5.71E+00	-0.028	8.88E+00
-0.152	7.97E-01	-0.037	5.76E+00	-0.027	8.99E+00
-0.151	8.17E-01	-0.036	5.94E+00	-0.026	9.10E+00
-0.150	8.40E-01	-0.035	5.94E+00	-0.025	9.21E+00
-0.149	8.62E-01	-0.034	6.07E+00	-0.024	9.33E+00
-0.148	8.84E-01	-0.033	6.20E+00	-0.023	9.45E+00
-0.147	9.03E-01	-0.032	6.26E+00	-0.022	9.55E+00
-0.146	9.25E-01	-0.032	6.31E+00	-0.021	9.67E+00
-0.145	9.47E-01	-0.030	6.50E+00	-0.020	9.78E+00
-0.144	9.76E-01	-0.030	6.52E+00	-0.019	9.90E+00
-0.143	9.99E-01	-0.029	6.63E+00	-0.018	1.00E+01
-0.142	1.02E+00	-0.027	6.76E+00	-0.017	1.01E+01
-0.141	1.05E+00	-0.026	6.87E+00	-0.016	1.03E+01
-0.140	1.07E+00	-0.025	6.93E+00	-0.015	1.04E+01

-0.139	1.09E+00	-0.025	7.00E+00	-0.014	1.05E+01
-0.138	1.12E+00	-0.023	7.11E+00	-0.013	1.06E+01
-0.137	1.14E+00	-0.022	7.28E+00	-0.012	1.07E+01
-0.136	1.18E+00	-0.022	7.34E+00	-0.011	1.08E+01
-0.135	1.21E+00	-0.021	7.43E+00	-0.010	1.10E+01
-0.134	1.24E+00	-0.019	7.51E+00	-0.009	1.11E+01
-0.133	1.26E+00	-0.019	7.64E+00	-0.008	1.12E+01
-0.132	1.29E+00	-0.017	7.79E+00	-0.007	1.13E+01
-0.131	1.32E+00	-0.017	7.79E+00	-0.006	1.14E+01
-0.130	1.36E+00	-0.016	7.98E+00	-0.005	1.16E+01
-0.129	1.38E+00	-0.014	8.09E+00	-0.004	1.17E+01
-0.128	1.41E+00	-0.013	8.17E+00	-0.003	1.18E+01
-0.127	1.44E+00	-0.012	8.29E+00	-0.002	1.19E+01
-0.126	1.47E+00	-0.012	8.40E+00	-0.001	1.21E+01
-0.125	1.51E+00	-0.010	8.43E+00	0.000	1.22E+01
-0.124	1.54E+00	-0.010	8.63E+00	0.001	1.23E+01
-0.123	1.58E+00	-0.009	8.69E+00	0.002	1.25E+01
-0.122	1.61E+00	-0.008	8.78E+00	0.003	1.26E+01
-0.121	1.64E+00	-0.006	8.93E+00	0.004	1.27E+01
-0.120	1.68E+00	-0.006	9.07E+00	0.005	1.28E+01
-0.119	1.73E+00	-0.005	9.15E+00	0.006	1.30E+01
-0.118	1.75E+00	-0.004	9.28E+00	0.007	1.31E+01
-0.117	1.79E+00	-0.003	9.46E+00	0.008	1.32E+01
-0.116	1.83E+00	-0.001	9.47E+00	0.009	1.34E+01
-0.115	1.88E+00	0.000	9.57E+00	0.010	1.35E+01
-0.114	1.91E+00	0.000	9.68E+00	0.011	1.36E+01
-0.113	1.95E+00	0.002	9.85E+00	0.012	1.38E+01
-0.112	1.98E+00	0.003	9.93E+00	0.013	1.39E+01
-0.111	2.03E+00	0.004	9.95E+00	0.014	1.40E+01
-0.110	2.09E+00	0.004	1.02E+01	0.015	1.42E+01
-0.109	2.13E+00	0.005	1.02E+01	0.016	1.43E+01
-0.108	2.17E+00	0.006	1.03E+01	0.017	1.44E+01
-0.107	2.20E+00	0.008	1.04E+01	0.018	1.46E+01
-0.106	2.25E+00	0.008	1.06E+01	0.019	1.47E+01
-0.105	2.28E+00	0.010	1.07E+01	0.020	1.48E+01
-0.104	2.33E+00	0.011	1.09E+01	0.021	1.50E+01
-0.103	2.38E+00	0.012	1.10E+01	0.022	1.51E+01
-0.102	2.42E+00	0.013	1.10E+01	0.023	1.52E+01
-0.101	2.47E+00	0.014	1.11E+01	0.024	1.54E+01
-0.100	2.53E+00	0.015	1.13E+01	0.025	1.55E+01
-0.099	2.59E+00	0.015	1.15E+01	0.026	1.57E+01
-0.098	2.64E+00	0.017	1.15E+01	0.027	1.58E+01
-0.097	2.69E+00	0.018	1.16E+01	0.028	1.59E+01
-0.096	2.74E+00	0.019	1.18E+01	0.029	1.61E+01
-0.095	2.80E+00	0.020	1.20E+01	0.030	1.62E+01
-0.094	2.84E+00	0.021	1.21E+01	0.031	1.64E+01
-0.093	2.88E+00	0.022	1.22E+01	0.033	1.65E+01

-0.092	2.94E+00	0.023	1.23E+01	0.033	1.67E+01
-0.091	3.01E+00	0.024	1.25E+01	0.034	1.68E+01
-0.090	3.05E+00	0.025	1.25E+01	0.035	1.70E+01
-0.089	3.10E+00	0.026	1.26E+01	0.036	1.71E+01
-0.088	3.17E+00	0.027	1.28E+01	0.037	1.73E+01
-0.087	3.25E+00	0.028	1.29E+01	0.038	1.74E+01
-0.086	3.30E+00	0.029	1.30E+01	0.039	1.76E+01
-0.085	3.35E+00	0.030	1.32E+01	0.040	1.77E+01
-0.084	3.41E+00	0.031	1.33E+01	0.041	1.78E+01
-0.083	3.49E+00	0.032	1.34E+01	0.042	1.80E+01
-0.082	3.53E+00	0.033	1.35E+01	0.043	1.81E+01
-0.082	3.53E+00	0.034	1.36E+01	0.044	1.83E+01

Data for Figure 25b.

	E (V/SHE)	i_{corr} (mA/cm^2)	Error ±
N_2	-0.26	0.007	0.12
Air	-0.14	0.367	0.06
O_2	-0.13	0.773	0.00

Data for Figure 26a.

pH 7		pH 5		pH 4		pH 3		pH 2		pH 1	
E	i	E	i	E	i	E	I	E	i	E	i
V/SHE	mA/cm^2	V/SHE	mA/cm^2	V/SHE	mA/cm^2	V/SHE	mA/cm^2	V/SHE	mA/cm^2	V/SHE	mA/cm^2
-0.42	-5.54	-0.42	-4.77	-0.40	-5.21	-0.42	-4.58	-0.32	-4.82	-0.33	-5.28
-0.42	-2.54	-0.42	-2.53	-0.40	-2.44	-0.42	-2.40	-0.33	-1.30	-0.33	-1.55
-0.42	-2.18	-0.42	-2.07	-0.41	-2.01	-0.42	-1.98	-0.33	-0.90	-0.33	-1.05
-0.42	-2.00	-0.42	-1.89	-0.41	-1.84	-0.42	-1.78	-0.33	-0.70	-0.33	-0.84
-0.42	-1.89	-0.42	-1.77	-0.41	-1.73	-0.42	-1.65	-0.33	-0.56	-0.34	-0.70
-0.43	-1.80	-0.42	-1.68	-0.41	-1.64	-0.42	-1.56	-0.33	-0.44	-0.34	-0.59
-0.43	-1.73	-0.43	-1.61	-0.41	-1.58	-0.42	-1.48	-0.33	-0.36	-0.34	-0.49
-0.43	-1.67	-0.43	-1.55	-0.41	-1.52	-0.42	-1.42	-0.33	-0.31	-0.34	-0.42
-0.43	-1.62	-0.43	-1.50	-0.41	-1.48	-0.43	-1.37	-0.33	-0.26	-0.34	-0.36
-0.43	-1.58	-0.43	-1.45	-0.41	-1.44	-0.43	-1.32	-0.33	-0.22	-0.34	-0.30
-0.43	-1.54	-0.43	-1.42	-0.41	-1.40	-0.43	-1.28	-0.33	-0.18	-0.34	-0.24
-0.43	-1.51	-0.43	-1.38	-0.41	-1.37	-0.43	-1.24	-0.34	-0.15	-0.34	-0.19
-0.43	-1.48	-0.43	-1.35	-0.42	-1.34	-0.43	-1.21	-0.34	-0.12	-0.34	-0.15
-0.43	-1.45	-0.43	-1.32	-0.42	-1.31	-0.43	-1.18	-0.34	-0.09	-0.34	-0.11
-0.43	-1.42	-0.43	-1.30	-0.42	-1.29	-0.43	-1.15	-0.34	-0.06	-0.35	-0.07
-0.44	-1.40	-0.43	-1.28	-0.42	-1.27	-0.43	-1.13	-0.34	-0.04	-0.35	-0.04
-0.44	-1.38	-0.44	-1.25	-0.42	-1.25	-0.43	-1.11	-0.34	-0.01	-0.35	0.00
-0.44	-1.36	-0.44	-1.24	-0.42	-1.23	-0.43	-1.09	-0.34	0.01	-0.35	0.03
-0.44	-1.34	-0.44	-1.22	-0.42	-1.21	-0.44	-1.07	-0.34	0.03	-0.35	0.06

-0.44	-1.33	-0.44	-1.20	-0.42	-1.19	-0.44	-1.05	-0.34	0.05	-0.35	0.09
-0.44	-1.31	-0.44	-1.19	-0.42	-1.18	-0.44	-1.03	-0.35	0.07	-0.35	0.12
-0.44	-1.30	-0.44	-1.17	-0.42	-1.16	-0.44	-1.02	-0.35	0.09	-0.35	0.14
-0.44	-1.28	-0.44	-1.16	-0.43	-1.15	-0.44	-1.00	-0.35	0.11	-0.35	0.17
-0.44	-1.27	-0.44	-1.14	-0.43	-1.14	-0.44	-0.99	-0.35	0.13	-0.35	0.19
-0.44	-1.26	-0.44	-1.13	-0.43	-1.13	-0.44	-0.97	-0.35	0.14	-0.36	0.22
-0.45	-1.25	-0.44	-1.12	-0.43	-1.12	-0.44	-0.96	-0.35	0.16	-0.36	0.24
-0.45	-1.23	-0.45	-1.11	-0.43	-1.10	-0.44	-0.95	-0.35	0.17	-0.36	0.26
-0.45	-1.22	-0.45	-1.10	-0.43	-1.09	-0.44	-0.94	-0.35	0.19	-0.36	0.28
-0.45	-1.21	-0.45	-1.09	-0.43	-1.09	-0.45	-0.93	-0.35	0.20	-0.36	0.30
-0.45	-1.21	-0.45	-1.08	-0.43	-1.08	-0.45	-0.92	-0.35	0.21	-0.36	0.32
-0.45	-1.20	-0.45	-1.07	-0.43	-1.07	-0.45	-0.91	-0.36	0.23	-0.36	0.34
-0.45	-1.19	-0.45	-1.06	-0.43	-1.06	-0.45	-0.90	-0.36	0.24	-0.36	0.36
-0.45	-1.18	-0.45	-1.05	-0.44	-1.05	-0.45	-0.89	-0.36	0.25	-0.36	0.38
-0.45	-1.17	-0.45	-1.04	-0.44	-1.04	-0.45	-0.88	-0.36	0.27	-0.36	0.40
-0.45	-1.17	-0.45	-1.02	-0.44	-1.04	-0.45	-0.87	-0.36	0.28	-0.37	0.41
-0.46	-1.16	-0.45	-1.01	-0.44	-1.02	-0.45	-0.87	-0.36	0.29	-0.37	0.43
-0.46	-1.15	-0.46	-1.01	-0.44	-1.01	-0.45	-0.86	-0.36	0.30	-0.37	0.45
-0.46	-1.15	-0.46	-1.00	-0.44	-1.01	-0.45	-0.85	-0.36	0.31	-0.37	0.47
-0.46	-1.14	-0.46	-0.99	-0.44	-1.00	-0.46	-0.85	-0.36	0.32	-0.37	0.49
-0.46	-1.13	-0.46	-0.99	-0.44	-0.99	-0.46	-0.84	-0.36	0.33	-0.37	0.50
-0.46	-1.13	-0.46	-0.98	-0.44	-0.99	-0.46	-0.83	-0.36	0.34	-0.37	0.52
-0.46	-1.12	-0.46	-0.97	-0.44	-0.98	-0.46	-0.83	-0.37	0.35	-0.37	0.54
-0.46	-1.12	-0.46	-0.97	-0.45	-0.98	-0.46	-0.82	-0.37	0.35	-0.37	0.56
-0.46	-1.11	-0.46	-0.96	-0.45	-0.97	-0.46	-0.82	-0.37	0.36	-0.37	0.57
-0.46	-1.11	-0.46	-0.96	-0.45	-0.97	-0.46	-0.81	-0.37	0.36	-0.38	0.59
-0.47	-1.10	-0.46	-0.95	-0.45	-0.96	-0.46	-0.81	-0.37	0.37	-0.38	0.60
-0.47	-1.10	-0.47	-0.95	-0.45	-0.96	-0.46	-0.80	-0.37	0.37	-0.38	0.62
-0.47	-1.09	-0.47	-0.94	-0.45	-0.95	-0.46	-0.80	-0.37	0.38	-0.38	0.63
-0.47	-1.09	-0.47	-0.94	-0.45	-0.95	-0.47	-0.79	-0.37	0.38	-0.38	0.65
-0.47	-1.09	-0.47	-0.93	-0.45	-0.94	-0.47	-0.79	-0.37	0.39	-0.38	0.66
-0.47	-1.08	-0.47	-0.93	-0.45	-0.94	-0.47	-0.78	-0.38	0.40	-0.38	0.68
-0.47	-1.08	-0.47	-0.92	-0.45	-0.94	-0.47	-0.78	-0.38	0.40	-0.38	0.70
-0.47	-1.08	-0.47	-0.92	-0.46	-0.93	-0.47	-0.77	-0.38	0.40	-0.38	0.71
-0.47	-1.07	-0.47	-0.92	-0.46	-0.93	-0.47	-0.77	-0.38	0.41	-0.38	0.72
-0.47	-1.07	-0.47	-0.91	-0.46	-0.93	-0.47	-0.76	-0.38	0.41	-0.39	0.73
-0.48	-1.07	-0.47	-0.91	-0.46	-0.92	-0.47	-0.76	-0.38	0.42	-0.39	0.75
-0.48	-1.06	-0.48	-0.90	-0.46	-0.92	-0.47	-0.75	-0.38	0.42	-0.39	0.76
-0.48	-1.06	-0.48	-0.90	-0.46	-0.92	-0.47	-0.75	-0.38	0.42	-0.39	0.77
-0.48	-1.06	-0.48	-0.90	-0.46	-0.91	-0.48	-0.75	-0.38	0.43	-0.39	0.78
-0.48	-1.05	-0.48	-0.89	-0.46	-0.91	-0.48	-0.74	-0.38	0.43	-0.39	0.80
-0.48	-1.05	-0.48	-0.89	-0.46	-0.91	-0.48	-0.74	-0.39	0.43	-0.39	0.81
-0.48	-1.05	-0.48	-0.89	-0.46	-0.90	-0.48	-0.73	-0.39	0.44	-0.39	0.82
-0.48	-1.04	-0.48	-0.88	-0.47	-0.90	-0.48	-0.73	-0.39	0.44	-0.39	0.84
-0.48	-1.04	-0.48	-0.88	-0.47	-0.90	-0.48	-0.73	-0.39	0.44	-0.39	0.85
-0.48	-1.04	-0.48	-0.88	-0.47	-0.89	-0.48	-0.72	-0.39	0.45	-0.40	0.86
-0.49	-1.03	-0.48	-0.87	-0.47	-0.89	-0.48	-0.72	-0.39	0.45	-0.40	0.87

-0.49	-1.03	-0.49	-0.87	-0.47	-0.89	-0.48	-0.72	-0.39	0.45	-0.40	0.88
-0.49	-1.03	-0.49	-0.87	-0.47	-0.88	-0.49	-0.71	-0.39	0.46	-0.40	0.90
-0.49	-1.03	-0.49	-0.87	-0.47	-0.88	-0.49	-0.71	-0.39	0.46	-0.40	0.91
-0.49	-1.02	-0.49	-0.86	-0.47	-0.88	-0.49	-0.71	-0.39	0.46	-0.40	0.92
-0.49	-1.02	-0.49	-0.86	-0.47	-0.87	-0.49	-0.70	-0.39	0.46	-0.40	0.94
-0.49	-1.02	-0.49	-0.86	-0.47	-0.87	-0.49	-0.70	-0.40	0.46	-0.40	0.95
-0.49	-1.02	-0.49	-0.85	-0.48	-0.87	-0.49	-0.70	-0.40	0.47	-0.40	0.96
-0.49	-1.02	-0.49	-0.85	-0.48	-0.87	-0.49	-0.69	-0.40	0.47	-0.40	0.97
-0.49	-1.01	-0.49	-0.85	-0.48	-0.86	-0.49	-0.69	-0.40	0.47	-0.41	0.98
-0.50	-1.01	-0.49	-0.85	-0.48	-0.86	-0.49	-0.69	-0.40	0.48	-0.41	0.99
-0.50	-1.01	-0.50	-0.84	-0.48	-0.86	-0.49	-0.68	-0.40	0.48	-0.41	1.00
-0.50	-1.00	-0.50	-0.84	-0.48	-0.85	-0.49	-0.68	-0.40	0.48	-0.41	1.01
-0.50	-1.00	-0.50	-0.84	-0.48	-0.85	-0.50	-0.68	-0.40	0.48	-0.41	1.02
-0.50	-1.00	-0.50	-0.84	-0.48	-0.85	-0.50	-0.67	-0.40	0.49	-0.41	1.03
-0.50	-1.00	-0.50	-0.83	-0.48	-0.85	-0.50	-0.67	-0.41	0.49	-0.41	1.04
-0.50	-0.99	-0.50	-0.83	-0.48	-0.84	-0.50	-0.67	-0.41	0.50	-0.41	1.05
-0.50	-0.99	-0.50	-0.83	-0.49	-0.84	-0.50	-0.66	-0.41	0.50	-0.41	1.06
-0.50	-0.99	-0.50	-0.82	-0.49	-0.84	-0.50	-0.66	-0.41	0.50	-0.41	1.07
-0.50	-0.99	-0.50	-0.82	-0.49	-0.84	-0.50	-0.66	-0.41	0.50	-0.42	1.08
-0.51	-0.99	-0.50	-0.82	-0.49	-0.83	-0.50	-0.66	-0.41	0.50	-0.42	1.10
-0.51	-0.99	-0.51	-0.82	-0.49	-0.83	-0.50	-0.65	-0.41	0.51	-0.42	1.11
-0.51	-0.98	-0.51	-0.81	-0.49	-0.83	-0.50	-0.65	-0.41	0.51	-0.42	1.11
-0.51	-0.98	-0.51	-0.81	-0.49	-0.83	-0.51	-0.65	-0.41	0.51	-0.42	1.12
-0.51	-0.98	-0.51	-0.81	-0.49	-0.83	-0.51	-0.64	-0.41	0.51	-0.42	1.13
-0.51	-0.98	-0.51	-0.81	-0.49	-0.82	-0.51	-0.64	-0.42	0.51	-0.42	1.14
-0.51	-0.98	-0.51	-0.80	-0.49	-0.82	-0.51	-0.64	-0.42	0.51	-0.42	1.16
-0.51	-0.97	-0.51	-0.80	-0.50	-0.82	-0.51	-0.64	-0.42	0.51	-0.42	1.17
-0.51	-0.97	-0.51	-0.80	-0.50	-0.82	-0.51	-0.63	-0.42	0.51	-0.42	1.17
-0.51	-0.97	-0.51	-0.80	-0.50	-0.82	-0.51	-0.63	-0.42	0.51	-0.43	1.18
-0.52	-0.97	-0.51	-0.79	-0.50	-0.81	-0.51	-0.63	-0.42	0.51	-0.43	1.19
-0.52	-0.97	-0.52	-0.79	-0.50	-0.81	-0.51	-0.63	-0.42	0.52	-0.43	1.20
-0.52	-0.96	-0.52	-0.79	-0.50	-0.81	-0.52	-0.62	-0.42	0.52	-0.43	1.21
-0.52	-0.96	-0.52	-0.79	-0.50	-0.81	-0.52	-0.62	-0.42	0.52	-0.43	1.22
-0.52	-0.96	-0.52	-0.78	-0.50	-0.80	-0.52	-0.62	-0.42	0.52	-0.43	1.23
-0.52	-0.96	-0.52	-0.78	-0.50	-0.80	-0.52	-0.61	-0.42	0.52	-0.43	1.24
-0.52	-0.95	-0.52	-0.78	-0.50	-0.80	-0.52	-0.61	-0.43	0.52	-0.43	1.24
-0.52	-0.95	-0.52	-0.78	-0.51	-0.80	-0.52	-0.61	-0.43	0.52	-0.43	1.25
-0.52	-0.95	-0.52	-0.77	-0.51	-0.80	-0.52	-0.61	-0.43	0.52	-0.43	1.26
-0.52	-0.95	-0.52	-0.77	-0.51	-0.79	-0.52	-0.61	-0.43	0.53	-0.44	1.27
-0.53	-0.95	-0.52	-0.77	-0.51	-0.79	-0.52	-0.60	-0.43	0.53	-0.44	1.28
-0.53	-0.94	-0.53	-0.77	-0.51	-0.79	-0.52	-0.60	-0.43	0.53	-0.44	1.29
-0.53	-0.94	-0.53	-0.76	-0.51	-0.79	-0.52	-0.60	-0.43	0.53	-0.44	1.29
-0.53	-0.94	-0.53	-0.76	-0.51	-0.78	-0.53	-0.60	-0.43	0.53	-0.44	1.30
-0.53	-0.94	-0.53	-0.76	-0.51	-0.78	-0.53	-0.59	-0.43	0.53	-0.44	1.31
-0.53	-0.93	-0.53	-0.76	-0.51	-0.78	-0.53	-0.59	-0.44	0.53	-0.44	1.32
-0.53	-0.93	-0.53	-0.76	-0.51	-0.78	-0.53	-0.59	-0.44	0.53	-0.44	1.33
-0.53	-0.93	-0.53	-0.75	-0.52	-0.78	-0.53	-0.59	-0.44	0.54	-0.44	1.33

-0.53	-0.93	-0.53	-0.75	-0.52	-0.77	-0.53	-0.58	-0.44	0.54	-0.44	1.34
-0.53	-0.93	-0.53	-0.75	-0.52	-0.77	-0.53	-0.58	-0.44	0.54	-0.45	1.35
-0.54	-0.92	-0.53	-0.75	-0.52	-0.77	-0.53	-0.58	-0.44	0.54	-0.45	1.36
-0.54	-0.92	-0.54	-0.74	-0.52	-0.77	-0.53	-0.58	-0.44	0.54	-0.45	1.36
-0.54	-0.92	-0.54	-0.74	-0.52	-0.76	-0.53	-0.58	-0.44	0.54	-0.45	1.37
-0.54	-0.92	-0.54	-0.74	-0.52	-0.76	-0.54	-0.57	-0.44	0.54	-0.45	1.38
-0.54	-0.91	-0.54	-0.74	-0.52	-0.76	-0.54	-0.57	-0.44	0.54	-0.45	1.39
-0.54	-0.91	-0.54	-0.73	-0.52	-0.76	-0.54	-0.57	-0.45	0.54	-0.45	1.39
-0.54	-0.91	-0.54	-0.73	-0.52	-0.76	-0.54	-0.57	-0.45	0.54	-0.45	1.40
-0.54	-0.91	-0.54	-0.73	-0.53	-0.75	-0.54	-0.57	-0.45	0.54	-0.45	1.41
-0.54	-0.91	-0.54	-0.73	-0.53	-0.75	-0.54	-0.57	-0.45	0.55	-0.45	1.41
-0.54	-0.90	-0.54	-0.72	-0.53	-0.75	-0.54	-0.56	-0.45	0.55	-0.46	1.42
-0.55	-0.90	-0.54	-0.72	-0.53	-0.75	-0.54	-0.56	-0.45	0.55	-0.46	1.43
-0.55	-0.90	-0.55	-0.72	-0.53	-0.74	-0.54	-0.56	-0.45	0.55	-0.46	1.43
-0.55	-0.90	-0.55	-0.72	-0.53	-0.74	-0.55	-0.56	-0.45	0.55	-0.46	1.44
-0.55	-0.90	-0.55	-0.71	-0.53	-0.74	-0.55	-0.56	-0.45	0.55	-0.46	1.45
-0.55	-0.89	-0.55	-0.71	-0.53	-0.74	-0.55	-0.56	-0.45	0.55	-0.46	1.46
-0.55	-0.89	-0.55	-0.71	-0.53	-0.73	-0.55	-0.56	-0.46	0.55	-0.46	1.46
-0.55	-0.89	-0.55	-0.71	-0.53	-0.73	-0.55	-0.55	-0.46	0.55	-0.46	1.47
-0.55	-0.89	-0.55	-0.71	-0.54	-0.73	-0.55	-0.55	-0.46	0.55	-0.46	1.47
-0.55	-0.89	-0.55	-0.70	-0.54	-0.73	-0.55	-0.55	-0.46	0.55	-0.46	1.48
-0.55	-0.89	-0.55	-0.70	-0.54	-0.72	-0.55	-0.55	-0.46	0.56	-0.47	1.48
-0.56	-0.88	-0.55	-0.70	-0.54	-0.72	-0.55	-0.55	-0.46	0.56	-0.47	1.49
-0.56	-0.88	-0.56	-0.69	-0.54	-0.72	-0.55	-0.55	-0.46	0.56	-0.47	1.50
-0.56	-0.88	-0.56	-0.69	-0.54	-0.72	-0.55	-0.54	-0.46	0.56	-0.47	1.50
-0.56	-0.88	-0.56	-0.69	-0.54	-0.71	-0.56	-0.54	-0.46	0.56	-0.47	1.51
-0.56	-0.87	-0.56	-0.69	-0.54	-0.71	-0.56	-0.54	-0.46	0.56	-0.47	1.52
-0.56	-0.87	-0.56	-0.68	-0.54	-0.71	-0.56	-0.54	-0.47	0.56	-0.47	1.52
-0.56	-0.87	-0.56	-0.68	-0.54	-0.71	-0.56	-0.54	-0.47	0.56	-0.47	1.53
-0.56	-0.87	-0.56	-0.68	-0.55	-0.70	-0.56	-0.54	-0.47	0.56	-0.47	1.53
-0.56	-0.87	-0.56	-0.68	-0.55	-0.70	-0.56	-0.54	-0.47	0.56	-0.47	1.54
-0.56	-0.86	-0.56	-0.67	-0.55	-0.70	-0.56	-0.53	-0.47	0.56	-0.48	1.54
-0.57	-0.86	-0.56	-0.67	-0.55	-0.70	-0.56	-0.53	-0.47	0.56	-0.48	1.55
-0.57	-0.86	-0.57	-0.67	-0.55	-0.70	-0.56	-0.53	-0.47	0.56	-0.48	1.56
-0.57	-0.86	-0.57	-0.67	-0.55	-0.69	-0.57	-0.53	-0.47	0.56	-0.48	1.56
-0.57	-0.86	-0.57	-0.66	-0.55	-0.69	-0.57	-0.53	-0.47	0.56	-0.48	1.57
-0.57	-0.86	-0.57	-0.66	-0.55	-0.69	-0.57	-0.53	-0.47	0.57	-0.48	1.57
-0.57	-0.85	-0.57	-0.66	-0.55	-0.69	-0.57	-0.53	-0.48	0.57	-0.48	1.58
-0.57	-0.85	-0.57	-0.65	-0.55	-0.68	-0.57	-0.53	-0.48	0.57	-0.48	1.58
-0.57	-0.85	-0.57	-0.65	-0.56	-0.68	-0.57	-0.53	-0.48	0.57	-0.48	1.59
-0.57	-0.85	-0.57	-0.65	-0.56	-0.68	-0.57	-0.52	-0.48	0.58	-0.48	1.59
-0.57	-0.84	-0.57	-0.65	-0.56	-0.68	-0.57	-0.52	-0.48	0.58	-0.49	1.60
-0.58	-0.84	-0.57	-0.65	-0.56	-0.68	-0.57	-0.52	-0.48	0.58	-0.49	1.61
-0.58	-0.84	-0.58	-0.64	-0.56	-0.68	-0.57	-0.52	-0.48	0.58	-0.49	1.61
-0.58	-0.84	-0.58	-0.64	-0.56	-0.67	-0.57	-0.52	-0.48	0.58	-0.49	1.61
-0.58	-0.83	-0.58	-0.64	-0.56	-0.67	-0.58	-0.52	-0.48	0.58	-0.49	1.62
-0.58	-0.83	-0.58	-0.64	-0.56	-0.67	-0.58	-0.52	-0.48	0.58	-0.49	1.62

-0.58	-0.83	-0.58	-0.64	-0.56	-0.67	-0.58	-0.52	-0.49	0.58	-0.49	1.63
-0.58	-0.83	-0.58	-0.64	-0.56	-0.67	-0.58	-0.52	-0.49	0.57	-0.49	1.63
-0.58	-0.82	-0.58	-0.63	-0.57	-0.67	-0.58	-0.52	-0.49	0.57	-0.49	1.64
-0.58	-0.82	-0.58	-0.63	-0.57	-0.67	-0.58	-0.52	-0.49	0.58	-0.49	1.64
-0.58	-0.82	-0.58	-0.63	-0.57	-0.66	-0.58	-0.52	-0.49	0.58	-0.50	1.65
-0.59	-0.82	-0.58	-0.63	-0.57	-0.66	-0.58	-0.51	-0.49	0.58	-0.50	1.65
-0.59	-0.81	-0.59	-0.63	-0.57	-0.66	-0.58	-0.51	-0.49	0.58	-0.50	1.66
-0.59	-0.81	-0.59	-0.62	-0.57	-0.66	-0.58	-0.51	-0.49	0.58	-0.50	1.66
-0.59	-0.81	-0.59	-0.62	-0.57	-0.66	-0.59	-0.51	-0.49	0.58	-0.50	1.67
-0.59	-0.81	-0.59	-0.62	-0.57	-0.66	-0.59	-0.51	-0.49	0.58	-0.50	1.67
-0.59	-0.80	-0.59	-0.62	-0.57	-0.65	-0.59	-0.51	-0.49	0.58	-0.50	1.68
-0.59	-0.80	-0.59	-0.62	-0.57	-0.65	-0.59	-0.51	-0.50	0.58	-0.50	1.68
-0.59	-0.80	-0.59	-0.61	-0.58	-0.65	-0.59	-0.51	-0.50	0.58	-0.50	1.69
-0.59	-0.80	-0.59	-0.61	-0.58	-0.65	-0.59	-0.51	-0.50	0.58	-0.50	1.69
-0.59	-0.80	-0.59	-0.61	-0.58	-0.65	-0.59	-0.51	-0.50	0.58	-0.51	1.69
-0.60	-0.80	-0.59	-0.61	-0.58	-0.64	-0.59	-0.51	-0.50	0.58	-0.51	1.70
-0.60	-0.80	-0.60	-0.61	-0.58	-0.64	-0.59	-0.50	-0.50	0.58	-0.51	1.70
-0.60	-0.79	-0.60	-0.60	-0.58	-0.64	-0.60	-0.50	-0.50	0.58	-0.51	1.71
-0.60	-0.79	-0.60	-0.60	-0.58	-0.64	-0.60	-0.50	-0.50	0.58	-0.51	1.71
-0.60	-0.79	-0.60	-0.60	-0.58	-0.64	-0.60	-0.50	-0.50	0.58	-0.51	1.72
-0.60	-0.79	-0.60	-0.60	-0.58	-0.63	-0.60	-0.50	-0.51	0.58	-0.51	1.72
-0.60	-0.79	-0.60	-0.59	-0.58	-0.63	-0.60	-0.50	-0.51	0.58	-0.51	1.73
-0.60	-0.79	-0.60	-0.59	-0.59	-0.63	-0.60	-0.50	-0.51	0.59	-0.51	1.73
-0.60	-0.79	-0.60	-0.59	-0.59	-0.63	-0.60	-0.50	-0.51	0.59	-0.51	1.73
-0.60	-0.78	-0.60	-0.59	-0.59	-0.63	-0.60	-0.50	-0.51	0.59	-0.52	1.74
-0.61	-0.78	-0.60	-0.59	-0.59	-0.62	-0.60	-0.50	-0.51	0.59	-0.52	1.74
-0.61	-0.78	-0.61	-0.58	-0.59	-0.62	-0.60	-0.50	-0.51	0.59	-0.52	1.75
-0.61	-0.78	-0.61	-0.58	-0.59	-0.62	-0.60	-0.50	-0.51	0.59	-0.52	1.75
-0.61	-0.78	-0.61	-0.58	-0.59	-0.62	-0.61	-0.49	-0.51	0.59	-0.52	1.75
-0.61	-0.78	-0.61	-0.58	-0.59	-0.62	-0.61	-0.49	-0.51	0.59	-0.52	1.76
-0.61	-0.78	-0.61	-0.57	-0.59	-0.61	-0.61	-0.49	-0.51	0.59	-0.52	1.76
-0.61	-0.77	-0.61	-0.57	-0.59	-0.61	-0.61	-0.49	-0.52	0.59	-0.52	1.77
-0.61	-0.77	-0.61	-0.57	-0.60	-0.61	-0.61	-0.49	-0.52	0.59	-0.52	1.77
-0.61	-0.77	-0.61	-0.57	-0.60	-0.61	-0.61	-0.49	-0.52	0.59	-0.52	1.77
-0.61	-0.77	-0.61	-0.57	-0.60	-0.61	-0.61	-0.49	-0.52	0.59	-0.53	1.78
-0.62	-0.77	-0.61	-0.56	-0.60	-0.60	-0.61	-0.49	-0.52	0.59	-0.53	1.78
-0.62	-0.77	-0.62	-0.56	-0.60	-0.60	-0.61	-0.49	-0.52	0.59	-0.53	1.79
-0.62	-0.76	-0.62	-0.56	-0.60	-0.60	-0.62	-0.48	-0.52	0.59	-0.53	1.79
-0.62	-0.76	-0.62	-0.56	-0.60	-0.60	-0.62	-0.48	-0.52	0.59	-0.53	1.79
-0.62	-0.76	-0.62	-0.55	-0.60	-0.60	-0.62	-0.48	-0.52	0.59	-0.53	1.80
-0.62	-0.76	-0.62	-0.55	-0.60	-0.59	-0.62	-0.48	-0.52	0.59	-0.53	1.80
-0.62	-0.70	-0.62	-0.52	-0.60	-0.55	-0.62	-0.48	-0.53	0.59	-0.53	1.80
-0.42	-4.91	-0.42	-4.60	-0.41	-5.21	-0.42	-5.30	-0.33	-4.93	-0.33	-4.91
-0.42	-2.31	-0.42	-1.79	-0.40	-2.24	-0.42	-2.17	-0.33	-1.07	-0.33	-1.09
-0.42	-1.97	-0.42	-1.63	-0.40	-1.95	-0.42	-2.05	-0.32	-0.80	-0.33	-0.80
-0.42	-1.80	-0.42	-1.53	-0.40	-1.80	-0.42	-1.86	-0.32	-0.65	-0.33	-0.63
-0.42	-1.67	-0.42	-1.45	-0.40	-1.70	-0.42	-1.73	-0.32	-0.51	-0.33	-0.53

-0.42	-1.57	-0.41	-1.39	-0.40	-1.62	-0.41	-1.63	-0.32	-0.42	-0.33	-0.43
-0.41	-1.49	-0.41	-1.33	-0.40	-1.56	-0.41	-1.54	-0.32	-0.35	-0.33	-0.38
-0.41	-1.42	-0.41	-1.28	-0.40	-1.50	-0.41	-1.47	-0.32	-0.27	-0.32	-0.31
-0.41	-1.36	-0.41	-1.24	-0.40	-1.45	-0.41	-1.41	-0.32	-0.23	-0.32	-0.26
-0.41	-1.31	-0.41	-1.20	-0.40	-1.40	-0.41	-1.36	-0.32	-0.17	-0.32	-0.21
-0.41	-1.26	-0.41	-1.16	-0.40	-1.36	-0.41	-1.31	-0.32	-0.13	-0.32	-0.17
-0.41	-1.21	-0.41	-1.13	-0.39	-1.32	-0.41	-1.26	-0.32	-0.08	-0.32	-0.14
-0.41	-1.17	-0.41	-1.09	-0.39	-1.29	-0.41	-1.22	-0.31	-0.04	-0.32	-0.09
-0.41	-1.13	-0.41	-1.06	-0.39	-1.25	-0.41	-1.18	-0.31	0.00	-0.32	-0.06
-0.41	-1.09	-0.41	-1.03	-0.39	-1.22	-0.41	-1.14	-0.31	0.04	-0.32	-0.03
-0.41	-1.06	-0.40	-0.99	-0.39	-1.19	-0.40	-1.10	-0.31	0.07	-0.32	0.00
-0.40	-1.02	-0.40	-0.96	-0.39	-1.16	-0.40	-1.07	-0.31	0.11	-0.32	0.03
-0.40	-0.99	-0.40	-0.94	-0.39	-1.13	-0.40	-1.04	-0.31	0.14	-0.32	0.03
-0.40	-0.96	-0.40	-0.92	-0.39	-1.11	-0.40	-1.00	-0.31	0.17	-0.31	0.05
-0.40	-0.93	-0.40	-0.89	-0.39	-1.08	-0.40	-0.97	-0.31	0.19	-0.31	0.08
-0.40	-0.90	-0.40	-0.87	-0.39	-1.06	-0.40	-0.94	-0.31	0.21	-0.31	0.11
-0.40	-0.88	-0.40	-0.85	-0.38	-1.03	-0.40	-0.92	-0.31	0.23	-0.31	0.13
-0.40	-0.85	-0.40	-0.83	-0.38	-1.00	-0.40	-0.89	-0.30	0.24	-0.31	0.15
-0.40	-0.83	-0.40	-0.81	-0.38	-0.98	-0.40	-0.87	-0.30	0.26	-0.31	0.18
-0.40	-0.81	-0.40	-0.79	-0.38	-0.96	-0.40	-0.84	-0.30	0.29	-0.31	0.19
-0.40	-0.78	-0.39	-0.77	-0.38	-0.94	-0.39	-0.82	-0.30	0.31	-0.31	0.21
-0.39	-0.76	-0.39	-0.75	-0.38	-0.91	-0.39	-0.79	-0.30	0.33	-0.31	0.22
-0.39	-0.74	-0.39	-0.73	-0.38	-0.90	-0.39	-0.77	-0.30	0.35	-0.30	0.24
-0.39	-0.72	-0.39	-0.71	-0.38	-0.88	-0.39	-0.75	-0.30	0.37	-0.30	0.26
-0.39	-0.70	-0.39	-0.69	-0.38	-0.86	-0.39	-0.73	-0.30	0.38	-0.30	0.28
-0.39	-0.68	-0.39	-0.67	-0.38	-0.84	-0.39	-0.71	-0.30	0.40	-0.30	0.28
-0.39	-0.66	-0.39	-0.66	-0.37	-0.82	-0.39	-0.69	-0.30	0.42	-0.30	0.30
-0.39	-0.64	-0.39	-0.64	-0.37	-0.80	-0.39	-0.67	-0.29	0.43	-0.30	0.31
-0.39	-0.63	-0.39	-0.62	-0.37	-0.79	-0.39	-0.65	-0.29	0.45	-0.30	0.32
-0.39	-0.61	-0.39	-0.61	-0.37	-0.77	-0.39	-0.63	-0.29	0.46	-0.30	0.34
-0.39	-0.59	-0.38	-0.59	-0.37	-0.75	-0.38	-0.61	-0.29	0.48	-0.30	0.34
-0.38	-0.57	-0.38	-0.57	-0.37	-0.73	-0.38	-0.59	-0.29	0.49	-0.30	0.36
-0.38	-0.56	-0.38	-0.56	-0.37	-0.72	-0.38	-0.58	-0.29	0.51	-0.29	0.37
-0.38	-0.54	-0.38	-0.54	-0.37	-0.70	-0.38	-0.56	-0.29	0.52	-0.29	0.38
-0.38	-0.53	-0.38	-0.53	-0.37	-0.68	-0.38	-0.54	-0.29	0.54	-0.29	0.39
-0.38	-0.51	-0.38	-0.51	-0.37	-0.67	-0.38	-0.52	-0.29	0.55	-0.29	0.40
-0.38	-0.49	-0.38	-0.49	-0.36	-0.65	-0.38	-0.51	-0.29	0.56	-0.29	0.41
-0.38	-0.48	-0.38	-0.48	-0.36	-0.64	-0.38	-0.49	-0.28	0.58	-0.29	0.42
-0.38	-0.46	-0.38	-0.46	-0.36	-0.62	-0.38	-0.47	-0.28	0.59	-0.29	0.43
-0.38	-0.45	-0.38	-0.45	-0.36	-0.61	-0.38	-0.46	-0.28	0.61	-0.29	0.44
-0.38	-0.43	-0.37	-0.43	-0.36	-0.59	-0.37	-0.44	-0.28	0.62	-0.29	0.45
-0.37	-0.42	-0.37	-0.42	-0.36	-0.58	-0.37	-0.43	-0.28	0.63	-0.29	0.46
-0.37	-0.41	-0.37	-0.41	-0.36	-0.56	-0.37	-0.41	-0.28	0.64	-0.28	0.47
-0.37	-0.39	-0.37	-0.39	-0.36	-0.55	-0.37	-0.39	-0.28	0.66	-0.28	0.48
-0.37	-0.38	-0.37	-0.38	-0.36	-0.53	-0.37	-0.38	-0.28	0.67	-0.28	0.49
-0.37	-0.36	-0.37	-0.36	-0.36	-0.52	-0.37	-0.36	-0.28	0.68	-0.28	0.50
-0.37	-0.35	-0.37	-0.35	-0.35	-0.50	-0.37	-0.35	-0.28	0.69	-0.28	0.51

-0.37	-0.34	-0.37	-0.33	-0.35	-0.49	-0.37	-0.34	-0.27	0.70	-0.28	0.52
-0.37	-0.32	-0.37	-0.32	-0.35	-0.47	-0.37	-0.32	-0.27	0.71	-0.28	0.53
-0.37	-0.31	-0.37	-0.31	-0.35	-0.46	-0.37	-0.31	-0.27	0.72	-0.28	0.54
-0.37	-0.30	-0.36	-0.29	-0.35	-0.45	-0.36	-0.29	-0.27	0.73	-0.28	0.55
-0.36	-0.28	-0.36	-0.28	-0.35	-0.43	-0.36	-0.28	-0.27	0.74	-0.28	0.56
-0.36	-0.27	-0.36	-0.27	-0.35	-0.42	-0.36	-0.26	-0.27	0.75	-0.27	0.58
-0.36	-0.26	-0.36	-0.25	-0.35	-0.41	-0.36	-0.25	-0.27	0.76	-0.27	0.58
-0.36	-0.24	-0.36	-0.24	-0.35	-0.39	-0.36	-0.24	-0.27	0.77	-0.27	0.59
-0.36	-0.23	-0.36	-0.23	-0.35	-0.38	-0.36	-0.22	-0.27	0.78	-0.27	0.60
-0.36	-0.22	-0.36	-0.21	-0.34	-0.37	-0.36	-0.21	-0.27	0.79	-0.27	0.61
-0.36	-0.21	-0.36	-0.20	-0.34	-0.35	-0.36	-0.20	-0.26	0.80	-0.27	0.62
-0.36	-0.19	-0.36	-0.19	-0.34	-0.34	-0.36	-0.18	-0.26	0.81	-0.27	0.63
-0.36	-0.18	-0.36	-0.17	-0.34	-0.33	-0.36	-0.17	-0.26	0.82	-0.27	0.64
-0.36	-0.17	-0.35	-0.16	-0.34	-0.31	-0.35	-0.16	-0.26	0.83	-0.27	0.65
-0.35	-0.15	-0.35	-0.15	-0.34	-0.30	-0.35	-0.14	-0.26	0.84	-0.27	0.66
-0.35	-0.14	-0.35	-0.13	-0.34	-0.29	-0.35	-0.13	-0.26	0.85	-0.26	0.67
-0.35	-0.13	-0.35	-0.12	-0.34	-0.28	-0.35	-0.12	-0.26	0.86	-0.26	0.68
-0.35	-0.12	-0.35	-0.11	-0.34	-0.26	-0.35	-0.11	-0.26	0.87	-0.26	0.69
-0.35	-0.11	-0.35	-0.10	-0.34	-0.25	-0.35	-0.09	-0.26	0.88	-0.26	0.71
-0.35	-0.09	-0.35	-0.08	-0.33	-0.24	-0.35	-0.08	-0.26	0.89	-0.26	0.72
-0.35	-0.08	-0.35	-0.07	-0.33	-0.23	-0.35	-0.07	-0.25	0.90	-0.26	0.74
-0.35	-0.07	-0.35	-0.06	-0.33	-0.21	-0.35	-0.06	-0.25	0.90	-0.26	0.75
-0.35	-0.06	-0.35	-0.04	-0.33	-0.20	-0.35	-0.04	-0.25	0.91	-0.26	0.76
-0.35	-0.04	-0.34	-0.03	-0.33	-0.19	-0.34	-0.03	-0.25	0.92	-0.26	0.77
-0.34	-0.03	-0.34	-0.02	-0.33	-0.18	-0.34	-0.02	-0.25	0.93	-0.26	0.78
-0.34	-0.02	-0.34	-0.01	-0.33	-0.16	-0.34	-0.01	-0.25	0.94	-0.25	0.80
-0.34	-0.01	-0.34	0.01	-0.33	-0.15	-0.34	0.00	-0.25	0.95	-0.25	0.81
-0.34	0.01	-0.34	0.02	-0.33	-0.14	-0.34	0.02	-0.25	0.95	-0.25	0.82
-0.34	0.02	-0.34	0.03	-0.33	-0.13	-0.34	0.03	-0.25	0.96	-0.25	0.84
-0.34	0.03	-0.34	0.04	-0.32	-0.12	-0.34	0.04	-0.25	0.97	-0.25	0.85
-0.34	0.04	-0.34	0.06	-0.32	-0.10	-0.34	0.05	-0.24	0.98	-0.25	0.87
-0.34	0.06	-0.34	0.07	-0.32	-0.09	-0.34	0.06	-0.24	0.99	-0.25	0.89
-0.34	0.07	-0.34	0.08	-0.32	-0.08	-0.34	0.07	-0.24	1.00	-0.25	0.90
-0.34	0.08	-0.33	0.10	-0.32	-0.07	-0.33	0.09	-0.24	1.00	-0.25	0.92
-0.33	0.09	-0.33	0.11	-0.32	-0.06	-0.33	0.10	-0.24	1.01	-0.25	0.94
-0.33	0.11	-0.33	0.12	-0.32	-0.04	-0.33	0.11	-0.24	1.02	-0.24	0.95
-0.33	0.12	-0.33	0.13	-0.32	-0.03	-0.33	0.12	-0.24	1.03	-0.24	0.97
-0.33	0.13	-0.33	0.15	-0.32	-0.02	-0.33	0.13	-0.24	1.04	-0.24	0.99
-0.33	0.14	-0.33	0.16	-0.32	-0.01	-0.33	0.14	-0.24	1.05	-0.24	1.01
-0.33	0.15	-0.33	0.17	-0.31	0.00	-0.33	0.15	-0.24	1.05	-0.24	1.02
-0.33	0.17	-0.33	0.18	-0.31	0.02	-0.33	0.16	-0.23	1.06	-0.24	1.04
-0.33	0.18	-0.33	0.20	-0.31	0.03	-0.33	0.18	-0.23	1.07	-0.24	1.06
-0.33	0.19	-0.33	0.21	-0.31	0.04	-0.33	0.19	-0.23	1.08	-0.24	1.08
-0.33	0.20	-0.32	0.22	-0.31	0.05	-0.32	0.20	-0.23	1.09	-0.24	1.10
-0.32	0.21	-0.32	0.23	-0.31	0.06	-0.32	0.21	-0.23	1.09	-0.24	1.11
-0.32	0.22	-0.32	0.25	-0.31	0.08	-0.32	0.22	-0.23	1.10	-0.23	1.13
-0.32	0.24	-0.32	0.26	-0.31	0.09	-0.32	0.23	-0.23	1.11	-0.23	1.15

-0.32	0.25	-0.32	0.27	-0.31	0.10	-0.32	0.24	-0.23	1.11	-0.23	1.17
-0.32	0.26	-0.32	0.28	-0.31	0.11	-0.32	0.25	-0.23	1.12	-0.23	1.18
-0.32	0.27	-0.32	0.30	-0.30	0.12	-0.32	0.26	-0.23	1.13	-0.23	1.20
-0.32	0.28	-0.32	0.31	-0.30	0.13	-0.32	0.27	-0.22	1.13	-0.23	1.22
-0.32	0.29	-0.32	0.32	-0.30	0.15	-0.32	0.28	-0.22	1.14	-0.23	1.23
-0.32	0.31	-0.32	0.33	-0.30	0.16	-0.32	0.29	-0.22	1.15	-0.23	1.25
-0.32	0.32	-0.31	0.35	-0.30	0.17	-0.31	0.30	-0.22	1.15	-0.23	1.27
-0.31	0.33	-0.31	0.36	-0.30	0.18	-0.31	0.31	-0.22	1.16	-0.23	1.28
-0.31	0.34	-0.31	0.37	-0.30	0.19	-0.31	0.32	-0.22	1.17	-0.22	1.30
-0.31	0.35	-0.31	0.38	-0.30	0.20	-0.31	0.33	-0.22	1.17	-0.22	1.31
-0.31	0.36	-0.31	0.40	-0.30	0.21	-0.31	0.34	-0.22	1.18	-0.22	1.33
-0.31	0.38	-0.31	0.41	-0.30	0.23	-0.31	0.35	-0.22	1.19	-0.22	1.34
-0.31	0.39	-0.31	0.42	-0.29	0.24	-0.31	0.36	-0.22	1.20	-0.22	1.36
-0.31	0.40	-0.31	0.43	-0.29	0.25	-0.31	0.37	-0.21	1.20	-0.22	1.37
-0.31	0.41	-0.31	0.45	-0.29	0.26	-0.31	0.38	-0.21	1.21	-0.22	1.39
-0.31	0.42	-0.31	0.46	-0.29	0.27	-0.31	0.39	-0.21	1.22	-0.22	1.40
-0.31	0.43	-0.30	0.47	-0.29	0.28	-0.30	0.40	-0.21	1.22	-0.22	1.41
-0.30	0.44	-0.30	0.48	-0.29	0.29	-0.30	0.41	-0.21	1.23	-0.22	1.42
-0.30	0.45	-0.30	0.50	-0.29	0.31	-0.30	0.42	-0.21	1.24	-0.21	1.44
-0.30	0.46	-0.30	0.51	-0.29	0.32	-0.30	0.43	-0.21	1.24	-0.21	1.45
-0.30	0.48	-0.30	0.52	-0.29	0.33	-0.30	0.44	-0.21	1.25	-0.21	1.46
-0.30	0.49	-0.30	0.53	-0.29	0.34	-0.30	0.45	-0.21	1.26	-0.21	1.47
-0.30	0.50	-0.30	0.54	-0.28	0.35	-0.30	0.46	-0.21	1.26	-0.21	1.48
-0.30	0.51	-0.30	0.56	-0.28	0.36	-0.30	0.47	-0.20	1.27	-0.21	1.50
-0.30	0.52	-0.30	0.57	-0.28	0.37	-0.30	0.48	-0.20	1.28	-0.21	1.51
-0.30	0.53	-0.30	0.58	-0.28	0.38	-0.30	0.49	-0.20	1.28	-0.21	1.52
-0.30	0.54	-0.29	0.59	-0.28	0.40	-0.29	0.50	-0.20	1.29	-0.21	1.53
-0.29	0.55	-0.29	0.61	-0.28	0.41	-0.29	0.51	-0.20	1.30	-0.21	1.54
-0.29	0.56	-0.29	0.62	-0.28	0.42	-0.29	0.52	-0.20	1.30	-0.20	1.55
-0.29	0.57	-0.29	0.63	-0.28	0.43	-0.29	0.53	-0.20	1.31	-0.20	1.56
-0.29	0.58	-0.29	0.64	-0.28	0.44	-0.29	0.54	-0.20	1.32	-0.20	1.57
-0.29	0.59	-0.29	0.65	-0.28	0.45	-0.29	0.55	-0.20	1.32	-0.20	1.58
-0.29	0.60	-0.29	0.67	-0.27	0.46	-0.29	0.56	-0.20	1.33	-0.20	1.59
-0.29	0.61	-0.29	0.68	-0.27	0.47	-0.29	0.57	-0.19	1.34	-0.20	1.59
-0.29	0.62	-0.29	0.69	-0.27	0.48	-0.29	0.58	-0.19	1.34	-0.20	1.60
-0.29	0.63	-0.29	0.70	-0.27	0.50	-0.29	0.59	-0.19	1.35	-0.20	1.61
-0.29	0.64	-0.28	0.71	-0.27	0.51	-0.28	0.60	-0.19	1.35	-0.20	1.62
-0.28	0.65	-0.28	0.72	-0.27	0.52	-0.28	0.61	-0.19	1.36	-0.20	1.63
-0.28	0.66	-0.28	0.74	-0.27	0.53	-0.28	0.61	-0.19	1.37	-0.19	1.64
-0.28	0.67	-0.28	0.75	-0.27	0.54	-0.28	0.62	-0.19	1.37	-0.19	1.64
-0.28	0.68	-0.28	0.76	-0.27	0.55	-0.28	0.63	-0.19	1.38	-0.19	1.65
-0.28	0.69	-0.28	0.77	-0.27	0.56	-0.28	0.64	-0.19	1.38	-0.19	1.66
-0.28	0.70	-0.28	0.78	-0.26	0.57	-0.28	0.65	-0.19	1.39	-0.19	1.67
-0.28	0.71	-0.28	0.79	-0.26	0.58	-0.28	0.66	-0.18	1.40	-0.19	1.67
-0.28	0.72	-0.28	0.80	-0.26	0.60	-0.28	0.67	-0.18	1.40	-0.19	1.68
-0.28	0.73	-0.28	0.81	-0.26	0.61	-0.28	0.68	-0.18	1.41	-0.19	1.69
-0.28	0.74	-0.27	0.83	-0.26	0.62	-0.27	0.69	-0.18	1.42	-0.19	1.70

-0.27	0.75	-0.27	0.84	-0.26	0.63	-0.27	0.70	-0.18	1.42	-0.19	1.70
-0.27	0.75	-0.27	0.85	-0.26	0.64	-0.27	0.71	-0.18	1.43	-0.18	1.71
-0.27	0.76	-0.27	0.86	-0.26	0.65	-0.27	0.71	-0.18	1.43	-0.18	1.72
-0.27	0.77	-0.27	0.87	-0.26	0.66	-0.27	0.72	-0.18	1.44	-0.18	1.72
-0.27	0.78	-0.27	0.88	-0.26	0.67	-0.27	0.73	-0.18	1.44	-0.18	1.73
-0.27	0.79	-0.27	0.89	-0.25	0.68	-0.27	0.74	-0.18	1.45	-0.18	1.74
-0.27	0.80	-0.27	0.90	-0.25	0.69	-0.27	0.75	-0.17	1.46	-0.18	1.74
-0.27	0.81	-0.27	0.91	-0.25	0.70	-0.27	0.76	-0.17	1.46	-0.18	1.75
-0.27	0.82	-0.27	0.92	-0.25	0.71	-0.27	0.77	-0.17	1.47	-0.18	1.75
-0.27	0.82	-0.26	0.93	-0.25	0.73	-0.26	0.77	-0.17	1.47	-0.18	1.76
-0.26	0.83	-0.26	0.94	-0.25	0.74	-0.26	0.78	-0.17	1.48	-0.18	1.77
-0.26	0.84	-0.26	0.95	-0.25	0.75	-0.26	0.79	-0.17	1.48	-0.17	1.77
-0.26	0.85	-0.26	0.96	-0.25	0.76	-0.26	0.80	-0.17	1.49	-0.17	1.78
-0.26	0.86	-0.26	0.97	-0.25	0.77	-0.26	0.81	-0.17	1.49	-0.17	1.78
-0.26	0.87	-0.26	0.98	-0.25	0.78	-0.26	0.82	-0.17	1.50	-0.17	1.79
-0.26	0.87	-0.26	0.99	-0.24	0.79	-0.26	0.83	-0.17	1.50	-0.17	1.80
-0.26	0.88	-0.26	1.00	-0.24	0.80	-0.26	0.83	-0.16	1.51	-0.17	1.80
-0.26	0.89	-0.26	1.01	-0.24	0.81	-0.26	0.84	-0.16	1.52	-0.17	1.81
-0.26	0.90	-0.26	1.02	-0.24	0.82	-0.26	0.85	-0.16	1.52	-0.17	1.81
-0.26	0.91	-0.25	1.02	-0.24	0.83	-0.25	0.86	-0.16	1.53	-0.17	1.82
-0.25	0.91	-0.25	1.03	-0.24	0.84	-0.25	0.87	-0.16	1.53	-0.17	1.82
-0.25	0.92	-0.25	1.04	-0.24	0.85	-0.25	0.88	-0.16	1.54	-0.16	1.83
-0.25	0.93	-0.25	1.05	-0.24	0.86	-0.25	0.88	-0.16	1.54	-0.16	1.83
-0.25	0.94	-0.25	1.06	-0.24	0.87	-0.25	0.89	-0.16	1.55	-0.16	1.84
-0.25	0.94	-0.25	1.07	-0.24	0.88	-0.25	0.90	-0.16	1.55	-0.16	1.84
-0.25	0.95	-0.25	1.08	-0.23	0.89	-0.25	0.91	-0.16	1.56	-0.16	1.85
-0.25	0.96	-0.25	1.09	-0.23	0.90	-0.25	0.92	-0.15	1.56	-0.16	1.85
-0.25	0.97	-0.25	1.10	-0.23	0.91	-0.25	0.93	-0.15	1.57	-0.16	1.86
-0.25	0.97	-0.25	1.10	-0.23	0.92	-0.25	0.93	-0.15	1.57	-0.16	1.86
-0.25	0.98	-0.24	1.11	-0.23	0.93	-0.24	0.94	-0.15	1.58	-0.16	1.87
-0.24	0.99	-0.24	1.12	-0.23	0.94	-0.24	0.95	-0.15	1.58	-0.16	1.87
-0.24	1.00	-0.24	1.13	-0.23	0.95	-0.24	0.96	-0.15	1.59	-0.15	1.88
-0.24	1.00	-0.24	1.14	-0.23	0.96	-0.24	0.97	-0.15	1.59	-0.15	1.88
-0.24	1.01	-0.24	1.15	-0.23	0.97	-0.24	0.97	-0.15	1.60	-0.15	1.89
-0.24	1.02	-0.24	1.15	-0.23	0.98	-0.24	0.98	-0.15	1.60	-0.15	1.89
-0.24	1.03	-0.24	1.16	-0.22	0.99	-0.24	0.99	-0.15	1.61	-0.15	1.90
-0.24	1.03	-0.24	1.17	-0.22	1.00	-0.24	1.00	-0.14	1.61	-0.15	1.90
-0.24	1.04	-0.24	1.18	-0.22	1.01	-0.24	1.00	-0.14	1.62	-0.15	1.91
-0.24	1.05	-0.24	1.19	-0.22	1.02	-0.24	1.01	-0.14	1.62	-0.15	1.91
-0.24	1.05	-0.23	1.19	-0.22	1.03	-0.23	1.02	-0.14	1.62	-0.15	1.91
-0.23	1.06	-0.23	1.20	-0.22	1.04	-0.23	1.03	-0.14	1.63	-0.15	1.92
-0.23	1.07	-0.23	1.21	-0.22	1.04	-0.23	1.04	-0.14	1.63	-0.14	1.92
-0.23	1.08	-0.23	1.22	-0.22	1.05	-0.23	1.04	-0.14	1.64	-0.14	1.93
-0.23	1.08	-0.23	1.22	-0.22	1.06	-0.23	1.05	-0.14	1.64	-0.14	1.93
-0.23	1.09	-0.23	1.23	-0.22	1.07	-0.23	1.06	-0.14	1.65	-0.14	1.94
-0.23	1.10	-0.23	1.24	-0.21	1.08	-0.23	1.06	-0.14	1.65	-0.14	1.94
-0.23	1.10	-0.23	1.24	-0.21	1.09	-0.23	1.07	-0.13	1.66	-0.14	1.94

-0.23	1.11	-0.23	1.25	-0.21	1.10	-0.23	1.08	-0.13	1.66	-0.14	1.95
-0.23	1.12	-0.23	1.26	-0.21	1.11	-0.23	1.09	-0.13	1.66	-0.14	1.95
-0.23	1.12	-0.22	1.27	-0.21	1.12	-0.22	1.10	-0.13	1.67	-0.14	1.96
-0.22	1.13	-0.22	1.27	-0.21	1.12	-0.22	1.10	-0.13	1.67	-0.14	1.96
-0.22	1.14	-0.22	1.28	-0.21	1.13	-0.22	1.11	-0.13	1.68	-0.13	1.97
-0.22	1.14	-0.22	1.29	-0.21	1.14	-0.22	1.12	-0.13	1.68	-0.13	1.97
-0.22	1.15	-0.22	1.29	-0.21	1.15	-0.22	1.12	-0.13	1.69	-0.13	1.97
-0.22	1.15	-0.22	1.30	-0.21	1.15	-0.22	1.13	-0.13	1.69	-0.13	1.98
-0.22	1.16	-0.22	1.30	-0.20	1.16	-0.22	1.13	-0.13	1.69	-0.13	1.98

Data for Figure 26b.

	N2	Air
pH	i_{corr} (mA/cm^2)	i_{corr} (mA/cm^2)
7	0.008	0.075
5	0.024	0.101
4	0.028	0.093
3	0.032	0.126
2	1.047	1.298
1	2.42	2.40